

NASA/TM-2006-213727



C-9 and Other Microgravity Simulations

Summary Report

Report prepared by
Space and Life Sciences Directorate
Human Adaptation and Countermeasures Office
Johnson Space Center, Houston

Lyndon B. Johnson Space Center
Houston, Texas

September 2006

THE NASA STI PROGRAM OFFICE . . . IN PROFILE

Since its founding, NASA has been dedicated to the advancement of aeronautics and space science. The NASA Scientific and Technical Information (STI) Program Office plays a key part in helping NASA maintain this important role.

The NASA STI Program Office is operated by Langley Research Center, the lead center for NASA's scientific and technical information. The NASA STI Program Office provides access to the NASA STI Database, the largest collection of aeronautical and space science STI in the world. The Program Office is also NASA's institutional mechanism for disseminating the results of its research and development activities. These results are published by NASA in the NASA STI Report Series, which includes the following report types:

- **TECHNICAL PUBLICATION.** Reports of completed research or a major significant phase of research that present the results of NASA programs and include extensive data or theoretical analysis. Includes compilations of significant scientific and technical data and information deemed to be of continuing reference value. NASA's counterpart of peer-reviewed formal professional papers but has less stringent limitations on manuscript length and extent of graphic presentations.
- **TECHNICAL MEMORANDUM.** Scientific and technical findings that are preliminary or of specialized interest, e.g., quick release reports, working papers, and bibliographies that contain minimal annotation. Does not contain extensive analysis.
- **CONTRACTOR REPORT.** Scientific and technical findings by NASA-sponsored contractors and grantees.

- **CONFERENCE PUBLICATION.** Collected papers from scientific and technical conferences, symposia, seminars, or other meetings sponsored or cosponsored by NASA.
- **SPECIAL PUBLICATION.** Scientific, technical, or historical information from NASA programs, projects, and mission, often concerned with subjects having substantial public interest.
- **TECHNICAL TRANSLATION.** English-language translations of foreign scientific and technical material pertinent to NASA's mission.

Specialized services that complement the STI Program Office's diverse offerings include creating custom thesauri, building customized databases, organizing and publishing research results . . . even providing videos.

For more information about the NASA STI Program Office, see the following:

- Access the NASA STI Program Home Page at <http://www.sti.nasa.gov>
- E-mail your question via the Internet to help@sti.nasa.gov
- Fax your question to the NASA Access Help Desk at (301) 621-0134
- Telephone the NASA Access Help Desk at (301) 621-0390
- Write to:
NASA Access Help Desk
NASA Center for AeroSpace Information
7121 Standard
Hanover, MD 21076-1320

NASA/TM-2006-213727



C-9 and Other Microgravity Simulations

Summary Report

Report prepared by
Space and Life Sciences Directorate
Human Adaptation and Countermeasures Office
Johnson Space Center, Houston

Lyndon B. Johnson Space Center
Houston, Texas

September 2006

**C-9 and Other Microgravity Simulations
Summary Report – September 30, 2006**

National Aeronautics and Space Administration
Lyndon B. Johnson Space Center

Prepared by: Noel C. Skinner 8/14/06
Noel C. Skinner, M.S. Date
C-9 Coordinator
Wyle Laboratories, Inc., Life Sciences Group

Approved by: Jeannie L. Nillen 8/25/06
Jeannie L. Nillen, MT(ASCP) Date
Manager Human Adaptation and Countermeasures Group
Wyle Laboratories, Inc., Life Sciences Group

Approved by: Todd T. Schlegel 8/14/06
Todd T. Schlegel, M.D. Date
Technical Monitor
Human Adaptation and Countermeasures Office
Reduced Gravity Program
NASA Johnson Space Center

Available from:

NASA Center for AeroSpace Information
7121 Standard Drive
Hanover, MD 21076-1320

National Technical Information Service
5285 Port Royal Road
Springfield, VA 22161

This report is also available in electronic form at <http://ston.jsc.nasa.gov/collections/TRS>

PREFACE

This document represents a summary of medical and scientific evaluations conducted aboard the C-9 or other NASA-sponsored aircraft from June 30, 2005, to June 30, 2006. Included is a general overview of investigations manifested and coordinated by the Human Adaptation and Countermeasures Office. A collection of brief reports that describe tests conducted aboard the NASA-sponsored aircraft follows the overview. Principal investigators and test engineers contributed significantly to the content of the report, describing their particular experiment or hardware evaluation. Although this document follows general guidelines, the format of individual reports varies to accommodate differences in experiment design and procedures. This document concludes with an appendix that provides background information concerning the Reduced Gravity Program.



CONTENTS

Overview of C-9 Flight Activities sponsored by the Human Adaptation and Countermeasures Office.....	1
Medical and Scientific Evaluations During Parabolic Flights	3
Prototype Flight Cytometer.....	5
A Countermeasure for Space Motion Sickness	9
Experimental Microfluidic System Interfaced to Cell Culture Bags for Real Time Analysis of Amino Acids and reGFP	13
Endotracheal Tube Suction Capability Test for ISS	19
Medical Operations Familiarization Flight.....	24
Preliminary Report of Reduced Gravity Tests of the Magnetic Field	27
TAGES – Transgenic Gene Expression System.....	30
Undergraduate Program Flights - Effect of Microgravity on Semicircular Canal and Vestibular Function.....	34
Undergraduate Program Flights - Re-hydration of Artificial Blood Polymers in Microgravity	40
Undergraduate Program Flights - Gravitational Effects on Cartilage Nutrition and Neutrophil Function.....	47
Undergraduate Program Flights – Free-Floating Resistance Exercises for Maintaining Postural Muscles in Weightlessness	53
Space Medicine C-9 Familiarization	58
Myotometric Measurements of Muscle during Changes in Gravitational Forces	64
A Low-Intensity Mechanical Countermeasure to Prohibit Osteoporosis in Astronauts during Long-Term Spaceflight (VIBE)	70
Minimally Invasive Diagnosis and Therapy of Microgravity Medical Contingencies.....	82
Vestibular Adaptation in Parabolic Flight	88
Microgravity Investigation of Crew Reactions in 0g (Adapt)	93
A Simple Countermeasure for Space Motion Sickness	100
Experimental Microfluidic System Interfaced to Cell Culture Bags For Real Time Analysis of Amino Acids	106
Microfluidic Ion Sensor Array.....	112
Predicting and Assessing Postural Reentry Disturbances.....	116
Medical Operations Support Team (MOST): Remote Guidance of Crew Medical Officers (CMO) Analogues through Space Relevant Medical Sciences	120
The Effects of Microgravity on the Binding Kinetics of Two Lipid Binding Proteins.....	126
An Advanced Portable Ion Analyzer for Water Quality Monitoring and Control	130
Prototype Flight Cytometer.....	143

CONTENTS (cont'd)

Evaluation of Hardware for Sampling of Water onboard ISS for Subsequent Microbial Testing	147
Microgravity Effects on Plant Boundary Layer.....	151
Medical Operations C-9 Familiarization Flight	158
Evaluation of the Effectiveness of Overhead Suspension Reduced-Gravity Analog in a Microgravity Environment	161
Aerosol Deposition in Fractional Gravity: Risk Mitigation for Martian and Lunar Habitats	172
Critical Care Skills in Microgravity: Validation and Application of Skill Assessment Toolkit.....	178
Rapid Development of Colorimetric Solid Phase Extraction Technology for Water Quality Monitoring: Evaluation of C-SPE and De-bubbling Methods in Microgravity	180
Appendix: Background Information about the C-9 and the Reduced-Gravity Program.....	190

Overview of Flight Activities Sponsored by the Human Adaptation and Countermeasures Office

NASA retired the KC-135 (931) in October 2004 and secured a C-9 aircraft as a replacement to support the Reduced Gravity Program. However, NASA's C-9 aircraft was not available for use by investigators until February 2006, due to persistent mechanical issues. In the interim, NASA Headquarters provided a unique opportunity when demonstration flights were completed in October 2005 aboard Zero G Incorporated's 727 aircraft.

As a summary for the year, from June 30, 2005 to June 30, 2006, nine weeks were specifically reserved for flights sponsored by the Human Adaptation and Countermeasures Office (HACO). In addition, during two weeks we were able to obtain seating for HACO customers with other organizations sponsoring these flight weeks. A total of forty flights with approximately forty parabolas per flight were completed. The average duration of each flight was two hours. The C-9 coordinator assisted principal investigators and test engineers of thirty-five different experiments and hardware evaluations in meeting the necessary requirements for flying aboard the C-9 or other NASA sponsored aircraft and in obtaining the required seating and floor space. HACO customers purchased a total of 382 seats. The number of seats supported and number of different tests flown by flight week are provided below:

Flight Week	Seats	# Tests Flown	Sponsor
Oct. 13 –14, 2005	24	5	HACO
Feb. 7 – 11, 2006	17	1	HACO
Mar. 7 – 10	28	4	Undergraduate Program
Mar. 23 – 24	4	1	Undergraduate Program
Apr. 11 –14	60	6	HACO
Apr. 18 – 21	64	5	HACO
Apr. 25 -28	56	2	HACO
May 9–12	14	3	HACO
May 23–26	27	3	HACO
June 13–16	72	4	HACO
June 21–23	16	1	HACO

Support was provided to the undergraduate program during two weeks in March 2006. Local and major network radio, television and newspaper journalists accompanied the students on some of these flights. A large ground crew from the respective academic institutions supported the in-flight experiments.

Other HACO sponsored flight opportunities are scheduled for weeks during July, August, and September 2006. Additional flights will be added throughout the remainder of calendar year 2006 to accommodate customers as needs arise.

Medical and Scientific Evaluations during Parabolic Flights

TITLE

Prototype Flight Cytometer

FLIGHT DATES

October 13 -14, 2005

PRINCIPAL INVESTIGATORS

Brian Crucian, Wyle Laboratories, Inc., Life Sciences Group
Mayra Nelman-Gonzalez, Wyle Laboratories, Inc., Life Sciences Group
Clarence Sams, NASA/Johnson Space Center



GOAL

To continue development/validation of a prototype spaceflight-compatible flow cytometer and an associated microgravity-compatible cell staining device for medical support during long-duration space missions. Two Zero-G Corp. evaluations of the developed hardware were performed in FY05.

OBJECTIVES

A spaceflight-compatible flow cytometer would be useful for the diagnosis of astronaut illness during long-duration spaceflight and for conducting in-flight research to evaluate the effects of microgravity on human physiology. Until recently, the primary limitations preventing the development of a spaceflight-compatible flow cytometer have been largely mechanical. Standard, commercially available flow cytometers are large, complex instruments that use high-

energy lasers and require significant training to operate. Standard flow cytometers function by suspending the particles to be analyzed inside a “sheath” fluid for analysis. This requires the presence of several liters of sheath fluid for operation and generates a corresponding amount of liquid hazardous waste. The particles are then passed through a flow cell, which uses the fluid mechanical property of “hydrodynamic focusing” to place the cells in single file (laminar flow) as they pass through a laser beam for scanning and evaluation. Many spaceflight experiments have demonstrated that fluid physics is dramatically altered in microgravity (MSF Fluid Physics Data Sheet-August 1997) and previous studies have shown that sheath fluid-based hydrodynamic focusing may also be altered during microgravity (Crucian et al, 2000). For these reasons, it is likely that any spaceflight compatible design for a flow cytometer would abandon the sheath fluid requirement. The elimination of sheath fluid would remove the problem of weight associated with large volumes of liquids as well as the large volume of liquid waste generated. It would also create the need for a method to create laminar particle flow distinct from the standard sheath fluid based method.

The spaceflight prototype instrument is based on a recently developed commercial flow cytometer possessing a novel flow cell design that creates single-particle laser scanning and evaluation without the need for sheath fluid-based hydrodynamic focusing. This instrument also possesses a number of other design advances that make it conditionally microgravity compatible: it is highly miniaturized and lightweight, uses a low energy diode laser, has a small number of moving parts, does not use sheath fluid and does not generate significant liquid waste. Although possessing certain limitations, the commercial cytometer functions operationally like a standard bench-top laboratory flow cytometer, aspirating liquid particle samples and generating histogram or dot-plot data in standard “FCS” file format. In its current configuration however, the cytometer is limited to three-parameter/two-color capability (two color photomultiplier tubes (PMTs) + forward scatter), does not allow compensation between colors, does not allow linear analysis and is operated by rather inflexible software with limited capabilities. This is due to the fact that the cytometer has been designed and marketed as an instrument specific to a few particular assays, not as a multi-purpose cytometer.

The NASA-JSC Center Director’s Discretionary Fund has funded the Cellular and Molecular Research (CMR) Laboratory to

1. construct a prototype flight instrument based on the framework of the commercial cytometer
2. perform ground-based and microgravity validation of the instrument
3. design and validate a set of medical assays compatible with the prototype instrument
4. design and validate a microgravity-compatible cell-staining device for sample processing that can interface with the instrument. In FY04 the initial stages of instrument design and validation were successfully completed, as well as the development of the cell staining unit and medical assays. The FY04 KC-135 evaluations that took place were as follows:

Flight #1	10-13-2004	Evaluation of 2005 engineering changes to instrument.
Flight #2	10-14-2004	Evaluation of 2005 engineering changes to instrument.

MATERIALS AND METHODS

Blood donors

Whole blood samples were obtained from adult donors into ACD anticoagulant vacutainers. This includes the KC-135 flight experiment and all developmental work performed in preparation for the experiment. The subjects had been screened by the NASA-JSC Test Subject Facility for most

major infectious diseases and were found to be in good health. Institutional Review Board (NASA-JSC) approval was obtained for this study and written informed consent was obtained from all subjects.

Cell staining

A complete 2-color antibody panel was formulated to resolve most major leukocyte subsets yet remain within the limitations of the instrument. The cell populations resolved included: leukocyte subsets, T cells, B cells, NK cells, T cell subsets, and activated T cells. Cell surface markers were stained prior to flight. For the bead-based cytometry samples either fluorescent calibration microspheres or linearity fluorescent microspheres were used.

Flow cytometry analysis

For ground-based analysis, a Beckman-Coulter XL flow cytometer was configured as a reference cytometer for 3-parameter/2-color analysis so that it would mimic the function of the cytometer. Analysis was performed using the XL as a reference cytometer, and ground-based control data was generated using the prototype flight cytometer. For data collection during microgravity, the sampling apparatus of the cytometer was altered for ease of operation during parabolic flight. To ensure data collection occurred during microgravity only, samples were mixed and affixed to the sampling probe and the instrument was primed prior to the initiation of the microgravity phase. Priming took place during the 2g phase between parabolas. Data collection was initiated as the parabola was initiated and ended as the aircraft exited the parabola.

RESULTS

In FY04-FY05, the basic configuration of the prototype flight cytometer was reduced-gravity validated, the associated cell-staining unit (interfaces with instrument) was developed and validated, the medical assay panel was developed and validated, and microgravity evaluation of all hardware was successfully performed. During these first two flights in FY06, the significant engineering changes were validated to not perturb the reduced-gravity function of the instrument.

Microgravity evaluation of instrument and associated hardware: The instrument, all associated hardware, and the panel of assays were all evaluated real-time in microgravity conditions onboard the Zero G Corp. aircraft. The sample delivery/processing hardware was found to function well during microgravity conditions, in a manner comparable to ground operation. All peripheral blood leukocyte subset data collected during microgravity were found to be essentially identical to ground data and reference cytometer control data. In short, the engineering modifications were found to be compatible with reduced-gravity operations.

As a consequence of miniaturization, the cooling fan was removed from the instrument. For these parabolic flights, internal temperature of the instrument was recorded via a digital thermometer. Internal core instrument temperature was found to peak at 32°C.

DISCUSSION

The flow cytometer is an extremely versatile laboratory instrument with a broad spectrum of uses in both clinical medicine and basic science research. It is therefore highly desirable to develop a spaceflight-compatible cytometer for use on the International Space Station. While currently limited in ability, the cytometer represents an attractive design option for the design of a spaceflight-compatible flow cytometer. It has the potential to be made completely microgravity compatible and serve as a prototype spaceflight instrument with relatively minimal alterations in design specifications.

The cytometer's level of miniaturization, use of a low-energy diode laser, and elimination of the sheath fluid requirement all uniquely meet the existing prerequisites for use during spaceflight. It is likely that the current limitations of this instrument could be overcome by modifying the software, and adding additional lasers, color PMTs, side scatter, color compensation ability and further miniaturization. The sample delivery apparatus of the cytometer is not microgravity-compatible and would require significant modifications. These limitations notwithstanding, the cytometer may be well suited to be the prototype from which a spaceflight-compatible flow cytometer is designed.

The successful microgravity evaluation of the cytometer, and the need to collect real-time experimental data onboard the ISS for both research and clinical diagnosis purposes, warrant the continued development of a spaceflight prototype flow cytometer. The versatility of the flow cytometer for general research (biological, microbial, environmental and physiological studies) and diagnostic medicine would be a major asset to the ISS/Lunar/Mars programs.

CONCLUSION

Significant engineering changes to the Prototype Flight Cytometer were performed and evaluated during reduced gravity.

REFERENCES

Crucian, B., Norman, J., Brentz, J., Pietrzyk, R., and Sams, C., Laboratory outreach: student assessment of flow cytometer fluidics in zero-gravity. *Laboratory Medicine* 31(10):569-572, 2000.

NASA-Marshall Space Flight Center (1997). Microgravity Research Division: Microgravity Fluid Physics Discipline Brochure. Available online at <http://mgnews.msfc.nasa.gov/db/fluid-phys.pdf> (PDF document) or <http://mgnews.msfc.nasa.gov/db/fluids/fluids.html> (HTML document).

PHOTOGRAPHS

JSC2005E41547
JSC2005E41550 to JSC2005E41552
JSC2005E41612 to JSC2005E41622
JSC 2005E41650 to JSC2005E41652
JSC2005E41674
JSC2006E18159 to JSC2006E18188

VIDEO

None

CONTACT INFORMATION

Brian Crucian, Ph.D.
Wyle Laboratories, Inc., Life Sciences Group
1290 Hercules, Suite 120
Houston, TX 77058
281-483-7061
brian.crucian-1@nasa.gov

TITLE

A Countermeasure for Space Motion Sickness

FLIGHT DATES

October 13-14, 2005

PRINCIPAL INVESTIGATOR

Millard F. Reschke
NASA/Johnson Space Center

CO-INVESTIGATORS

Jeffrey Somers
Veteran's Affairs Medical Center

R. John Leigh
Wyle Laboratories, Inc., Life Sciences Group



GOAL

The goal of this study was to determine the efficacy of the parabolic flight experimental protocol and the reliability of the goggles and audio hardware.

OBJECTIVES

- The primary objective was to validate our test procedures and protocol.
- The second objective was to determine the dependability of the Ferro-electric (FE-1) goggles and their respective drivers.
- The third objective was to ascertain the reliability and necessity of the audio hardware.

METHODS AND MATERIALS

Four flyers flew during these verification flights: two flyers served as test subjects, one flyer served as a test operator and the other flyer served as a videographer. The test subjects sat in the first row of seats to allow room for whole-body movements, and so the operator could be in constant contact with the subjects, close enough to lay the subjects on the floor if they became motion sick. An audio box was fastened under one of the subject's seats. The audio box allowed communication between the operator and the subjects and provided a metronomic beep via iPod shuffle. The operator's voice could be heard through the subjects' left earphone while the beep could be heard through the subjects' right earphone. All audio (operator, subjects, and tone) was recorded on four individual digital voice recorders. A motion sickness score sheet contained a list of motion sickness symptoms and their equivalent Miller-Graybiel rating score. It also had a table on which the test operator could record the symptoms that the subjects reported and acquire a sum total motion sickness score. Subjects were trained prior to the flight on how to recognize and report the Miller-Graybiel motion sickness symptoms as well as how to self-rate their symptoms on a scale of 1-20 (1 = normal, no motion sickness). The subjective self-rating score gives the operator another tool to monitor the subject's level of motion sickness.

Once the plane reached altitude, subjects donned the FE-1 goggles, goggle driver with pushbutton, and audio headset, and the operator donned his/her audio headset.

The subjects remained seated upright in their chairs, seatbelts fastened tightly with their eyes closed and heads completely still during the 2g portions of the parabola. At the onset of the microgravity portions of the parabola, the subjects would push a handheld pushbutton that was connected to the driver to cause the goggles to flash at 4 Hz for 30 seconds. Once the button was pressed, the subjects would open their eyes and perform 90° en bloc head and body pitch movements at a frequency of 0.5 Hz to serve as a motion sickness stimulus. The frequency of the movement was directed by a metronomic beep that would sound once per second. The subject would move pitch-down or pitch-up when they heard the tone. Hearing the announcement "Feet down, coming out", the subjects would sit upright with their heads still while closing their eyes until the next microgravity portion. Once the announcement was made, the operator would ask the subjects to report any symptoms they were experiencing. The subjects would verbally report their symptoms to the operator and the operator would add up the total motion sickness score. The test was terminated either when the subject reached a Miller-Graybiel score of eight (moderate malaise) or when the subject asked to stop.

RESULTS

One of the subjects became moderately motion sick, and this was believed to be caused by minuscule head movements during the 2g portions of the parabolas, and not as a result of the body movements during the microgravity portions. Head movements during hyper-g can generate motion-sickness symptoms that cannot be prevented by strobe goggles. However, we found that when the subject lay supine on the floor with nose pointing to the ceiling during the 2g portions to eliminate all possible head movements, the subject's motion sickness symptoms would subside. Therefore, it may be desirable to have the subjects lie on the floor of the plane in the supine position during the 2g portions of the parabolas instead of sitting upright in the seat. Then, during the microgravity portions, the subjects would begin the en bloc head and torso movements from the supine to upright seated position on the floor. This would ensure that the subject's head is stabilized during 2g. Since our experimental protocol was fashioned after the

study performed in 1984 by Lackner and Graybiel on the KC-135, we will keep the current upright seating configuration for the remainder of the study.

One of the goggles did not work properly, but we realized afterward that we were using a depleted 9V battery. The goggles were then tested on the ground and they worked properly. Also, the subjects reported that the goggles developed condensation during the body movements. To correct this, the subjects were instructed to apply anti-fog wipes to the lenses during the breaks between parabolas, which alleviated the problem.

There were no technical problems associated with the audio hardware. However, it was noticed that the operator's voice could be heard clearly by the subject even if the operator is speaking with the microphone turned off. That discovery might eliminate the need for the operator to wear the audio headset.

DISCUSSION

The motion sickness that resulted from the 2g portions of the parabolas in the one subject has led to the future implementation of neck braces to serve as head restraints. These goggles are not intended to inhibit or prevent coriolis force induced motion sickness and the neck braces should eliminate most of those forces. This will result in a more accurate depiction of the ability of the goggles to prevent motion sickness.

Also, because the subjects were able to hear the operators clearly even when the microphone was turned off, the operator's microphone was not played through the headsets, although the headsets remained part of the equipment setup to allow the subjects to hear the iPod beeps as well as allow us to record the subjects' comments throughout the flight. The operators will also continue to wear the operator microphone connected to a voice recorder to record everything said during the flight.

CONCLUSION

The flights enabled us to determine the efficacy of our protocol and hardware. The protocol appears to be an effective means of assessing the success of treating microgravity-induced motion sickness with stroboscopic vision. The hardware, except for very minor issues (i.e., using an old battery in the goggles driver), proved to be robust and effective. The changes that will be made, as stated in the discussion section, are the addition of neck braces to eliminate unwanted head movements and the removal of some of the audio setup.

REFERENCES

Graybiel, A., Wood, C., Miller, E.F. and Cramer, D.B. Diagnostic criteria for grading the severity of acute motion sickness. *Aerospace medicine*. 39,453-455, 1968.

PHOTOGRAPHS

JSC2005E41522
JSC2005E41554
JSC2005E41556 to JSC2005E4158
JSC2005E41563 to JSC2005E4165
JSC2005E41568
JSC2005E41572 to JSC2005E41574
JSC2005E41612
JSC2005E41637
JSC2005E41655 to JSC2005E41660
JSC2005E41687 to JSC2005E4189
JSC2005E4190 to JSC2005E4196

VIDEO

None

CONTACT INFORMATION

Millard F. Reschke, Ph.D.
Human Adaptation and Countermeasures Office
Johnson Space Center
Houston, Texas 77058
Tel: (281) 483-7210
FAX: (281) 244-5734
Email: millard.f.reschke@nasa.gov

Jeffrey T. Somers, M.S.
Wyle Laboratories, Inc.,
Life Sciences Group
1290 Hercules, Suite 120
Houston, TX 77058
Tel: (281) 483-7485
FAX: (281) 244-5734
Email: jeffrey.t.somers@nasa.gov

TITLE

Experimental Microfluidic System Interfaced to Cell Culture Bags
for Real Time Analysis of Amino Acids and reGFP

FLIGHT DATES

October 13 -14, 2005

PRINCIPAL INVESTIGATORS

Steve Gonda, NASA/Johnson Space Center
Christopher Culbertson/Kansas State University

CO-INVESTIGATORS

Greg Roman, Kansas State University
Amanda Meyer, Kansas State University
Sandra Geffert, University of Houston



GOAL

The ultimate goal of this project is to integrate microfluidic devices with NASA space bioreactor systems. In such a system, the microfluidic device would provide real-time feedback control of the bioreactor by monitoring pH, glucose, and lactate levels in the cell media. It also would provide an analytical capability to the bioreactor in extraterrestrial environments for monitoring bioengineered cell products and health changes in cells due to environmental stressors. Such integrated systems could be used as biosentinels both in space and on planet surfaces.

OBJECTIVES

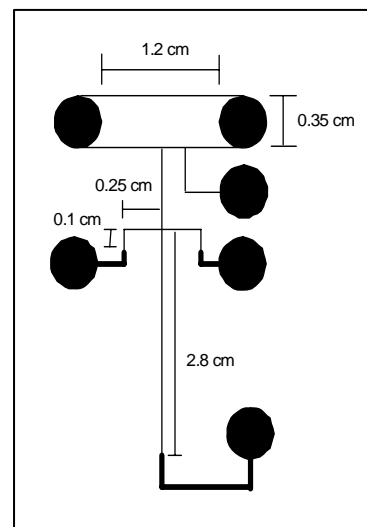
To demonstrate the ability of microfabricated devices to repeatedly and reproducibly sample microliter volumes from flight-certified cell culture bags and perform capillary electrophoretic separations in microgravity, lunar gravity, Martian gravity and hypergravity (1.8g).

METHODS AND MATERIALS

The portable microfluidic device developed for these tests was contained in a Bud box enclosure (NBA10148), which had exterior dimensions of 30 cm wide x 18 cm deep x 40 cm high. The microchips, in their custom-machined two-part polymethyl methacrylate holder, were attached to an x-y positioning plate (ST1XY-S; Thor Labs Inc.; Newton, New Jersey) and positioned above a microscope objective (CD-240-M40X; Creative Devices, Neshanic Station, New Jersey). This objective was used to focus the excitation light, a blue laser beam at 473 nm. The laser beam was reflected off a dichroic mirror (505 DRLP; Omega Optical, Brattleboro, Vermont) prior to being focused into the microchip channel by the microscope objective. The fluorescence from the labeled amino acids or the native fluorescent recombinant enhanced green fluorescent protein (reGFP) was collected by the same microscope objective, passed through the dichroic mirror, a 1.0 mm pinhole, and a 505 nm longpass filter (505ALP, Omega Optical) prior to being detected at a channel photomultiplier tube (MD972; Perkin Elmer; Fremont, California). The PMT was powered by a 5-volt power supply. The gain was manually controlled by a potentiometer which had a locking mechanism to prevent accidental change.

The high voltages used for making injections and performing the electrophoretic separations on the microchip were provided by two independent high-voltage power supplies capable of 125 mA outputs at up to 8 kV (C80; Emco High Voltage Corp.). Each high-voltage power supply was powered by a 15 V DC source. The HV output was determined by a 0-5 V DC control signal provided by a National Instruments AO card (DAQCard AO-2DC). The power supplies each occupied only 19 cm³ and weighed 51 g, making them very suitable for portable applications. The entire instrument was controlled and data was acquired using in-house written LabVIEW software run on a laptop computer.

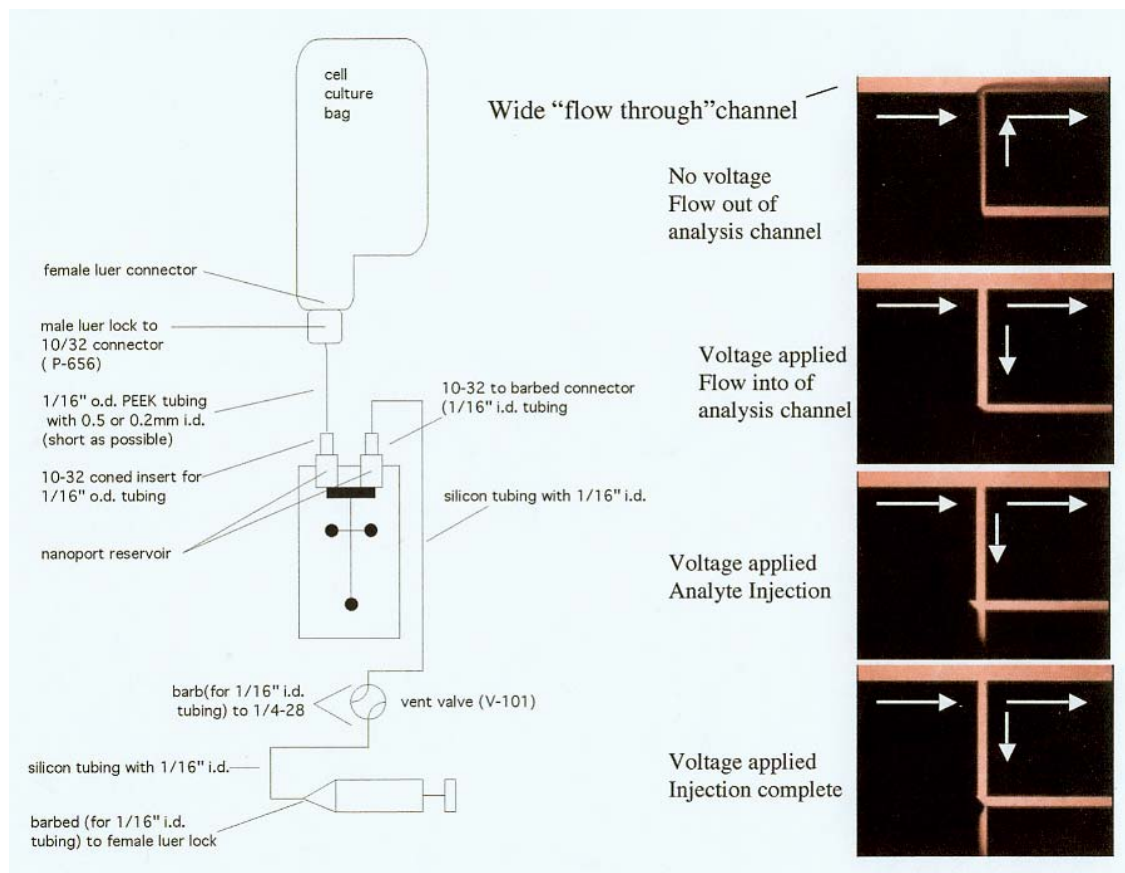
A “flow-through” channel chip was designed and is illustrated at right. This chip features a large fluidic channel, located near the top of the microchip, which offers a low fluidic resistance. This channel is etched to a depth of ~ 150 microns and a width of about 0.35 cm. The low fluidic resistance of this large channel allows for the rapid flow and movement of fluid through this channel. The flow-through channel serves as an interface between the macroscale external fluidics, which will deliver a sample from either a cell culture bag or a bioreactor and the on-chip microfluidics that are designed to perform capillary electrophoresis separations of amino acids and proteins, specifically reGFP. We used a two-step etch process to fabricate the microfluidic channels with a depth of 20 μm. This provided for a large fluidic resistance to hydrodynamic flow through the microfluidic channels so that pressure caused by the external fluidics did not significantly affect the electrophoretic separations.



The goal of this experiment was to validate the fluidic interface between the microfluidic chip and the external fluidic network including the cell culture bag. To accomplish this goal, several

different samples were placed in a series of cell culture bags. Each cell culture bag contained differences not only in the number of analytes, but also in the concentration of the analytes. The different samples in each bag would allow us to characterize the fluidic interface and the time it takes for a sample to reach the injector and allow us to use the quantitative ability of the electrophoretic separations for determining differences in concentration of amino acids and proteins.

Illustrated on the following page is a schematic of the flow-through chip connected to the external fluidics. A series of charged-coupled device (CCD) images was collected, demonstrating the combination of hydrodynamic fluid flow through the wide flow-through channel with the electrokinetic injection and separation of amino acids into the microfluidic channels. A flow rate of $\sim 250 \mu\text{L}/\text{min}$ could be achieved through the wide flow through channel. This allowed rapid real-time analysis of the contents of the cell culture bag. The time it takes for the analyte to travel from the cell culture bag to the cross injector was 1-5 min depending on the flow rate from the pump.



Sample Preparation

The following samples were mixed separately in three 10 mL cell culture bags using 10 mM sodium tetraborate at a pH of 9.3:

- 1 μM serine-FITC, 1 μM arginine-FITC and 1 μM glutamic acid-FITC
- 2 μM of serine-FITC, 2 μM arginine-FITC, 2 μM glutamic acid-FITC and 2 μM proline-FITC
- 400 nM reGFP and 500 nM reGFP

The solutions were stored at 8° C until used. A four-way valve made it possible to connect these bags in parallel with the microfluidic device. Each cell culture bag was sampled for 15 min during flight before switching to another sample.

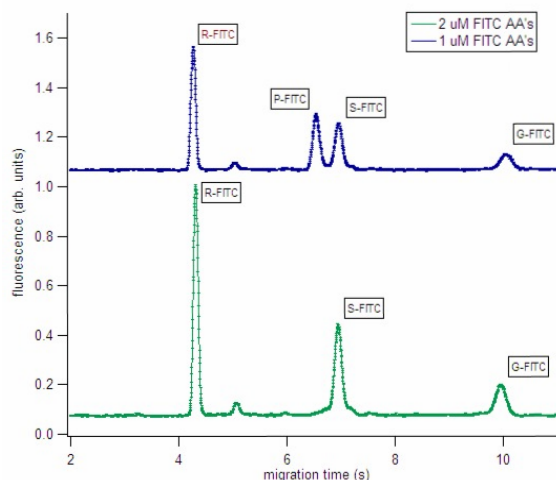
Chip Preparation and Operation

Chip preparation consisted of flushing a 50/50 (v/v) 1M NaOH/methanol solution through the channels, followed by water and then the run buffer. The electrophoretic separations were carried out in a pH 9.3, 10 mM sodium tetraborate buffer. Gated injections between 0.025 and 0.1 s were performed to introduce the sample into the separation channel. The separation distance was 2 cm and the field strength in the separation channel was ~ 1000 V/cm. Laser light scattering off the channel walls was used to align the device.

RESULTS/DISCUSSION

We demonstrated a reproducible interface between the cell culture bags and microfluidic channels of the microchip. The microchip was capable of performing rapid capillary electrophoresis separations of both FITC derivatized amino acids and reGFP in a reduced-gravity environment.

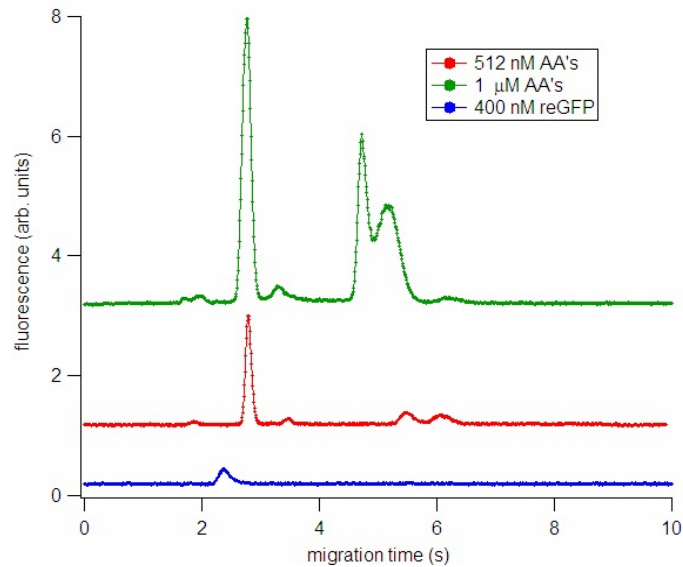
Shown below is an example of two different sample bags being separated on the flow-through chip in 0g. The first sample contained two μM of the FITC-derivatized amino acids arginine, serine and glutamic acid. The second sample contained 1 μM of the FITC-derivatized amino acids arginine, proline, serine and glutamic acid. The time it takes for the sample to move from the cell culture bag to the cross injector on the microchip was approximately 3 min. The peak area of each lower concentration analyte was decreased by 50 percent. A few good characteristics for this separation include the constant baseline, reproducible migration times and high efficiencies.



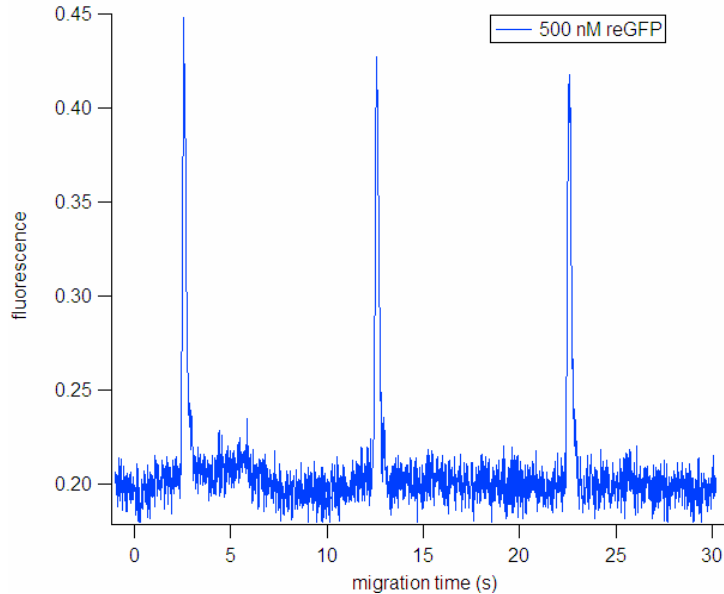
In addition to separating amino acids, we have also examined the separation of both amino acids and reGFP using the flow-through chips. Shown below is a series of solutions containing

- 1 μM FITC-derivatized amino acids
- 512 nM FITC-derivatized amino acids
- 400 nM reGFP

All solutions were dissolved in 10 mM sodium borate. We were able to move the sample from the cell culture bags to the microfluidic chip in less than 1 min using 500 $\mu\text{L}/\text{min}$ flow rates in the flow-through channel. The fast flow-rate sampling caused a few peaks to broaden, but continued to allow the separation of a series of amino acids and reGFP at reduced and hyper gravities. The top electropherogram shows arginine, proline and serine peaks in order from left to right. The middle electropherogram shows a reduced concentration of the same amino acids that were present in the top electropherogram. Finally, the bottom electropherogram shows the reGFP peak. Again, each electropherogram represents a different sample bag connected to the chip in parallel.



Below is a series of injections of reGFP from a cell culture bag containing 500 nM reGFP dissolved in sodium tetraborate. These three injections were performed in a 0g environment produced by flying 1 parabola of 25 seconds. The approximate migration time of the reGFP was 2.5 s.



CONCLUSION

We have demonstrated a microchip capable of performing rapid sampling of microliter volumes that are subsequently separated and quantified using capillary electrophoresis in reduced- and hyper-gravity environments. The results have validated our delivery method between the external fluidics and the on-chip microfluidics. The optimal flow rate through the flow-through channel was $\sim 250 \mu\text{L}/\text{min}$. Using the device we have developed thus far we are ready to perform separations of reGFP secreted in to cell media in a cell culture bag and electrophoretically migrate it to a cross injector for separation and quantification.

PHOTOGRAPHS

JSC2005E41522
JSC2005E41544 to JSC2005E41546
JSC2005E41548 to JSC2005E41549
JSC2005E41567
JSC2005E41612
JSC2005E41648 to JSC2005E41649
JSC2005E4153 to JSC2005E41654
JSC2005E41675

VIDEO

None

CONTACT INFORMATION

Dr. Christopher Culbertson
e-mail: culbert@ksu.edu

TITLE

Endotracheal Tube Suction Capability Test
for the International Space Station

FLIGHT DATE

October 13, 2005

PRINCIPAL INVESTIGATORS

Bonnie Paul, Wyle Laboratories, Inc., Life Sciences Group
Jimmy Wu, Wyle Laboratories, Inc., Life Sciences Group
Shannon Melton, Wyle Laboratories, Inc., Life Sciences Group



GOAL

To demonstrate that current inventory on the station may be used to provide emergency endotracheal tube suctioning

OBJECTIVES

1. Demonstrate emergency endotracheal tube (ETT) suction capability on station using the large syringe inventory (35 mL and Toomey syringe) and 10 Fr ETT suction catheter that are currently in the station medical kits.
2. Demonstrate emergency ETT suction capability on station using currently flown large syringe inventory (35 mL and Toomey syringe) and the 14 Fr ETT suction catheter that has been approved for station use.
3. Photo-document capabilities.

4. Provide evidence-based recommendation for best emergency ETT suction setup for current station medical operations using inventory already approved for flight.

INTRODUCTION

The ISS Health Maintenance System (HMS) Medical Kit includes a means of establishing an airway using an intubating laryngeal mask airway (ILMA) and endotracheal tube (ETT). It also includes a 10 Fr ETT suction catheter. The station suction device is equipped with a tonsil tip suction catheter for superficial oral suctioning. The ETT suction catheter is not compatible with this device. A 70 mL Toomey syringe and a 35 mL syringe tip syringe are available in the HMS kit and are compatible with the ETT suction catheter. In October 2004, a ground based study was performed using the 70 mL Toomey syringe and both the 10 Fr and 14 Fr Kendall ETT suction catheters. The 14 Fr catheter outperformed the 10 Fr catheter and the recommendation for change was made to engineering. The 35 mL syringe is part of the ILMA kit and was added to the test design after the ground-based study was complete. A microgravity study was designed to test the use of a 10 Fr and 14 Fr ETT suction catheter with the 70mL and 35mL syringes.

METHODS

Ultrasound gel thinned with water was used as a sputum substitute and added to a one-pint Rubbermaid container. The container was attached to the inside of a plastic tub using Velcro. The tub was then secured to the crew medical restraint system (CMRS) (Figure 1). Green dye was added to the gel for recording purposes.



Figure 1.

The ILMA ETT was placed into the ultrasound gel to simulate the diameter and length required of the suction catheter. The suction catheters were taped at the appropriate insertion length for ease of handling in flight. For sterility purposes they will not be taped on station. A second

plastic tub containing a similar Rubbermaid container filled with water was used for cleaning between catheter uses.

We began our suction parabolas using the 35 mL syringe and 10 Fr ETT suction catheter to mimic the current station inventory using what we felt would be the best syringe. A fair amount (check video for quantity) was suctioned within the microgravity parabola timeframe.

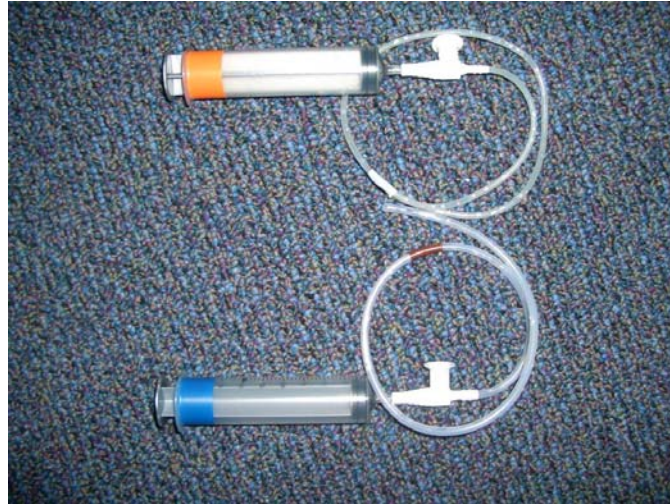


Figure 2.

Figure 2 illustrates the suction configuration using the 35 mL syringe with 10 Fr catheter (top) and 14 Fr catheter (bottom). The juncture between the syringe and catheter was secure, with no separation during use. It was easy to maintain suction using a finger over the suction catheter hole.

We then switched to the Toomey syringe configuration, again using both the 10 Fr and 14 Fr catheters. The juncture between the four parts was variable and often fell apart. We tried to tape all of the junctures, which kept the pieces together, but this led to leaks in the system and inefficient suction.



Figure 3. Toomey syringe with 14Fr ETT catheter, untaped



Figure 4. Toomey syringe with 14F catheter, taped junctures

RESULTS/DISCUSSION

The 70mL Toomey syringe and 35mL ILMA syringe are both currently onboard the station. Of the two syringes, the 35 mL ILMA syringe outperforms the 70 mL Toomey syringe significantly due to its two-part construction vs. four-part construction, with its only juncture being between the syringe and the catheter. The 35 mL volume should not be a concern, and steps will be added to the procedure for emptying the syringe between suction runs to maximize volume.

The 14 Fr ETT suction catheter is not manifested on the ISS; however, it has been approved for flight through the EHS/HMS SPRT for addition into the kit and is superior to the 10 Fr ETT suction catheter in performance.

We recommend that the ideal temporary emergency ETT suction setup would consist of the 35 mL syringe and 14 Fr ETT suction catheter. We recommend that the 14 Fr ETT suction catheter be manifested on the next available flight. The 10 Fr ETT suction catheter may be used in the event of an emergency prior to the addition of the 14 Fr ETT suction catheter.

As a final note, this should not be considered a final solution in ETT suctioning. Syringe suction is appropriate as an emergency stop-gap for transports and our current ISS operations. However, if airway management continues to be part of our operations, a method of continuous suction needs to be developed to allow for definitive airway management and sterile technique, especially for a long-duration mission where return is not feasible and the risk of secondary infection is high.

FUTURE PLANS

1. A procedure for ETT suctioning needs to be developed incorporating the use of the 35 mL syringe. (See Appendix A)
2. Present findings to the flight surgeons and HMS system problem resolution team.
3. The ILMA cue card should be modified to include a statement to re-stow the syringe after use, or place it in a Ziploc bag with sterile gauze and the ETT suction catheter and tape it to the head of the CMRS once the ILMA has been placed.

PHOTOGRAPHS

JSC2005E41522

JSC2005E41612

JSC2005E41639 to JSC2005E41647

JSC2005E41663 to JSC2005E41673

JSC2005E41678 to JSC2005E41681

JSC2005E41684 to JSC2005E41686

VIDEO

None

CONTACT INFORMATION

Bonnie Paul, RN, BSN

Wyle Laboratories, Inc., Life Sciences Group

1290 Hercules Suite 120

Houston, Texas 77058

(281) 212-1354

BPaul@wylehou.com

TITLE

Medical Operations Familiarization Flight

FLIGHT DATES

October 14, 2005

PRINCIPAL INVESTIGATOR

Jessica Hughlett, Wyle Laboratories, Inc., Life Sciences Group

CO-INVESTIGATORS

Corinne Williams, Wyle Laboratories, Inc., Life Sciences Group

Brent Temple, Wyle Laboratories, Inc., Life Sciences Group

Chris Van Velson, Wyle Laboratories, Inc., Life Sciences Group

David Rubin, Wyle Laboratories, Inc., Life Sciences Group



OBJECTIVES

Familiarize medical operations personnel with the effects of microgravity on medical equipment and procedures, as well as the required process of conducting a C-9 and other microgravity simulations flight. This will give medical operations personnel a better insight into conditions the crew is required to work under for nominal and off-nominal medical operations procedures.

METHODS AND MATERIALS

Three stations were set up

1. Intubation – this involved the use of an intubation mannequin, along with the proper tools (intubating laryngeal mask airway (ILMA), endotracheal tube, laryngoscope, syringe, lubrication, and Ambu bag). We were positioned at the top of the head of the “supine”

mannequin and we practiced intubation using both the ILMA and laryngoscope to insert a breathing tube.

2. IV – this involved the use of a Teflon catheter, IV bag, syringes, etc. This procedure involved inserting the Teflon catheter into a mannequin arm.
3. CPR – this involved the use of the crew medical restraint system (CMRS) and a CPR mannequin. CPR was performed by sitting on the side of the mannequin, straddling the mannequin, and taking an inverted position with feet pushing off the ceiling of the plane.

The procedures utilized during the flight are published in the International Space Station Integrated Medical Group (IMG) Medical Checklist, JSC-48522.

All personnel flying were trained on these procedures prior to flight.

RESULTS

All three stations were successfully completed. The Intubation Station was performed first. This required multiple attempts, as adaptation to parabolic flight had not occurred. Both methods seemed to be approximately equal in difficulty in microgravity. While performing CPR, it became evident that there is a significant difference in the ease and efficacy of the three methods. The one performed with the greatest ease is the inverted method, currently preferred on-orbit. The IV station was the last performed, and the IV was successfully placed.

All procedures took more time to complete than on the ground. It was also more difficult to keep track of all supplies than expected. Learning techniques for proper restraint of both materials and personnel was a key component to performing the procedures.

DISCUSSION

This familiarization flight will be extremely beneficial in supporting the crew and console operations. A greater understanding and appreciation of the difficulties the crew faces due to their environment was gained. This experience will provide a better ability to walk the crew through any procedure, not just the ones performed during the flight. Learning first-hand the difficulties involved in operating in the microgravity environment will be an extremely valuable tool for flight controllers and instructors.

CONCLUSION

The familiarization flight experience will be a very beneficial knowledge base for working with the crew. The flight really gave a deeper appreciation of this fact. As flight controllers/instructors, we need to have constant awareness of the conditions the crew is under. Performing these highly critical medical activities is difficult enough, but if the ground support can't fully understand the activities from the viewpoint of a floating crewmember there will be a gap in the basic understanding of the procedure. It also demonstrated that the procedures, as written, could be successfully performed on orbit. This was a successful flight for Medical Operations.

PHOTOGRAPHS

JSC2005E41522
JSC2005E41539 to JSC2005E41541
JSC2005E41553
JSC2005E41555
JSC2005E41559 to JSC2005E41562
JSC2005E41566
JSC2005E41569 to JSC2005E41571
JSC2005E41575
JSC2005E41577
JSC2005E41581 to JSC2005E41583

VIDEO

None

CONTACT INFORMATION

Ms. Jessica Hughlett
Wyle Laboratories, Inc., Life Sciences Group
1290 Hercules Suite 120
Houston, TX 77058
(281) 212-1283
jessica.l.hughlett@nasa.gov

TITLE

Preliminary Report of Reduced Gravity Tests of the Magnetic Field

FLIGHT DATES

February 7 and 9-11, 2006

PRINCIPAL INVESTIGATOR

Karl H. Hasenstein, University of Louisiana at Lafayette

CO-INVESTIGATORS

Susan Mopper, University of Louisiana at Lafayette

Dan Povinelli, University of Louisiana at Lafayette

Peter Scherp, University of Louisiana at Lafayette

Joseph Benjamin, Bionetics Inc., Kennedy Space Center



OBJECTIVE

The objective of the investigation was to assess the effectiveness of high gradient magnetic fields (HGMF) on the displacement of starch grains during periods of weightlessness.

METHODS AND MATERIALS

Schedule

Each day, 40 (4×10) parabolas were flown. The total of 160 parabolas resulted in a robust data set that was analyzed after returning to the laboratory. The analysis is still going on as of the writing of this report (4/20/2006) and is expected to be completed by fall 2006.

Design

A magnetic system consisting of two NdFeB magnets ($50 \times 50 \times 12$ mm) was assembled around a plastic spacer that accommodates wedges of different shape (Figure 1) and a cuvette with three different types of starch (corn, wheat, and potato). A video microscope was constructed to observe the displacement of starch grains as a function of distance and shape of the magnetic wedge and the type of starch (Figures 2 & 4).

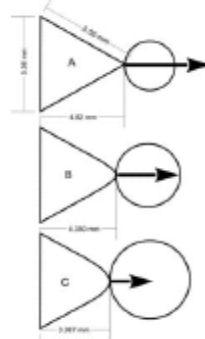


Figure 1: Wedge design to generate a high-gradient magnetic field. The base dimensions of the wedges were identical to the original design (A) used in the experiment on STS-107, but the height and roundness differed to reduce the magnetic force (arrows) but increase the effective area (circles).

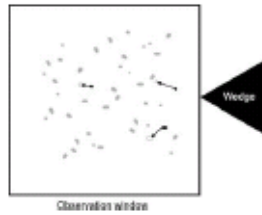


Figure 2: Path of magnetic particles suspended in water. The arrows indicate the direction and velocity of movements during the weightlessness period. The path is not measurable under regular 1g conditions, because the magnetic force would be reduced to a pulse that depends on the rate of sedimentation.



Figure 3: Assembly of the hardware on the floor of the C-9 plane as secured during take-off and landing.

RESULTS/DISCUSSION

The design of the apparatus allowed continuous recording of the relative movement of starch grains during the parabolic flights. Although some opportunities were missed because of lighting conditions and poorly suspended grains, the overall data set clearly shows that

- 1) The high-gradient magnetic field did repel starch grains
- 2) The extent of displacement was a function of wedge shape
- 3) The displacement was a function of the starch type
- 4) The velocity of displacement was a function of wedge and starch type

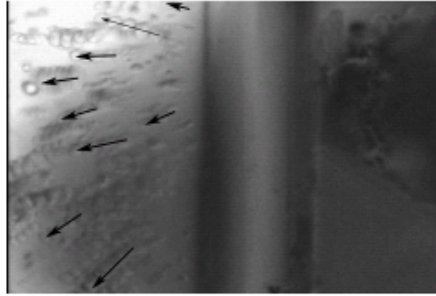


Figure 4. Superimposed image sequence shows the displacement of particles in five one-second intervals. The arrows indicate the movement of each particle over time. It is obvious that the particles moved different distances. The arrows emanate from the tip of the wedge (dark silhouette on the right). The dependence of the movement on the distance between wedge and particle and the size of the particle will be analyzed by a motion analysis system. The combined total of more than 120 data files will provide a robust analysis of the effective force field. The test was an extension of the ill-fated flight experiment on the Space Shuttle *Columbia* (STS-107) and was necessary to verify if, in the absence of gravity, a mechanical (ponderomotive) displacement of starch-filled organelles (amyloplasts) effected a stronger than expected curvature in the shuttle experiment. The video data that were down-linked from STS-107 represented the only basis for the hypothesis that the implied curvature resulted from stronger than expected influence of the HGMF. The reduced-gravity flight supported that scenario as correct. Although of short duration, the weightlessness on the C-9 allowed us to examine our original concept and was sufficient to isolate the HGMF effect. Despite the incomplete analysis, the data indicate that the HGMF effect on biological systems in weightlessness (microgravity) is stronger than initially assumed.

PHOTOGRAPHS

JSC2006e03060

JSC2006e03093 to JSC2006e03099

JSC2006e03512 to JSC2006e03523

JSC2006e03639 to JSC2006e03656

VIDEO

- Zero G Science Feb. 7 - 9, 2006 week, Master: 720859

Videos available from Imagery and Publications Office (GS4), NASA/JSC.

CONTACT INFORMATION

Karl Hasenstein, Ph.D

University of Louisiana at Lafayette/Biology Dept

300 East St Mary Blvd.

Lafayette, LA 70503

Hasenstein@louisiana.edu

TITLE

TAGES – Transgenic Gene Expression System

FLIGHT DATES

April 7-10, 2006

PRINCIPAL INVESTIGATOR

Robert Ferl, University of Florida

CO-PRINCIPAL INVESTIGATORS

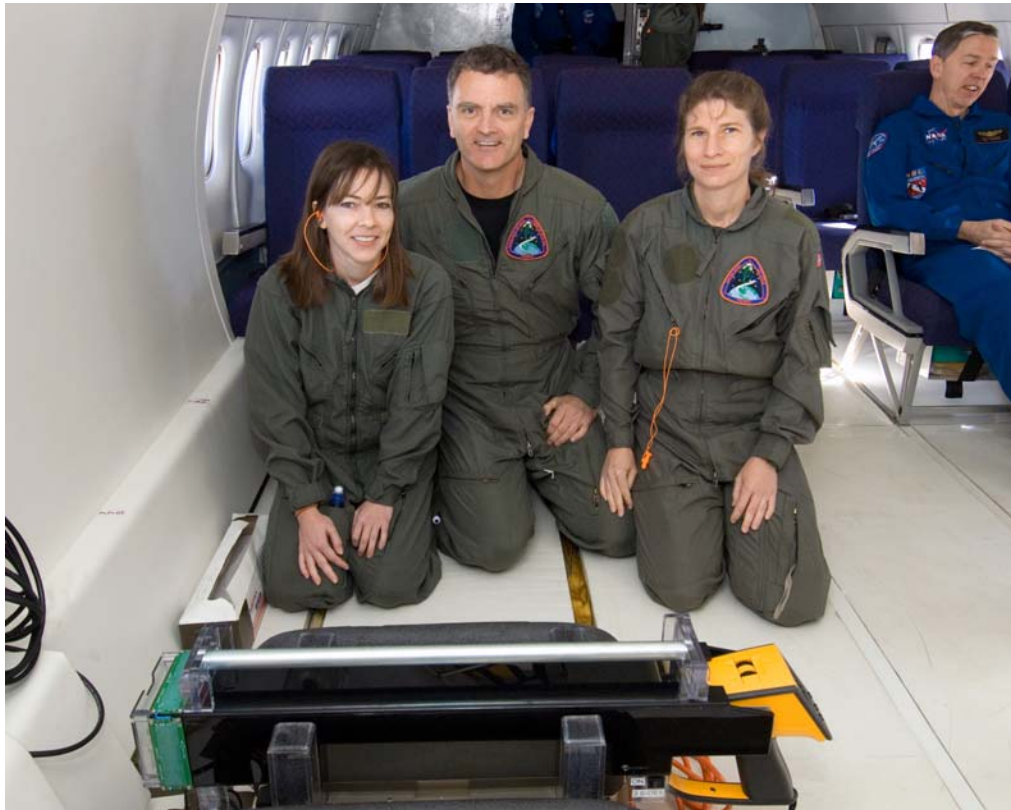
Anna-Lisa Paul, University of Florida

Kelly Norwood, Bionetics Inc., Kennedy Space Center

Meghan Kruger, Bionetics Inc., Kennedy Space Center

Matt Regan, Bionetics Inc., Kennedy Space Center

Richard Meshberger, Bionetics Inc., Kennedy Space Center



GOAL

To test plant biological samples for reaction to altered-gravity environments at the level of gene expression and to monitor the distribution of surface temperature in plant leaves in altered gravity environments. Transgenic plants engineered with gene reporters designed to respond to specific types of abiotic environments were used to report stress induced by parabolic flight. GUS gene reporters provided tissue-specific data, and GFP reporters were used to provide tissue

for subsequent molecular analyses, and for real-time thermal imaging to monitor temperature distribution in leaves during parabolas.

OBJECTIVES

The first objective is to determine the extent of thermal variation on the surface of Arabidopsis leaves during parabolic flight. There is recent evidence that a microgravity environment may influence changes in leaf surface temperatures that are not seen in similar 1g environments. Kitaya et al. (2003) demonstrated that in a 20-second period of milligravity provided during parabolic flight, the surface temperature of a sweet potato leaf could vary by almost 2°C. It is our goal to utilize thermal imaging technologies to monitor Arabidopsis plants through a series of parabolic flights. Data will be collected in the form of digital images collected with a Fluke Thermal Imager. In addition, plants engineered with gene reporters designed to respond to heat stress will be used to gather tissue-specific gene expression data (HSF18/GUS). The second goal is to further develop the genome level; genetic analyses were initiated with the April 2003 KC-135 experiments. The results from the April 2003 data indicate that numerous genes associated with auxin metabolism are up-regulated in response to parabolic flight (22,000-gene array chips from Affymetrix). Several of these genes have been implicated in gravity sensing. The genetic analyses in the current C-9 flight will further dissect the role of auxin metabolism as related to parabolic flight stress. These experiments also have the potential to address the environmental differences between the C-9 and KC-135 aircraft; even subtle differences between the internal environments may be reflected in different patterns of gene expression in the experimental plants. The third goal is to use plants engineered with gene reporters designed to respond to variations in temperature and stress metabolism to gather tissue-specific gene expression data. These experiments are set to repeat previous observations of flight-induced Adh/GUS expression in shoots, and to extend those observations by including three new stress gene reporters: TCH4/GUS, GSH2/GUS and HSP18/GUS. Environmental parameters such as temperature and atmospheric pressure were monitored with HOBO data loggers for correlation with patterns in gene expression.

INTRODUCTION

The TAGES (Transgenic Arabidopsis Gene Expression System) project seeks to make a contribution to our understanding of stress imposed by the spaceflight environment on plants. This environment may affect the ability of plants to process critical biological signals, such that the perception of certain signals may be inappropriately processed into a stress response. Central to the TAGES are genetically engineered plants that serve as monitors and reporters of their environment. Transgenic Arabidopsis engineered with the Adh/GUS transgene flew on STS-93 and revealed that the spaceflight environment disrupted an aspect of calcium-mediated signal transduction. The current TAGES experiment utilizes a gene reporter that can be visualized non-destructively (green fluorescent protein - GFP). GFP fluoresces green when illuminated with 470 nm blue light, thus any tissues in which GFP is being expressed can be identified in vivo with the proper combination of illumination and camera filters. Plants engineered with the GFP reporter facilitate telemetric data collection, and represent a significant savings of crew time for flight experiments. Previous studies have indicated that KC-135 flights induce interesting patterns of stress gene activation. The current experiments were designed to extend those observations with additional gene reporter systems (TCH4/GUS, GSH2/GUS and HSP18/GUS) to evaluate thermal imaging hardware, and to replicate and extend the gene expression analyses of April 2003.

METHODS AND MATERIALS

Subjects

Transgenic Arabidopsis plants of various genotypes and ages.

Instruments

Experiment 1 and Experiment 2 (experiment numbers refer to designations in the TAGES C-9 parabolic flight plan document of March 2006) – Harvesting and staining kits consisted of forceps and 13 ml conical tubes pre-filled with either x-gluc stain or RNA later. Experiment 3 – Fluke Ti30 thermal imager, the hardware designed to create a focal-length tube of lighted dead air space, plus a supporting computer connected to an accelerometer and HOBO data loggers to monitor temperature and cabin air pressure.

Procedure

Experiment 1 and Experiment 2 – During the 1g turn periods, plants were harvested from the appropriate plates with forceps and placed into stain/fix tubes. Experiment 3 – Thermal imaging was conducted throughout the flight, both in a free-floating configuration and held stationary in a cradle anchored to the floor. In addition, we tested the effects of lighting, dead air space and free-floating techniques during the data collection periods.

RESULTS

The data collection portion of the experiment went flawlessly. Samples from Experiments 1 and 2 were collected, stored and transported back to UF without incident to await biochemical analyses. The thermal imaging of Experiment 3 was also successful and occasionally exceeded our expectations. The data clearly show that leaves are less able to dissipate heat during periods of reduced gravity. The differences between 0g and 2g were observed to be as much as 2 degrees Celsius.

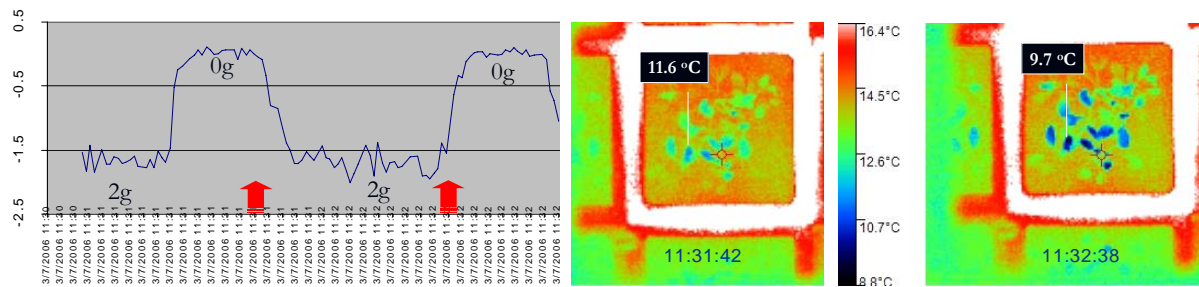


Figure 1 – An accelerometer tracing (left) is annotated with times during the flight and the approximate G forces. The arrows indicate the points at which the thermal images (right) were collected. The thermal images are annotated with the time stamp and a temperature reading for an individual leaf.

CONCLUSION

Data from previous KC-135 experiments suggest that parabolic flights do indeed alter gene expression patterns, with genes associated with auxin metabolism prominently featured. The experiments conducted with the current C-9 flights will replicate the initial experiment and address issues that might arise from environmental factors associated with the two aircraft. One significant difference between the KC-135 and the C-9 is related to internal cabin pressures.

While the KC-135 exhibits wide parabolic-associated variations in pressure (3 kPa), the C-9 was very stable with variations of only 0.4 kPa. The thermal imaging data supports the concept that convective cooling has a large impact of the surface temperature of leaves. These data will contribute to our understanding of seemingly heat-related stress responses of plants during spaceflight when the cabin and growth chamber temperature readings suggest that the environment is well below a heat-stress threshold.

PHOTOGRAPHS

JSC2006EO6737 to JSC2006EO6750
JSC2006EO6932 to JSC2006EO6933
JSC2006EO6934 to JSC2006EO6943
JSC2006EO7186 to JSC2006EO7216
JSC2006EO7999 to JSC2006EO8020

VIDEO

- Zero G March 6 - 10, 2006, Master: 720751

Videos available from Imagery and Publications Office (GS4), NASA/JSC.

CONTACT INFORMATION

Robert Ferl, Ph.D.
Biotechnology and Horticultural Sciences
University of Florida
Gainesville, FL 32611-0690

TITLE

Undergraduate Program Flights - Effect of Microgravity on Semicircular Canal and Vestibular Function

FLIGHT DATES

March 7-8, 2006

PRINCIPAL INVESTIGATORS

William Bishop, Johns Hopkins University

Ondrej Juhasz, Johns Hopkins University

Anthony Ngo, Johns Hopkins University

Ravi Pathak, Johns Hopkins University



INTRODUCTION

The main purpose of flying our experiment on the C-9 was to verify that a 0g environment does not affect the vestibular system, specifically the semicircular canals. The vestibulo-ocular reflex (VOR) allows humans to maintain their visual focus while shaking their head back and forth. It has not been absolutely verified whether the semicircular canals are the main cause of the VOR or if some part of the brain corrects for the movement of the head. With our experiment, we hoped to provide further evidence that the semicircular canals are the main cause of the VOR.

The semicircular canals are located in the inner ear. They serve to sense rotational accelerations of the head. The canals are filled with a fluid called endolymph, and upon acceleration of the head, the momentum of the fluid displaces the cupola, which has the same density as the

endolymph. The cupola is a membrane that spans the canal, and is attached to hair cells at one end. The hair cells sense the deformation of the cupola and send signals to the head indicating acceleration. Our plan was to build a working model of the semicircular canal and test it in a microgravity environment.

METHODS AND MATERIALS

We constructed a model of the semicircular canal using a plastic tube bent into the shape of a circle. The cupola was modeled by encasing the same fluid as is used in the canal between two thin plastic/rubber sheets to maintain the same specific gravity. The fluid we used to model the endolymph was a pure silicone fluid called polydimethylsiloxane.

To encase the apparatus, we constructed a rectangular box out of Lexan, and to prevent any possible fluid leaks in the case, we sealed all junctions with rubber. We also placed Styrofoam padding around the outside edges of the box for safety purposes.

For the purposes of data acquisition, we used the following equipment: an accelerometer, a rate sensor, a data acquisition attachment (Datastick DAS-1294), a Palm Pilot, and a video camcorder. The accelerometer and rate sensor were each input to a channel on the Datastick. The Datastick was then attached to the Palm Pilot, which we used to collect and store all the data received from the accelerometer and rate sensor. We then placed the video camcorder inside our Lexan box and positioned it so that it took footage of our cupola (the thin rubber sheet inside the tube). In order to analyze our data effectively, we synchronized the readings taken from the accelerometer and rate sensor with the footage of the deflecting cupola.



Figure 1.a. General view of our model with all components attached.

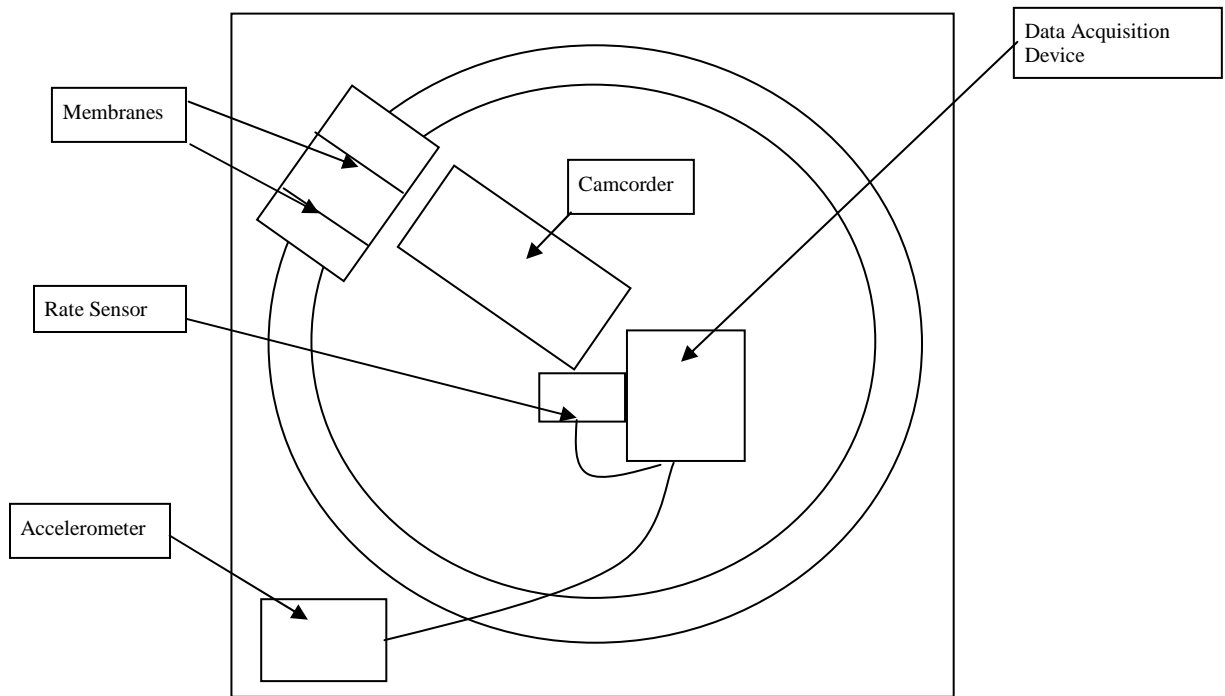


Figure 1.b. Component view of our model

To perform our experiment, the two flyers held the container on opposite sides. In 0g, the two flyers together exerted rotational forces in the horizontal plane of the container. We tried to exert a range of forces, and we repeated this method for about 25-30 parabolas.

In our original plan for our experiment, we wanted to take three sets of data: one at 0g, one at 1g, and one at 1.8g. We were able to successfully collect data for the 1g environment on the ground level prior to our flight days, and we were able to collect data for 25-30 parabolas of 0g on each flight day after getting used to being in the microgravity environment. However, because we were not able to effectively maneuver in the 1.8g environment, we were not able to collect any data for that part. Still, we always viewed collecting data for 1.8g as a bonus and were satisfied with our readings for 0g and 1g.

Data analysis was performed using the MATLAB computing environment. We exported the raw video from the camcorder and using Adobe Premier, we were able to take still shots of the membrane as it was deflecting. The images were then taken into MATLAB, where we manually selected the maximum deflection. Our biggest concern was the ability to synchronize the data from the Palm Pilot to the times we had for the pictures. This proved to be challenging, but by using both the gravitational acceleration data and the rate sensor data, we feel that we matched them well.

As the fluid membranes were moved, the rate sensors picked up the varying accelerations. The mean negative deflection for 0g was -107.5 ± 13.4 pixels, with rate sensor voltages being $1.453 \pm .017$ V. The mean negative deflection for 1g was -106.2 ± 8.4 pixels, with voltages being $1.339 \pm .012$ V. The positive deflections were 131.3 ± 21.1 pixels for 0g and 136.6 ± 28.6 pixels for 1g. The voltages were $1.598 \pm .041$ V for 0g and $1.435 \pm .044$ V for 1g. Negative deflections were measured when the membrane moved leftward on the picture and positive deflections moved the membrane to the right.

We also attempted to use water as another fluid to simulate semicircular canal deficiency. This data, however, proved to be too erratic, and our experimental setup proved ill equipped to measure the deflections. We would have had to sample at a much higher frequency to have been able to collect any good water data.

DISCUSSION

The semicircular canals are responsible for sensing rotational acceleration of the head. When a rotational acceleration takes place, the inertia of the endolymph causes a deflection in the cupola. We hypothesized that the semicircular canals would behave identically regardless of the gravity environment they were placed in. Data were collected both in 0g and in 1g.

During one of our flight days the semicircular canal was filled with water while the cupola was filled with a high-viscosity fluid. This was done to model how the canals would react to a deficiency, such as alcohol impairment, in different gravity environments. Unfortunately, the data for this flight were poor. The membrane that modeled the cupola deflected back and forth in response to minuscule forces. It is our belief that this occurred due to the fact that there was a considerable difference in the viscosity of the two fluids. Perhaps if we had chosen another liquid instead of water that had a higher viscosity, our data would have been better.

During the other flight day the entire model was filled with the same high-density fluid. This was done to model the semicircular canal of a normal person in different gravity environments. This setup provided us with much better data. As we had hypothesized, the canals acted as if they were gravity insensitive. Even though there was some variability in the data when the same force was applied in either 0g or 1g, the cupola deflected approximately the same amount.

One oversight that occurred in this experiment was that the camera was set up to record at 30 Hz while our data acquisition device was set up to record at 4 Hz. This made matching some of the data a little difficult. However, this experiment still provided us with good and reliable data. Our results have provided us with some evidence that the reason phenomena such as the vestibular ocular reflex are preserved in space is that the semicircular canals are in fact gravity insensitive.

PHOTOGRAPHS

JSC2006EO6807 to JSC2006EO6808

JSC2006EO6817 to JSC2006EO6818

JSC2006EO6823

JSC2006EO6882

JSC2006EO6894 to JSC2006EO6898

VIDEO

- Zero G March 6 - 10, 2006, Master: 720751

Videos available from Imagery and Publications Office (GS4), NASA/JSC.

CONTACT INFORMATION

Ondrej Juhasz, Johns Hopkins University
Johns Hopkins University
3400 North Charles Street
Baltimore, MD 21218
ojuhasz2@gmail.com

TITLE

Undergraduate Program Flights - Rehydration of Artificial Blood Polymers in Microgravity

FLIGHT DATES

March 7-8, 2006

PRINCIPAL INVESTIGATOR

David Gillikin, North Carolina State University

CO-INVESTIGATORS

Chris Page, North Carolina State University

Chris Thomas, North Carolina State University

Christine Watson, North Carolina State University



GOAL

The goal of this experiment was to enhance the availability of medications in 0g by determining an effective means of quickly hydrating bio-polymers. Whether on deployment to an orbiting space station or on a future mission to Mars, astronauts face constant risks, including electrocution, severe burns, and even radiation. Treatments may require immediate and routine transfer of plasmas, fluids, and other medications (Blood 50). In such situations dehydrated polymersomes or micelles would need to be re-hydrated as quickly as possible without getting air into the mixture. Some of the major polymers being explored for their biological friendly nature and are polyethylene oxide block copolymers (Miller, 2006). These materials are not only stronger than biological cells but are capable of being dehydrated, which makes them ideal for bioencapsulation and long-term storage (Meng, 2005). Artificial blood products composed of

bio-polymers can take several minutes to hydrate in the presence of gravitational buoyancy. However, in space there is no buoyancy and the hydration process becomes much more difficult and much slower. Therefore an effective means of quickly hydrating bio-polymers in 0g would greatly enhance the practicality of using dehydrated medications in space. A series of tests was performed in 0g to determine if a combination of artificial gravity and vibration could enhance the hydration rate of the medical polymers.

OBJECTIVES

The objective of this experiment was to determine an effective means of hydrating bio-polymers quickly in a 0g environment. It was hypothesized that, in 0g hydration of bio-polymers would be slow without being enhanced by vibration. To test this hypothesis an experiment was performed in 0g in which various combinations of artificial gravity and vibration were induced on samples of bio-polymer and solvent to determine the most effective method of hydration. The parameters needed to determine the effectiveness of each combination were the mass of bio-polymer that dissolves in solvent, the frequency and magnitude of vibration induced, and the magnitude of the artificial gravity induced.

METHODS AND MATERIALS

Solute: Pluronic F87 Prill, manufactured by BASF

Solvent: Distilled water

A combined vibrator and centrifuging device was used with special test tubes to test whether a combination of vibration and artificial gravity could enhance hydration. Various accelerations from 0 to approximately 9g were tested. There were two vibration settings, high and low. The frequency for the high setting was 25 Hertz with an impulse magnitude of 0.247 Newtons. The frequency for the low setting was 15 Hertz with amplitude of 0.089 Newtons.

The test tubes consist of three chambers separated by a filter. See Figure 1. The filter keeps the polymer in Chamber 3 while the solvent remains in Chamber 1. During the onset of microgravity, the plug between Chamber 1 and 2 is opened. The artificial gravity induced forces the solvent into Chamber 2 where it passes through the filter into Chamber 3 to mix with the polymer. At the return of gravity, the water and any dissolved polymer in the test tube is allowed to drain out of Chamber 3 and back all the way to Chamber 1. Then the plug is resealed. The amount of polymer which dissolved can be determined either by a spectrophotometer or by taking mass measurements of the contents remaining in each chamber. The latter method was used. In this method the mass of polymer remaining in Chamber 3 was recorded as well as the mass of the hydrant and dissolved polymer in Chamber 1. To account for dissolved polymer remaining in the filter paper the new mass of the filter paper, was also recorded.

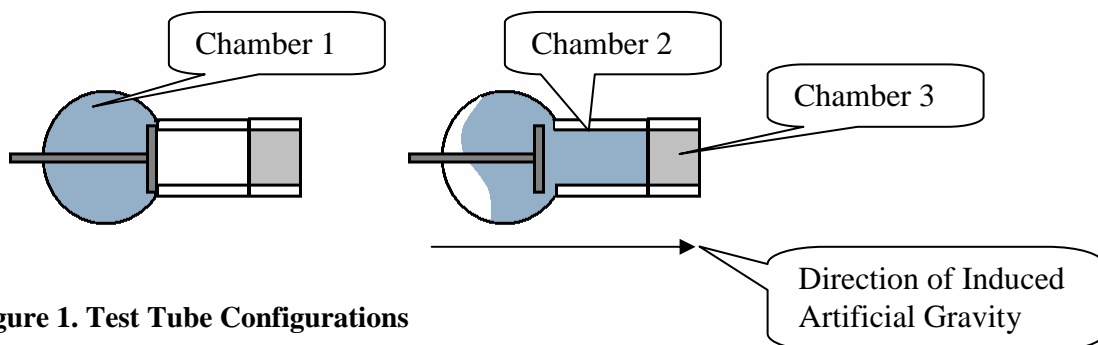


Figure 1. Test Tube Configurations

Since 5 grams of polymer were originally placed in Chamber 3, the mass of polymer remaining in Chamber 3 indicates how much polymer dissolved. The other mass measurements can be used to determine the uncertainty in the results. Any difference in the total amount of polymer and solvent present before and after the experiment is considered an error or uncertainty measurement. Since the filter paper weighs 0.005 grams and 20 grams of solvent were put into Chamber 1 initially, the total mass after the experiment should be 25.005 grams. Any change would indicate an error or uncertainty. It is likely that some decrease in mass would be due to solvent evaporation, but to be thorough any mass decrease post flight was treated as uncertainty in the amount of polymer dissolved.

RESULTS

The experimental data from Day 1 are listed in Table 1 below. The table lists the masses of polymer, solvent, and filter remaining after each trial.

Table 1. Day 1 Experimental Data

Trial #	Polymer Mass Remaining (grams)	Solvent Mass Remaining (grams)	Filter Paper Mass (grams)
1	4.989	20.000	0.015
2	4.955	20.023	0.015
3	4.966	20.014	0.017
4	4.891	20.077	0.016
5	4.939	20.037	0.022
6	4.888	20.061	0.017
7	4.935	20.040	0.026
8	4.872	20.105	0.018
9	4.844	20.126	0.011
10	4.807	20.170	0.009

The recorded control data are listed in Table 2. This includes the data collected to determine the amount of artificial gravity induced on the samples. Notice that the radius remains the same for all samples because this radius value is fixed in the centrifuging machine. The gs were calculated based on 9.81 m/s^2 acceleration for Earth's gravity.

Table 2 Day 1 Control Data

Trial #	G's	Radius (m)	Revolutions	Time (s)	Vibration Setting
1	0.000	0.100	0.000	22.820	Low
2	0.166	0.100	16.000	24.910	High
3	0.341	0.100	25.000	27.160	Low
4	0.418	0.100	19.000	18.640	High
5	0.567	0.100	24.000	20.220	Low
6	0.725	0.100	31.000	23.100	High
7	0.740	0.100	27.000	19.910	Low
8	0.821	0.100	33.000	23.100	High
9	0.905	0.100	26.000	17.340	Low
10	0.931	0.100	31.000	20.380	High

Table 3. Day 1 Calculated Data

Trial #	Polymer Hydrated (grams)	Uncertainty (grams)	Percent Uncertainty (%)
1	0.011	0.001	9.091
2	0.045	0.012	26.667
3	0.034	0.008	23.529
4	0.109	0.021	19.266
5	0.061	0.007	11.475
6	0.112	0.039	34.821
7	0.065	0.004	6.154
8	0.128	0.010	7.812
9	0.156	0.024	15.385
10	0.193	0.019	9.845

Table 3 above lists the calculated data for Day 1. These data includes the amount of polymer that was hydrated and the uncertainty in this calculation. The uncertainty was based on the decrease in mass of the sample. Any decrease in mass was treated as uncertainty in the polymer hydrated. The effect of vibration and artificial gravity on the hydration rate is depicted in Figure 2 and shows the comparison between low and high vibration.

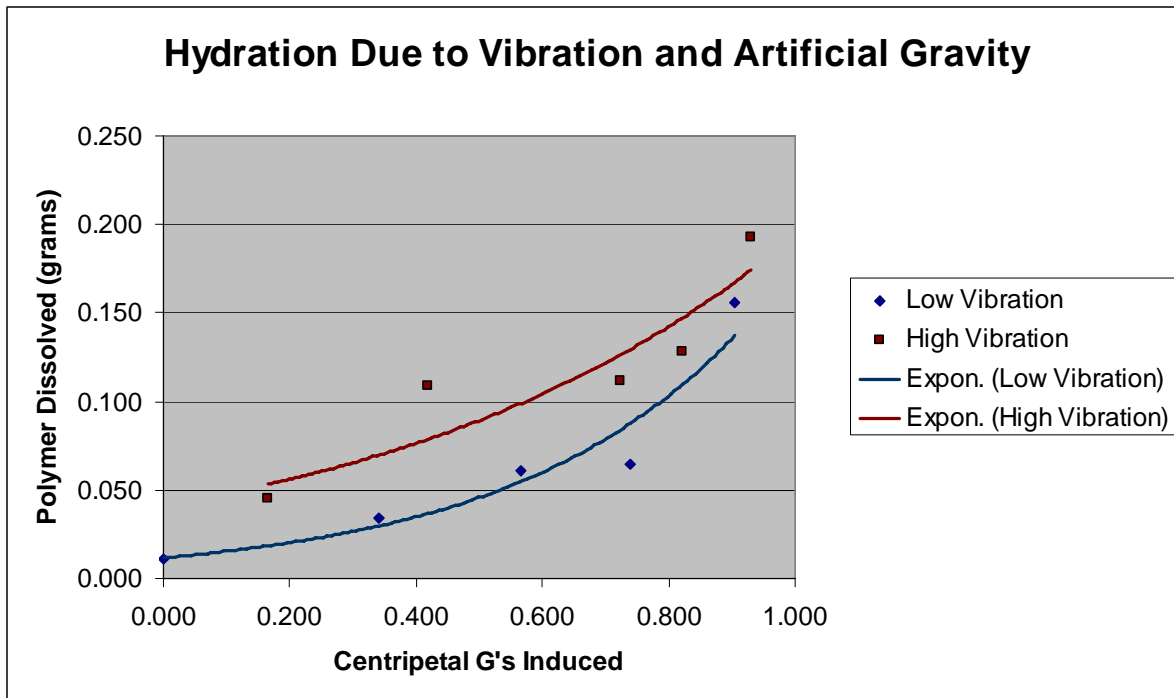


Figure 2. Day 1 Hydration Due to Vibration and Artificial Gravity

Table 4. Day 2 Experimental Data

Trial #	Polymer Mass Remaining (grams)	Solvent Mass Remaining (grams)	Filter Paper Mass (grams)
1	4.973	19.892	0.030
2	4.817	19.576	0.018
3	4.959	19.344	0.015
4	4.474	19.947	0.023
5	4.309	19.820	0.029
6	4.117	19.469	0.024
7	4.965	19.764	0.015
8	4.402	19.124	0.024
9	4.587	19.172	0.025
10	4.409	19.365	0.017

The experimental results from Day 2 are listed in Table 4 above. Notice that the polymer and solvent mass remaining is much smaller than that on day one. The control data for Day 2 are listed in Table 5. The radius is still fixed, but the revolutions and time were recorded. It is likely that these mass readings will produce high uncertainty values.

Table 5. Day 2 Control Data

Trial #	G's	Radius (m)	Revolutions	Time (s)	Vibration Setting
1	0.000	0.100	0.000	21.673	Low
2	0.018	0.100	4.000	18.841	High
3	0.028	0.100	7.000	26.322	Low
4	0.066	0.100	11.000	27.072	High
5	0.285	0.100	17.000	20.184	Low
6	0.577	0.100	25.000	20.877	High
7	0.453	0.100	21.000	19.802	Low
8	0.723	0.100	32.000	23.881	High
9	0.996	0.100	31.000	19.705	Low
10	0.905	0.100	35.000	23.339	High

Table 6. Day 2 Calculated Data

Trial #	Polymer Hydrated (grams)	Uncertainty (grams)	Percent Uncertainty (%)
1	0.027	0.110	407.407
2	0.183	0.594	324.590
3	0.041	0.687	1675.610
4	0.526	0.561	106.654
5	0.691	0.847	122.576
6	0.883	1.395	157.984
7	0.035	0.261	745.714
8	0.598	1.455	243.311
9	0.413	1.221	295.642
10	0.591	1.214	205.415

Table 6 lists the calculated data for Day 2. Note that the uncertainty percentage is well over 100% for Day 2's data. The hydrated polymer is plotted as a function of the vibration and artificial gravities induced in Figure 3. Notice that there is no apparent trend to the data and no strong relationship to the control variables.

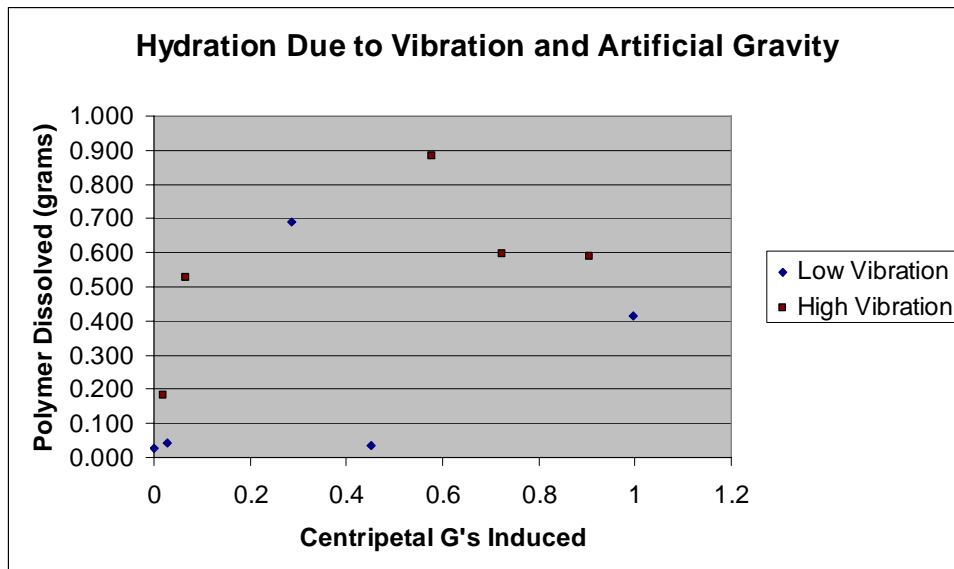


Figure 3. Day 2 Hydration Due to Vibration and Artificial Gravity

DISCUSSION

The results indicate that there is a significant mass drop in the test samples from Day 2, which indicates that there may have been a leak in the test tube apparatus. The cause of this leak is not known, but the lack of precision and high uncertainty calculation in the data from Day 2 leads to this conclusion. There is also high uncertainty in the data collected from Day 1; however, it is not nearly as high as the uncertainty from Day 2. The highest uncertainty from Day 1 was less than 35% while the highest uncertainty from Day 2 were 1652%. Some mass loss could be due to evaporation of the solvent, but clearly the data from Day 2 is in error. In comparing the calculated dissolved amount of polymer with the artificial gravity and vibration induced for Day 2's samples, no trend could be discerned. The data show no strong response to the control variables. Nonetheless, there is no known reason to consider that the data from Day 1 is in error. While vibration did not have as strong an effect as expected on hydration in Day 1's experiments, it did indicate that there was a large enough effect at low artificial gravities for vibration to significantly enhance hydration and solubility.

CONCLUSION

The objective of this experiment was to determine whether a combination of vibration and artificial gravity could significantly enhance the hydration rate of bio-polymers. To determine if a combination was effective, certain parameters needed to be obtained. These parameters include the mass of polymer that dissolved, the frequency of the vibration induced, the magnitude or force amplitude of the vibration induced, and the magnitude of the artificial g's induced on each test sample. The results were that there is some evidence that vibration increased the hydration rate of the polymer despite the fact that data from Day 2 of testing did not yield useful results. The data from Day 2 indicates a significant mass drop in the test samples after experimenting, which indicates that there may have been a leak in the test tube apparatus. The cause of this leak

is not known, but the lack of a trend in the results indicates that some extraneous factor has skewed the results. Nonetheless, the results from Day 1 of testing yielded useful results. They indicated that the increase in hydration due to vibration is not as significant as was expected. Vibration increased the amount of hydrated polymer by only about 30% at the highest artificial gravity tested. Essentially the rate of hydration was more responsive to increase in the artificial gravity than vibration. It is noteworthy, however, that vibration seemed to have a more influential effect, over 100% on hydration at low artificial gravities. Perhaps this may prove useful for bio-encapsulating medications having components and aggregates of different densities that must not be separated out during hydration. Enhancing hydration at low gs would enable one to more effectively prepare medications in 0g. Nonetheless, the most significant influence tested on hydration appears to be artificial gravity. Vibration does seem to improve hydration in reduced gravity enough that it is likely that higher frequency or magnitude vibrators could more significantly improve hydration at higher artificial gravities.

REFERENCES

- “Blood Transfusions: Playing it Safe.” Editorial. Nursing96 April 1996, Springhouse Corporation. Springhouse, Pa. 50-52.
- Miller, Karen. “Artificial Cells.” NASA—Artificial Cells. 14 Oct. 2003. National Aeronautics and Space Administration. 10 Oct. 2003
- Meng F, Engbers GH, Feijen J., Biodegradable polymersomes as a basis for artificial cells: encapsulation, release and targeting. [Journal of Controlled Release](#) [Volume 101, Issues 1-3](#) , 3 January 2005, Pages 187-198

PHOTOGRAPHS

JSC2006EO6769 to JSC2006EO6773
JSC2006EO6849
JSC2006EO6858 to JSC2006EO6859

VIDEO

- Zero G March 6 - 10, 2006, Master: 720751

Videos available from Imagery and Publications Office (GS4), NASA/JSC.

CONTACT INFORMATION

David Gillikin

dmgillik@ncsu.edu

Phone: (704) 254-5751

Chris Thomas

cmthomas@ncsu.edu

Phone: (919)824-0920

Chris Page

cdpage@ncsu.edu

Phone: (704) 201-9702

Christine Watson

cawatson@ncsu.edu

Phone: (919)512-0660

TITLE

Undergraduate Program Flights - Gravitational Effects on Cartilage Nutrition and Neutrophil Function

FLIGHT DATES

March 9-10, 2006

PRINCIPAL INVESTIGATOR

Brenda Klement, Morehouse School of Medicine

CO-INVESTIGATORS

Daniel von Deutsch, Morehouse School of Medicine

Doug Paulsen, Morehouse School of Medicine

STUDENT CO-INVESTIGATORS

Ruby Flowers, Morehouse School of Medicine

Albert von Deutsch, Morehouse School of Medicine

Allyson Belton, Morehouse School of Medicine



GOAL

Exposure to a microgravity environment has been reported to cause several health concerns in the human body including compromised musculoskeletal and immune systems. Articular cartilage is a component of the musculoskeletal system and is present in the moveable joints. Pronounced decreases occur in bone and muscle mass after even short spaceflights. Changes in any of the musculoskeletal components during long space missions could reduce astronaut mobility during and after flight.

Neutrophils are circulating white blood cells that play an important role in the body's immune system. In the presence of bacteria and foreign particles (as well as oxidative and physical stress), neutrophils can degranulate and release myeloperoxidase (MPO) and the reactive oxygen species hypochlorous acid (HOCl). In activated neutrophils, MPO is the enzyme that produces HOCl from peroxide (H_2O_2) and chloride anion (Cl) substrates. The function of HOCl is to combat infection. However, if too much is released, the result will be the onset of inflammation and oxidative damage to the surrounding cells and tissues. Studies have shown that neutrophils may be activated during spaceflight reducing their normal function. A disturbance in an astronaut's immune system could lead to a greater susceptibility to pathogens and infections during spaceflight and upon return to Earth.

Two sets of experiments were conducted to address the issue of astronaut health and mobility. The goal of one of the projects was to determine if diffusion of nutrients through cartilage is altered by a decreased or increased gravitational environment. The goal of the second project was to determine if transitional gravitational changes (continuous cycles of microgravity, hypergravity and standard 1 gravity) cause neutrophils to become activated and release the pro-oxidative enzyme myeloperoxidase (MPO).

OBJECTIVES

- Determine the quantity of fluorescent glucose that diffuses into cartilage tissue during a 20-second interval of microgravity
- Determine the quantity of fluorescent glucose that diffuses into cartilage tissue during a 20-second interval of hypergravity.
- Determine the extent of MPO release from human neutrophils exposed to transitional gravitational forces.

METHODS AND MATERIALS

Cartilage Component

Bovine articular cartilage was collected from an Atlanta-area slaughterhouse and placed into culture. The cartilage pieces were shipped to Houston the day before each flight. Prior to flight they were inserted into rubber rings and each was anchored inside a 10cc syringe. Each syringe also contained 1ml of phosphate buffered solution (PBS). Upon entry into the microgravity component of the parabola, a glucose solution from another syringe was added to the PBS in the cartilage syringe. Near the end of the microgravity component this solution was removed and a solution of colored mineral oil was added. The mineral oil covered the cartilage and prevented the glucose from leaving the cartilage during the remainder of the flight. After each experiment, the syringes were stowed in a cooler containing ice packs. The same procedure was used for the experiments conducted during the hypergravity phases of the parabolas. Controls at standard 1g were performed during the turnaround in flight and after the flight was complete. After landing, the cartilage plugs were packed in dry ice, where they were stored until the return to MSM, when they were transferred to a $-20^{\circ}C$ freezer.

Neutrophil Component

Human neutrophils have, on average, only a 24-hour life span, so it was necessary to obtain fresh whole human blood from our flight and ground crew personnel for these experiments. On each flight day blood was drawn from the fliers and ground crew personnel. The neutrophils were isolated and suspended in culture medium. The cells were inserted into specialized Cell Max Chamber culture devices. These chambers contained a filter membrane for the cells to rest on but allowed culture medium to flow around them during the experiment. After the cells were collected and put into culture chambers, they were incubated at 37°C until they were loaded onto the aircraft (see timeline in **Figure 1**).

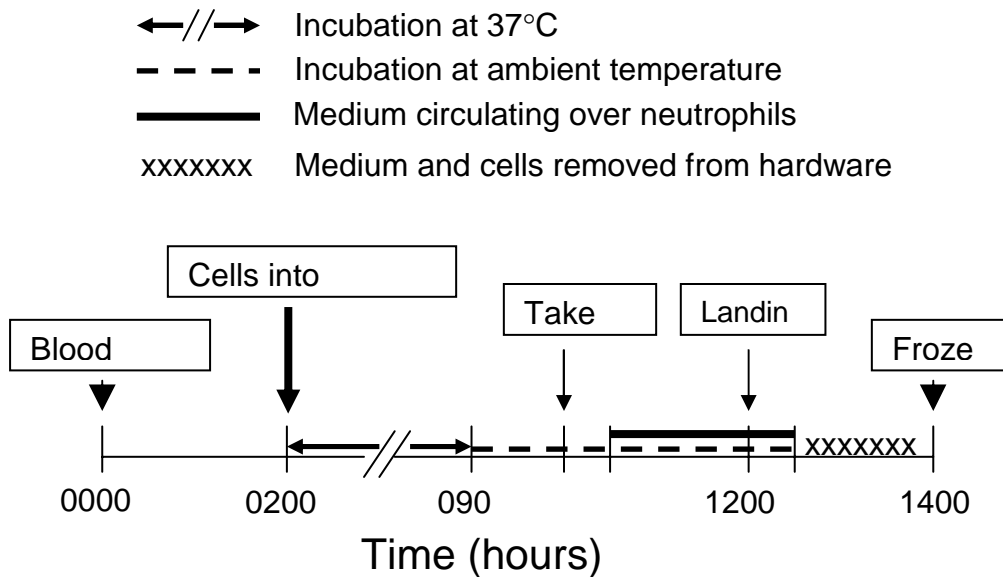


Figure 1. Timeline showing important events in the neutrophil experiment.

Immediately before the parabolas began, the peristaltic pump was turned on so that the culture medium would continuously circulate over the cells. The flow rate was set to 1.0 mL per minute. The medium was allowed to circulate throughout the duration of the flight and was stopped after landing. Subsequently, the medium was removed from the circulation lines and the cell module detached from the system for removal of the cells. The medium and cells were frozen on dry ice and carried back to MSM for analysis.

RESULTS

Analyses of our ground and flight samples will begin in mid-May after final exams. Thus, results are not yet available to show if changes in gravity can modulate the diffusion of nutrients in cartilage or exacerbate neutrophil activation. However, data are presented below (Tables 1 - 3) to show the number of samples collected on each flight day and the estimated time required to complete the biochemical analyses from each experiment.

Samples of three solutions from the cartilage nutrition experiment have been measured to compare the amount of fluorescence to the amount present in the original solution (Figure 2). A difference was seen in the amount of fluorescence, suggesting that at least the standard 1g control experiments were successful and that glucose diffused into the cartilage. We anticipate

that the difference in fluorescence between the samples and original stock solution is the amount that diffused into the tissue. This can be determined after the tissue component is analyzed. The solutions from all experiments will be analyzed and compared to the stock solution.

Table 1. Number Of Nutrient Diffusion Experiments Conducted.

Experimental Conditions	Flight day 1	Flight day 2	Total	Estimated Time Required for Analysis
Microgravity	12	15	27	6 Days
Hypergravity	6	3	9	2 Days
In-Flight Control (1 gravity)	8	9	17	4 Days
Post-Flight Control (1 gravity)	0	6	6	2 Days
Total	26	33	59	14 Days

At the conclusion of the neutrophil experiment after each flight, the cells were removed from the culture device and counted. The number of cells retrieved from each culture chamber is listed in Table 2. There were fewer live cells on day 2 than on day 1 because of a problem encountered during the isolation procedure on day 2. However, when the percent live cells on the two days were compared, they were nearly equivalent.

Table 2. Table of Cell Counts for both flight days.

Day 1				Recovered	% Live Cells	Day 2				Recovered	% Live Cells		
				cell density						cell density			
				per mL						per mL			
a	Live	dead	total			a	Live	dead	total				
	142	11	153	30,600	92.8%		68	6	74	14,800	91.9%		
	108	5	113	22,600	95.6%		88	18	106	21,200	83.0%		
	average	125	8	133	26,600		94.0%	average	78	12	90	18,000	86.7%
b	Live	dead	total			b	Live	dead	total				
	103	8	111	55,500	92.8%		109	17	126	25,200	86.5%		
	78	8	86	43,000	90.7%		78	16	94	18,800	83.0%		
	average	90.5	8	98.5	49,250		91.9%	average	93.5	16.5	110	22,000	85.0%
c	Live	dead	total			c	Live	dead	total				
	175	10	185	46,250	94.6%		85	7	92	18,400	92.4%		
	119	8	127	31,750	93.7%		56	3	59	11,800	94.9%		
	average	147	9	156	39,000		94.2%	average	70.5	5	75.5	15,100	93.4%
d	Live	dead	total			d	Live	dead	total				
	113	5	118	23,600	95.8%		33	3	36	7,200	91.7%		
	156	13	169	33,800	92.3%		39	4	43	8,600	90.7%		
	average	134.5	9	143.5	28,700		93.7%	average	36	3.5	39.5	7,900	91.1%
e	Live	dead	total			e	Live	dead	total				
	179	7	186	37,200	96.2%		185	11	196	39,200	94.4%		
	166	16	182	36,400	91.2%		193	9	202	40,400	95.5%		
	average	172.5	11.5	184	36,800		93.8%	average	189	10	199	39,800	95.0%
				Averages:	36,070	93.6%					Averages:	20,560	90.3%
				Standard Dev:	9,442	1.6%					Standard Dev:	11,248	4.4%

The types of assays, number of samples, and estimated time required for analysis are presented in Table 3. The quantity of MPO and nitric oxide (NO) produced by the neutrophils and the amounts released into the cell culture medium will be measured.

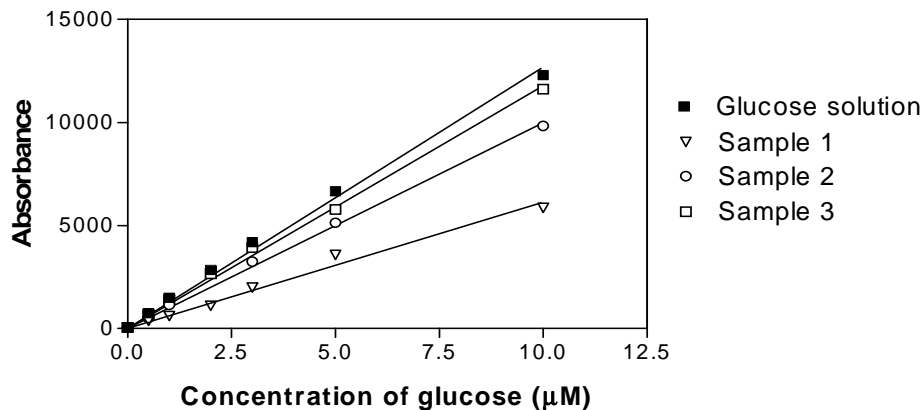


Figure 2. Graph showing standard curves of glucose solution. The original stock solution of glucose contains the highest level of fluorescence. Aliquots of solution from three of the control samples were measured.

In addition, levels of lipid peroxidation will be assessed in both the cell homogenates and culture medium. The total protein content will also be determined for each cell sample. However, before the samples are analyzed an additional blood draw will be performed to isolate neutrophils in order to establish levels of maximal release. These neutrophils will be exposed to lipopolysaccharides (LPS), which will cause them to release MPO and NO in a process called degranulation. This will constitute a maximal response and the samples from the flight experiments will be compared to these. Individual samples will all be run in triplicate for each assay.

Table 3. Scheduled Tests and Time for Analyses.

Tests	Control Samples		LPS Control Positive Samples **		Flight Sample		Totals Assays	Time (days) per assay***
	Media # Samples	Cell # Samples	Media # Samples	Cell # Samples	Media # Samples	Cell # Samples		
1 Myeloperoxidase (MPO)*	10	10	5	5	10	10	50	5
2 IL-6	10	10	5	5	10	10	50	5
3 Lipid peroxidation (LPO)	10	10	5	5	10	10	50	5
4 Total Protein	n/a	10	n/a	5	n/a	10	25	5
Total Number of Assays	30	40	15	20	30	40	175	20

- * Reagent is on back order.
- ** A separate blood draw must take place to have fresh cells (IRB approved). Fresh cells will be treated with LPS to stimulate 100% release of MPO and IL-6.
- *** Includes time for sample preparation, running the assays and data/statistical analyses. Note: Samples will be run in triplicate by the students.

DISCUSSION

The samples from our C-9 flight experiments will begin to be analyzed following final examinations around the middle of May. We have numerous biological samples, 59 from the cartilage experiment and 20 from the neutrophil experiment, and each must be analyzed individually. Since many of the assays require several hours to conduct, full workdays are required that are not broken up by attending classes. In addition, several chemicals required for

the neutrophil assays were on backorder and have just arrived (May 8, 2006). Our student team members are almost finished with classes for the semester and will soon be able to devote their attention to conducting the individual analyses, preparing graphs, and writing up final results in publication format. This should be completed by the end of July.

It was planned that one cartilage nutrient diffusion experiment would be conducted on each of 20-25 microgravity episodes and 10 hypergravity episodes of the parabolas. However, it was more difficult than anticipated to conduct an experiment during back-to-back parabolas. Therefore, an experiment was conducted, on average, every other parabola during the microgravity components. The second flyer, in addition to overseeing the operation of the neutrophil experiment, conducted some of the nutrient diffusion experiments. This was especially helpful during the hypergravity component of the parabolas. Therefore, fewer microgravity and hypergravity experiments were conducted than was originally planned. The tissues not used during the flight were used as extra standard 1g controls.

The blood collection and neutrophil preparation went well, although it would have helped to have additional ground crew to assist in the preparation. The only hindrance to the experiments was insufficient time allotted to collect all the cells and medium from the individual circulation lines after the first flight. In this instance, the problem was that the aircraft was scheduled to conduct other flight experiments immediately following the student flight, so recovery of cells and medium from our hardware was rushed. Since preliminary results from the recovered cell counts indicated high percentages of live cells, the impact resulting from this problem may be minimal to none. Otherwise, the experiment went as planned and no other problems were encountered.

CONCLUSION

A substantial number of samples were collected from experiments conducted on the C-9 during our two flight days. A total of 59 tissue samples and their respective solution samples were collected from the nutrient diffusion in cartilage experiments. These included experiments conducted during the microgravity and hypergravity components of the parabolas, as well as standard 1g in-flight and post-flight controls. Blood was successfully drawn from our flight team and ground crew on both days and the neutrophils were isolated. Ten individual groups of neutrophils were flown during the 2 flight days (5 on each day). These neutrophils, as well as the medium in which they were incubated, will be analyzed for the total amount of MPO, lipid peroxidase and nitric oxide. Total protein will also be measured in the cell samples. These time-consuming assays will be conducted after the spring semester is complete, so that the students will have uninterrupted time to work in the laboratories.

PHOTOGRAPHS

JSC2006EO7219

JSC2006EO7220 to JSC2006EO7224

JSC2006EO7257

JSC2006EO7261 to JSC2006EO7262

JSC2006EO7268

JSC2006EO7282 to JSC2006EO7290

VIDEO

- Zero G March 6 - 10, 2006, Master: 720751

Videos available from Imagery and Publications Office (GS4), NASA/JSC.

TITLE

Undergraduate Program Flights
Free-Floating Resistance Exercises for Maintaining Postural Muscles in Weightlessness: A
Reflight and Enhancement of the 2004 Study

FLIGHT DATES

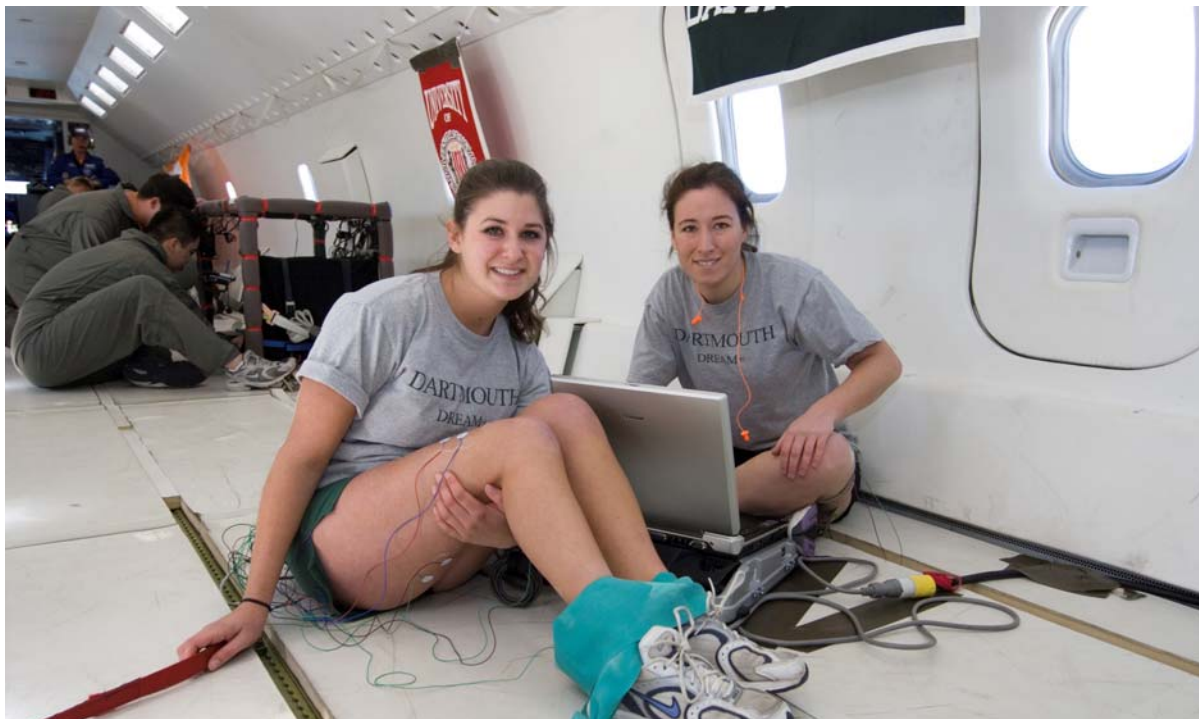
March 23-24, 2006

PRINCIPAL INVESTIGATOR

Abigail Davidson, Dartmouth College

CO-INVESTIGATORS

Lauren Edgar, Dartmouth College
Jennifer Tonneson, Dartmouth College



ABSTRACT

Multiple studies have shown reductions in muscle cross-section area and strength in weightlessness. This affects mainly the anti-gravity (postural) muscles. Currently, astronauts use the following regimen for exercise and training in space: a 1-hour session of aerobic conditioning 2 days/week, a 1-hour session of resistive exercise 6 days/week, interval training 4 days/week, and EVA training as needed. For the 2004 NASA Reduced Gravity Student Flight Opportunity, a group of students from Dartmouth College tested the effects of short, intense resistive exercises on the activation of postural muscles. These simple exercises could be done by the astronauts at any time during the day, without special equipment, to help maintain the antigravity muscles. They called these exercises the Dartmouth Resistance Exercises for Antigravity Muscles (DREAM). Observation of the electromyogram (EMG) recording on the KC-135 in 2004

indicated that the DREAM exercises were indeed effective in muscle activation. Also, the exercises could be performed easily in weightlessness.

Over the academic year of 2005-2006, our group expanded upon the successful initial demonstration of these exercises by (a) testing new exercises that also activated postural muscles, (b) providing visual feedback on muscle activation during the exercises so the crewmember could calibrate muscle activation (c) improving the EMG data analysis. Using a surface electromyography (sEMG) to quantify the results, we recorded the stimulation of muscles from these exercises in a microgravity environment. We also developed a software package to analyze the results.

In conclusion, our exercise regimen was easy to perform in a microgravity environment. The targeted exercises the subjects performed activated muscles in a 0g environment similar to how they were activated in a 1g environment whereas the one universal exercise we used did not. Muscle activation also varied with concentration from the subject.

INTRODUCTION

Muscle atrophy is a severe problem for astronauts in a microgravity environment. Without the force of gravity, muscle groups that are normally activated by everyday activities (standing up, sitting down, etc.) atrophy due to lack of stimulation. The affects are similar to those of people confined to bed rest on Earth. The muscle groups most significantly affected by extended time spent in a microgravity environment are the five main postural muscle groups.

In order to minimize these detrimental affects, astronauts engage in a rigorous workout regimen during their time in flight. The current routine for astronauts consists of multiple hour-long exercise sessions per week. These exercises are grouped into the categories of aerobic conditioning, resistive exercise, interval training, and EVA training. This complete workout schedule demands at least twelve hours of exercise per week not including the EVA training, which is completed as needed¹. However, research in animal subjects has indicated that shorter intense exercise sessions may be just as (or possibly more) effective than these longer exercise programs. Furthermore, the equipment currently used by astronauts to complete their exercises accommodates only one astronaut at a time, so that the crewmembers must schedule when they use the exercise equipment.

The DREAM exercises developed by the Dartmouth team during the 2004 Reduced Gravity Student Flight Opportunities Program provide short bursts of exercise to the five main postural muscle groups to avoid atrophy. These exercises were also designed to be performed with minimal equipment (a portable resistance band or a nylon strap) so that astronauts could perform these exercises at their convenience.

The primary reasons for the 2005-2006 re-flight were to gather further data on the existing exercises, test new methods of exercise execution, solve data acquisition and analysis problems, and provide feedback to the user on muscle activation.

The re-flight used the same exercises described in DREAM along with one other that triggers the hip abductors. In addition, the test subjects executed these exercises in a different fashion for a potentially more efficient workout, using the “extend and hold” method as opposed to the “extension-contraction” method of 2004.

The data from 2004 and 2006 were then analyzed to compare the relative effectiveness of the exercises in a 0g environment compared to the effectiveness in a 1g environment.

METHODS AND MATERIALS

Procedure

Before boarding the C-9, test subjects attach the electrodes and take impedance measurements. The ground electrode attaches to the subject's inner ankle, and pairs of electrodes are placed on the following muscle groups:

- calf
- quadriceps
- hamstring
- hip abductors
- erector spinae (lower back)

On-board Protocol

The subject performs two sets of each of the five DREAM+ exercises during the first ten dives, while the other subject is monitoring their progress on the EMG. After 10 parabolas, the fliers switch, and the second test subject repeats the protocol for the next 10 dives. The remaining 10 parabolas are used for make-ups and additional data collection if necessary. The exercise protocol is as follows:

- 1) Calf exercise (extend and hold): The non-elastic nylon band wraps around the bottom of the ball of the foot, with leg extended, and the subject holds one end of the band in each hand. Subject points and holds her toe for approximately 10 seconds, flexing the calf.
- 2) Quad exercise (extend and hold): The non-elastic nylon band is placed under the ball of the foot, with leg at a 90-degree angle. The subject holds one end of the band in each hand, and extends her leg about halfway. Resistance is provided by the subject's arms pulling on the band, while the leg pushes the band in the opposite direction. The subjects hold the position for 10 seconds.
- 3) Biceps femoris, hamstring (extend and hold): The green Thera Band is tied in a loop, and rests on the top of the foot of the stationary leg and the back of the heel of the exercising leg. Both legs are extended most of the way. The subject tries to bend the exercising leg to a 90-degree angle, and holds for about 10 seconds.
- 4) Hip abductors (extend and hold): The green Thera Band is tied in a loop and wrapped twice around the subject's ankles. The subject's legs are extended, and she tries to spread her legs apart and holds for 10 seconds.
- 5) "Pullsquat" (extend and hold): The non-elastic nylon band wraps around the ball of both feet and the subject holds one end of the band in each hand. The subject starts by bending at the waist to form a 90-degree angle. The subject pushes against the canvas band with her feet while pulling up with her back, trying to activate as many muscles as possible. She holds the exercise for 10 seconds.

During each parabola, the recording researcher cues the subject (experimenting researcher) to begin, then pushes the record button on the EMG unit. After approximately 10 seconds the recording researcher stops recording and cues the subject to stop the exercise.

Post-Flight Activity

Following the flight, the subjects perform 3 sets of each of the 5 DREAM+ exercises to be used as a baseline. Additionally, each subject performs a set of daily activities, which include walking,

sitting down, standing up, walking up steps, toe raises, and picking up an object. Each normal exercise is repeated for sessions of 10-15 seconds.

Equipment

The computer used onboard the C-9 is a Dell Latitude D800. The Thera-bands are 6 feet in length and 6 inches in width. The nylon band is approximately 0.079 inches in length and approximately 1.5 inches in width. The foot loop needed for several of the exercises is obtained by tying a loop in the Thera-band. The length may also be adjusted per use according to the resistance desired.

RESULTS

The output of our EMG was microvolts per unit time. The binary data from the EMG were exported into MATLAB, where we summed the amplitudes of the activated muscle to determine total activation. The sample rate was 320 Hz. Using 10 seconds of muscle activation, we determined total activation (summed the amplitudes) and divided by the total number of data points (3200) to find the average activation per sample.

We then used these numbers to determine the mean activation (in μV) for each muscle for each exercise. The data from 0g and 1g were then compared by using a paired sample t-test. Table 1 shows the results from the pullsquat exercise, N=7 (we were not able to analyze the data from one of the 2004 subjects).

Table 1

Muscle	μ Flight	μ Ground	P- Value
Calf	24.0	43.1	0.0214
Quad	60.0	100	0.0146
Hamstring	27.5	34.8	0.0947
Hip	34.4	19.1	0.0381
Back	83.8	84.6	0.942

The mean activation for each muscle is given in μV . The muscles highlighted are the ones with a P-Value <0.1, indicating a significant difference between populations. Table 2, however, shows the results from the four targeted exercises (N=7 for calf, quad, and hamstring, N=5 for hip).

Table 2

Muscle	μ Flight	μ Ground	P- Value
Calf	147	161	0.597
Quad	54.2	66.8	0.0751
Hamstring	161	149	0.746
Hip	138	171	0.448

Table 2 indicates no significant difference between 0g and 1g activation except for the quadriceps.

Dissecting these results, we predict that the discrepancy between 0g and 1g activation for the pullsquat comes from the way it was performed in 1g. We performed the pullsquat standing up, initially hypothesizing that muscle activation from loading due to a subject's body weight would be negligible compared to loading from the exercise. Since the leg and hip muscles, however, show significantly higher mean activations in 1g than in 0g, we believe that our initial hypothesis was incorrect.

CONCLUSION

All of the test subjects noted how easy the exercises were to perform in weightlessness. They also noted how helpful it was to have feedback from the person recording the results on the EMG. Because the targeted exercises produce similar values for mean 0g and mean 1g, we may conclude that they are most effective for exercising the leg muscles and hip muscles. However the pullsquat is sufficient for achieving similar activation in a 0g and 1g environment.

For future work we would like to calibrate the amount of muscle activation a subject achieves in her daily life. We intend to use a wireless EMG that a subject can carry around throughout the day so we may determine the total amount of activation she achieves throughout the day. Then we can better calibrate how much activation we wish to achieve through our exercise regimen.

REFERENCES

1. Jay Buckey, personal communication.
2. Wildrick JJ et al, "Effect of a 17 day spaceflight on contractile properties of human soleus muscle fibres," *The Journal of Physiology* 516.3 (1999). 915-930.
3. Leblanc A. et al, "Muscle volume, MRI relaxation times (T2), and body composition after spaceflight," *Journal of Applied Physiology* 89(6) (2000). 2158-2164.
4. Edgerton, V.R. and R.R. Roy, "Neuromuscular adaptations to actual and simulated spaceflight." In Fregly, M.J. and C.M. Blatteis, eds., *Handbook of Physiology, Section 4 Environmental Physiology*. New York, NY, Oxford. 1996, 721-764

PHOTOGRAPHS

JSC2006E10173
JSC2006E10177 to JSC2006E10178
JSC2006E10187 to JSC2006E10191
JSC2006E10194 to JSC2006E10198
JSC2006E10544
JSC2006E10559 to JSC2006E10561
JSC2006E10564 to JSC2006E10567
JSC2006E10570
JSC2006E10579 to JSC2006E10584
JSC2006E10597 to JSC2006E10598

VIDEO

- Zero G flights March 20 -24 , 2006, Master: DV0520

Videos available from Imagery and Publications Office (GS4), NASA/JSC.

TITLE

Space Medicine C-9 Familiarization Flight

FLIGHT DATE

April 11, 2006

PRINCIPAL INVESTIGATOR

David Stanley, Wyle Laboratories, Inc., Life Sciences Group

CO-INVESTIGATORS

Erin Taschner, Wyle Laboratories, Inc., Life Sciences Group

Chris Goetter, Wyle Laboratories, Inc., Life Sciences Group

Rick Scheuring, University of Texas Medical Branch

Bob Tweedy, Barrios Technology



GOAL

To familiarize Space Medicine Branch personnel with the effects of a 0g environment through performing activities that utilize the medical equipment and procedures in order to better facilitate crew training and biomedical engineering support for ISS procedures.

OBJECTIVES

All co-investigators accomplished the following objectives:

PRE-FLIGHT

1. Attend pre-flight briefing and participate in ground-based practiced session
2. Attend Test Readiness Review (TRR)
3. Attend Medical Briefing
4. Conduct final inventory of all hardware and supplies and transport equipment to Ellington Field for scheduled reporting time
5. Properly load and secure hardware onto aircraft

IN-FLIGHT

1. Experience and evaluate the effects of microgravity on intravenous insertion and drug administration, and on medical fluids
2. Experience and evaluate the effects of microgravity on cardiopulmonary resuscitation (CPR), patient restraint, and rescuer restraint
3. Experience and evaluate the effects of microgravity on using two different types of instruments used in intubation

POST-FLIGHT

1. Unload hardware from aircraft
2. Prepare a C-9 final report

INTRODUCTION

As new personnel join the Space Medicine Branch, it is critical that they understand the effects of microgravity while using medical procedures, hardware, and supplies. The familiarization flight provided personnel with a better understanding of the effects of microgravity for use of medical procedures, patient and rescuer restraint, and medical training for spaceflight. Using the procedures to perform the tasks on the familiarization flight allows the operator to understand the limitations imposed by microgravity, helps in the composition of procedures for spaceflight, and helps operators assist astronauts in on board procedure execution.

The flight process also provided experience in flight test plan preparation and execution, and final report preparation. In addition, first-time flyers gained insight on their performance level in microgravity for future flights.

METHODS AND MATERIALS

An initial training session was held to familiarize the new flyers with the documentation and skills necessary to fly on the C-9. The documentation required for requesting and reporting a C-9 flight was covered in detail and the co-investigators were given a template for writing their final reports. A skill session on the medical procedures that would be attempted during flight was also held. Flyers were introduced to the tasks required at each station and were given additional time to build confidence in their skills by practicing these tasks.

The procedures and equipment were divided into three stations. These stations included an intubation station, an IV administration station and a CPR station.

The intubation station was composed of a plastic model of the human head/neck/chest that is designed specifically for practicing the establishment of an airway. Two methods of intubation were practiced; the intubating laryngeal mask airway (ILMA) device (Figure 1) and the laryngoscope (Figure 2) and endotracheal tube. The established medical checklist procedures for the insertion of these devices were followed.



Figure 1. ILMA



Figure 2. Laryngoscope

The IV administration station consisted of an artificial human arm with the correct anatomic landmarks for practicing intravenous catheter insertion. The arm and IV equipment (Figure 3) were fixed to a small metal table. The procedures for establishing peripheral intravenous access were followed and procedures for injecting medication into the intravenous line were practiced. A Tubex drug injection system was used for this purpose. The established medical checklist procedure for this technique was followed.

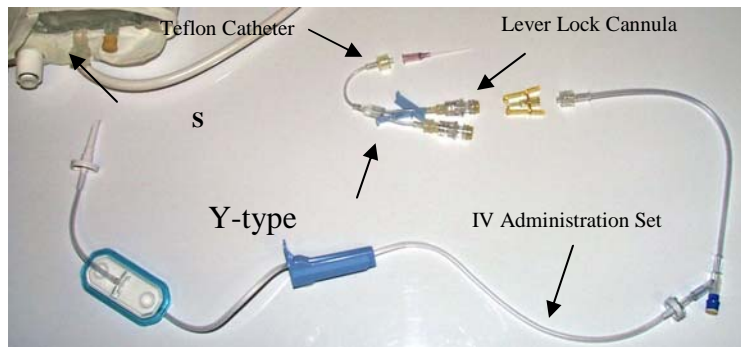


Figure 3. IV Equipment

Finally, the CPR station was established to practice performing cardiopulmonary resuscitation on a simulated ill crewmember. The Crew Medical Restraint System (CMRS) was deployed and utilized to immobilize the simulated ill crewmember. Three approaches to performing CPR were practiced for the designated crew medical officer (CMO): (1) CMO beside the patient, (2) CMO straddled on the patient, and (3) handstand position.

During the flight, the co-investigators were stationed as outlined in Table 1.

Table 1. C-9 Familiarization Flight Procedure Assignments

<i>Parabolas</i>		0-10	11 - 20	21 - 30	31 -40
<i>Activities</i>	CPR	Tweedy	Scheuring	Goetter	Taschner
	CPR	Scheuring	Tweedy	Taschner	Goetter
	IV	Taschner	Goetter	Tweedy	Scheuring
	Intubation	Goetter	Taschner	Scheuring	Tweedy

RESULTS

Intubation Station

The medical checklist procedures were followed for the insertion of the ILMA. The lack of gravitational influence made it necessary to secure all small loose objects so that they would not drift away. The laryngoscope/endotracheal tube method of intubation was performed according to established procedures. Both of these methods were repeated twice. All the objectives for this station were met.

IV Station

The insertion of an intravenous catheter was achieved using the standard procedures. Intravenous fluid tubing was connected to the catheter. Afterward, Tubex drug injection was practiced. The management of sharp waste was particularly important due to the tendency of objects to float in simulated microgravity. All the objectives for this station were met.



Figure 4. Bob Tweedy



Figure 5. Erin Taschner

CPR Station

The CMRS was deployed and secured to the aircraft floor pre-flight. The simulated ill crewmember (mannequin) was secured to the CMRS following established procedures for the use of the restraint system. The designated CMO was able to perform CPR in all three of the positions desired: straddled, inverted, and side-by-side. The inverted position was clearly the most effective position as the other two positions required significant counter-pressure from restraints. All the objectives for this station were met.



Figure 6 Subject performing CPR in the inverted position.

DISCUSSION

Performing the medical operations procedures on the C-9 flight gave the co-investigators a greater understanding of the conditions involved in space operations. This knowledge will prove very useful for the co-investigators, especially during any on orbit contingency situation or training session.

Experiencing weightlessness presented many difficulties that the co-investigators did not originally expect. They found the lack of control while floating to be the most difficult aspect of weightlessness. The lack of control was most apparent while performing time-critical medical activities. The co-investigators spent a larger amount of time securing themselves and maintaining proper positioning than originally anticipated. This time would most likely be reduced with extended exposure to microgravity. With this information, the co-investigators will be able to make more accurate and effective recommendations to a crewmember during nominal and emergency situations.

This familiarization flight will be extremely beneficial in supporting the crew and console operations. A greater understanding and appreciation of the difficulties the crew faces due to their environment was gained. This experience will provide a better ability to walk the crew through any procedure, not just the ones performed during the flight.

CONCLUSION

Overall, the objectives of the C-9 Familiarization Flight were met. All co-investigators agreed that the C-9 Familiarization Flight and associated training provided them with an excellent knowledge level from which to conduct their own flights. This was a very valuable training session and is highly recommended for all BMEs, Flight Surgeons, and instructors. It is especially beneficial for anyone who will train astronauts to perform complex tasks that require the use of lots of loose equipment.

PHOTOGRAPHS

- None

VIDEO

- None

Videos available from Imagery and Publications Office (GS4), NASA/JSC.

CONTACT INFORMATION

David Stanley
Wyle Laboratories, Inc., Life Sciences Group
1290 Hercules Suite 120
Houston, TX 77058
dstanley@wylehou.com

TITLE

Myotonometric Measurements of Muscle during Changes in Gravitational Forces

FLIGHT DATES

April 12, 2006

PRINCIPAL INVESTIGATOR

Charles T. Leonard, University of Montana

CO-INVESTIGATORS

Daniel L Feedback, NASA/Johnson Space Center

James Sykes, University of Montana

Eric Kruger, University of Montana



GOAL

Assess operational characteristics and reliability of the Myotonometer, a portable medical device that quantifies muscle tone and strength, while gravitational forces are changing.

OBJECTIVES

1) Perform correlational analysis comparing myotonometric measurements of resting and contracting muscle at 0 and 1g. 2) Determine intra-rater reliabilities of myotonometric measurements at 0g. 3) Obtain inter-rater reliabilities of myotonometric measurements at 0g. 4) Descriptive and anecdotal information relating to the feasibility and constraints of obtaining myotonometric measurements of muscle health in a 0g environment.

It is hypothesized the myotonometric measurements of the soleus muscle will be the same regardless of whether measurements are acquired in 0 or 1g. It is also hypothesized that intra- and inter-rater reliabilities will be very high, matching similar published results acquired in 1g.

METHODS AND MATERIALS

Instrument = Myotonometer

The Myotonometer is a patented¹, FDA-approved electronic instrument that measures muscle stiffness (tone/compliance) by quantifying resistance, measured as millimeters of tissue displacement per unit of a perpendicularly applied force of a hand-held probe. An examiner presses a probe onto the skin overlying the desired muscle to a pre-prescribed force level. Computational software instantaneously computes and displays force-displacement characteristics of the muscle. Measurements obtained from a relaxed muscle reflect resting muscle stiffness. Measurements taken during maximal voluntary contractions (MVCs) provide a measure of voluntary muscle activation capabilities of the muscle (strength). This is possible because muscle stiffness increases proportionally with increasing levels of muscle contraction and joint torque.^{2,3,4,5}

Measurements are highly reliable at 1g.^{6,7,5}

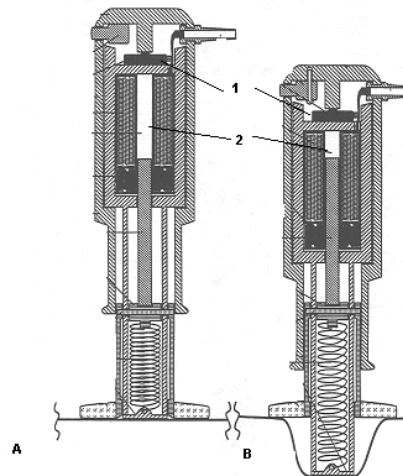


Figure 1. Myotonometer probe diagram. A) Illustrates probe positioned on skin overlying muscle to be tested. B) Illustrates pressure being applied by the examiner. Outer Plexiglas collar remains relatively motionless on the skin while the inner probe compresses underlying tissue. 1= force transducer; 2= electromagnetic coil assembly that measures tissue displacement. Probe is connected to laptop computer for data storage and analysis.

The Myotonometer probe measures 13.5 x 3.7 centimeters and weighs 15 ounces. It is powered by a computer USB port.



Figure 2. Photograph of Myotonometer being used to measure soleus muscle compliance during a 0g parabolic trial aboard the C-9 aircraft.

Subjects and Procedures

Four investigators also served as subjects. Measurements were obtained during 28 parabolas. It was possible, using one instrument, to obtain measurements of resting tone and tone change during soleus MVCs of two subjects during each parabola. Each investigator measured the soleus muscle of the other 3 flyers. Each investigator obtained 3 recordings of a subject's resting and contracted soleus tone during 3 separate 0g parabolas. An equal number of measurements were obtained on the ground at 1g. Each subject's data at 0g were compared to data obtained at 1g to determine whether the measurements differed and to determine the degree of correlation. Data were also analyzed for the degree of intra- and inter-rater reliabilities.

RESULTS

Intra- and Inter-rater Myotonometric Measurement Reliabilities

Myotonometer intra- and inter-rater reliabilities were $r > 0.90$ during 1g measurements. The Myotonometer worked well in 0g, but reliability statistical analysis became a moot point secondary to examiners having difficulty stabilizing adequately in 0g. All examiners had difficulties centering the Myotonometer probe over the muscle in the same location during each parabola. The inability of the examiners to accurately place the hand-held probe over the same spot on the muscle during each trial negatively affected reliabilities, not Myotonometer performance.

Correlation Between Myotonometric Measurements at 0 and 1g

As above, correlational analysis was not possible secondary to unreliable examiner positioning of probe over muscle during 0g trials.

Differences in Myotonometric Measurements During 0 and 1g

There was an apparent trend toward increased muscle stiffness (decrease in compliance) in 0g when compared to 1g measurements (Figure 3).

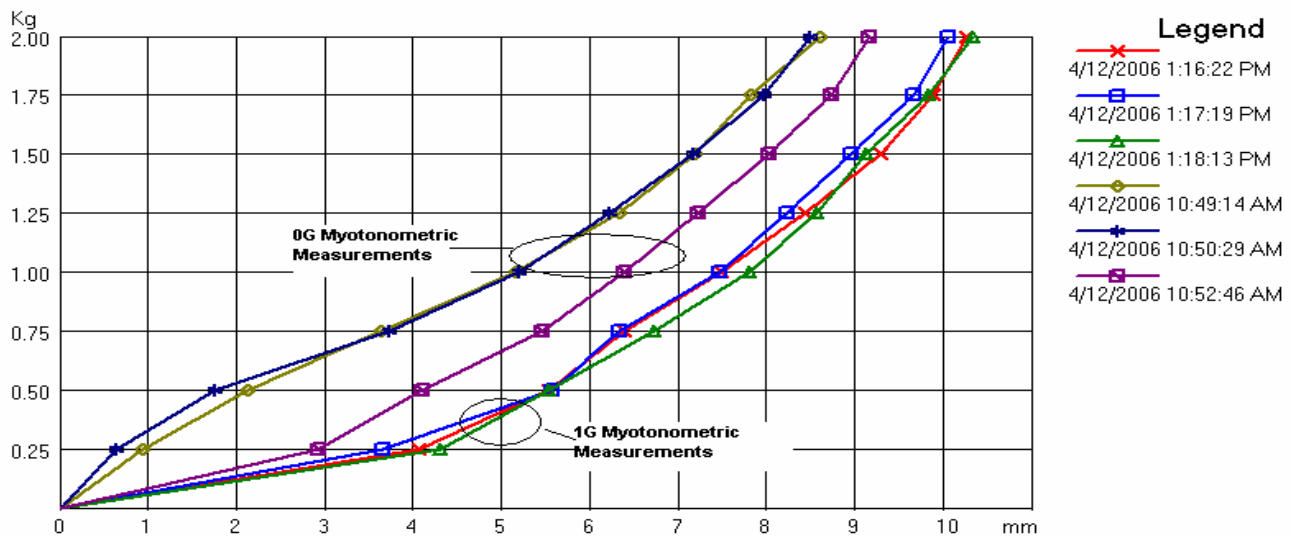


Figure 3. Myotonometric measurements of soleus muscle at rest during 0 and 1g

This figure shows 3 measurements obtained during 1g and 3 measurements obtained at 0g. It illustrates the high reliability of measurements at 1g and more variance at 0g. It also illustrates the trend toward an increase in muscle stiffness during 0g (less muscle displacement per unit of applied force).

DISCUSSION

The Myotonometer has been shown to produce valid measurements of resting muscle tone^{8,9} and strength^{4,10}. Myotonometric measurements of muscle stiffness (tone/compliance) are highly correlated with surface electromyographic (sEMG)¹¹ and joint torque measurements^{4,5}. The myotonometer has distinct advantages over sEMG and torque measurements that include its portability, ease of use and ability to measure two characteristics of muscle health (tone and strength) in a single testing session that requires less than 1 minute to obtain and display results. Additionally, it is possible to obtain measurements of a single muscle (not just total joint torque).

The Myotonometer worked well in the 0g environment. There were no technical difficulties or malfunctions during parabolic flight. Unfortunately, correlational and reliability statistics were not appropriate secondary to examiner error. The error related to the inability of examiners to obtain measurements from the same location on the soleus muscle during each measurement trial. In order for precise measurements to be obtained myotonometric measurements must be obtained from the same location on the muscle during each trial. This was not possible during the present experiments because our strapping and stabilization procedures were not adequate and examiners struggled to maintain their positions during 0g.

Of interest was a general trend for all subjects to have increased muscle stiffness during 0g, as evidenced by less muscle displacement per unit of applied force (Figure 1). Additional experiments, correcting for potential confounding influences of examiner stabilization problems, would be needed to validate this preliminary finding. Previous results obtained induced 0g during parabolic flight by other investigators, indicate that alpha motor neuron excitability, measured by H-reflex change, increases during 0g^{12,13}. These results are consistent with, and possibly help to explain, presently reported results.

CONCLUSION

The Myotonometer, a portable hand-held computerized device that requires no external power supply, performed well during parabolic flight. Conceivably, the device could be used to monitor astronaut muscle health during prolonged exposures to microgravity and to assess efficacy of muscle health interventions. Astronauts could self-test and assess changes in specific muscles over time. Flight surgeons would be able to use myotonometry data to monitor the efficacy of specific countermeasures to muscle atrophy and to selectively tailor participation of individual crew members in these countermeasures based on these measurements as an indicator of skeletal muscle health.

REFERENCES

1. Leonard CT and Mikhailenok EL. Apparatus for Measuring Muscle Tone. Patent 09/295277(6063044): 5-16-2000.
2. Cannon SC, Zahalak GI. The mechanical behavior of active human skeletal muscle in small oscillations. *Journal of Biomechanics*. 1982;15:111-21.
3. Leonard C, Brown J, Price T, Queen SA, Mikhailenok EL. Comparison of surface electromyography and myotonometric measurements during isometric contractions. *Electromyography and Kinesiology*. 2004;14:709-14.
4. Bizzini M, Mannion AF. Reliability of a new, hand-held device for assessing skeletal muscle stiffness. *Clinical Biomechanics*. 2003;18:459-61.
5. Arokoski JP, Surakka J, Ojala T, Kolari P, Jurvelin JS. Feasibility of the use of a novel soft tissue stiffness meter. *Physiological Measurement*. 2005;26:215-28.
6. Leonard C, Deshner W, Romo J, Suoja E, Fehrer S, Mikhailenok E. Myotonometer intra- and inter-rater reliabilities. *Arch Phys Med Rehabil*. 2003;84:928-32.
7. Aarrestad DD, Williams MD, Fehrer SC, Mikhailenok E, Leonard CT. Intra- and inter-rater reliabilities of the Myotonometer when assessing the spastic condition of children with cerebral palsy. *Journal of Child Neurology*. 2004;19:894-902.
8. Leonard CT, Stephens JU, Stroppel SL. Assessing the spastic condition of individuals with upper motor neuron involvement: validity of the Myotonometer. *Archives of Physical Medicine and Rehabilitation*. 2004;82:1416-20.
9. Rydahl SJ, Brouwer BJ. Ankle stiffness and tissue compliance in stroke survivors: A validation of Myotonometer measurements. *Archives of Physical Medicine and Rehabilitation*. 2004;85:1631-7.
10. Gubler HC, Marx BJ, Leonard CT. Comparison of the Myotonometer with sEMG and isokinetic dynamometry as measures of muscle strength during isometric knee extension. *Journal of Orthopedic and Sports Physical Therapy*. 2005;35:85-6.
11. Leonard CT, Brown JS, Price TR, Queen SA, Mikhailenok EL. Comparison of surface electromyography and myotonometric measurements during voluntary isometric contractions. *J. Electromyogr. Kinesiol*. 2004;14:709-14.
12. Ohira Y, Nomura T, Kawano F, Soduh M, Ishihara A. Responses of Hoffman-reflex in human soleus to gravity and/or fluid shift. *J Gravit Physiol*. 2002;9:129-30.

13. Miyoshi T, Hotta K, Yamamoto S, Nakazawa K, Akai M. Somatosensory graviception inhibits soleus H-reflex gain in humans during walking. *Exp Brain Res.* 2006;169:135-8.

PHOTOGRAPHS

JSC2006E14452 to JSC2006E14470

VIDEO

- None

Videos available from Imagery and Publications Office (GS4), NASA/JSC.

CONTACT INFORMATION

Charles T. Leonard, Ph.D.
Director, The Motor Control Research Laboratory
School of Physical Therapy and Rehabilitation Sciences
The University of Montana
Missoula, MT 59803
Charles.leonard@umontana.edu
Phone: 406 243 2710

TITLE

A Low-Intensity Mechanical Countermeasure to Prohibit Osteoporosis in Astronauts During Long-Term Spaceflight (VIBE)

FLIGHT DATES

April 14, 2006

PRINCIPAL INVESTIGATOR

Clinton Rubin, State University of New York at Stony Brook



GOAL

The osteoporosis that develops in microgravity is one of the greatest hurdles to an extended human presence in space. Earth-based animal and human studies have demonstrated that extremely low-magnitude mechanical loading, if imposed at a high frequency, is strongly anabolic to the skeleton and can serve to inhibit the bone loss that typically parallels disuse. This experiment is designed to evaluate the efficacy of this unique biomechanical countermeasure to inhibit the microgravity-induced osteoporosis. To achieve this in a non-invasive, non-pharmacologic way would have tremendous impact in space, and would also address the bone loss that plagues over 20 million people worldwide each year on Earth.

OBJECTIVES

The general objectives for the VIBE Experiment was to evaluate the feasibility of transmitting whole body vibrations in weightlessness and demonstrate that the subject could use, and the prototype equipment function, in 0g. Effective transmission of these vibrations is essential to the potency of the VIBE treatment as a bone and muscle wasting countermeasure. Ground-based experiments have shown that applying a load (approximately 60% of body weight) to the shoulders allows a high degree of signal transmission. These experiments modeled

weightlessness by placing subjects in a recumbent position. This position serves to remove gravitational forces in the main loading axis. Flight experiments on the C-9B provide a critical test to evaluate device performance in microgravity prior to flight aboard the ISS, and therefore represent a critical step in the VIBE Experiment's development. Data from these tests confirmed results obtained in the recumbent ground-based model. Aside from this critical proof of principle in microgravity, the current device setup and design was evaluated with respect to its utility and ease of use for subjects in microgravity.

OUTCOMES

Four subjects successfully used the vibrating platform during the parabolic flights. The vest was easily donned, and the coupling via the harness system rapidly executed. Full extension was well tolerated, and the vibration felt by all subjects. Output from the plate demonstrated that, even with shifting during stance, and thus variations in the axial force generated by the subject, the plate quickly adapted to retain a 0.3g, 30Hz acceleration through the subject, at 60% of the applied force. The C-9 flight test of the equipment and feasibility of the protocol was considered a success by all measures.

METHODS AND MATERIALS

The C-9 VIBE experiment protocols were conducted very similarly to how they will be conducted on board the International Space Station. The VIBE subjects equipped themselves with the VIBE Harness and entered the suspension system (VIBE C-9 Fixture). The VIBE Plate attached to the Long Duration Foot Restraint (LDFR) was hung from the suspension system. Meanwhile, the subject squatted to attach the VIBE Subject Loading Device (VLD) cord to each of the VLD canister clips using carabineers, thus connecting the subject to the VIBE Plate. The VLD cord was equipped with numerous D-rings that could be used to adjust the amount of load until 60% of the subject's body weight was applied in total to the harness. The subjects placed their feet onto VIBE Plate and extended their legs as if they were standing. Reference figure 1a below for a view of the setup.



Figure 1a. VIBE Subject on board the C-9 standing on the HRF VIBE Plate during micro-g, receiving the vibratory signal while being loaded to VIBE Plate at 60% body weight.

One accelerometer was attached to the top surface of the VIBE Plate using double-sided tape. It was placed between the subject's ankles. The second accelerometer was attached to a bite bar using double sided tape. The bite bar was wrapped in cellophane for cleanliness, and placed into the mouth of the subject. The subject used his/her molars to grip the bar, so that it exits the mouth at a 90-degree angle to the body. Due to a data recording dysfunction, the transmissibility experiments are not reported here, but, by report of all subjects, transmissibility was considered very high in each participant.

Following the setup, the VIBE Plate was activated once 40 lbs of force was exceeded. Recordings were made at 1000 Hz for 20-30 seconds during the 0g portion of the parabola using a LabVIEW program generated by the VIBE team. Following the 0g portion, the VLD canister carabiner was relocated to a different D-ring on the VLD cord in order to increase or decrease the load on the subject, and the measurements were repeated for each subject. This was repeated incrementally 4 to 6 times, depending on the height/weight of the subject until the lowest force was achieved. Subjects were rotated so that recordings were made of several individuals.

Figure 1b shows the output readings from the device itself, with the line that starts higher indicating force through the harness, and the line that starts lower indicating peak-to-peak acceleration. Note that as the force fell below 40 pounds (e.g., knees bent), the plate shut down, as designed. Further, with shifting of posture on the plate, and thus altering the total force imparted through the harness system, the 0.3g peak-to-peak acceleration kept constant, indicating that the closed-loop feedback system worked effectively.

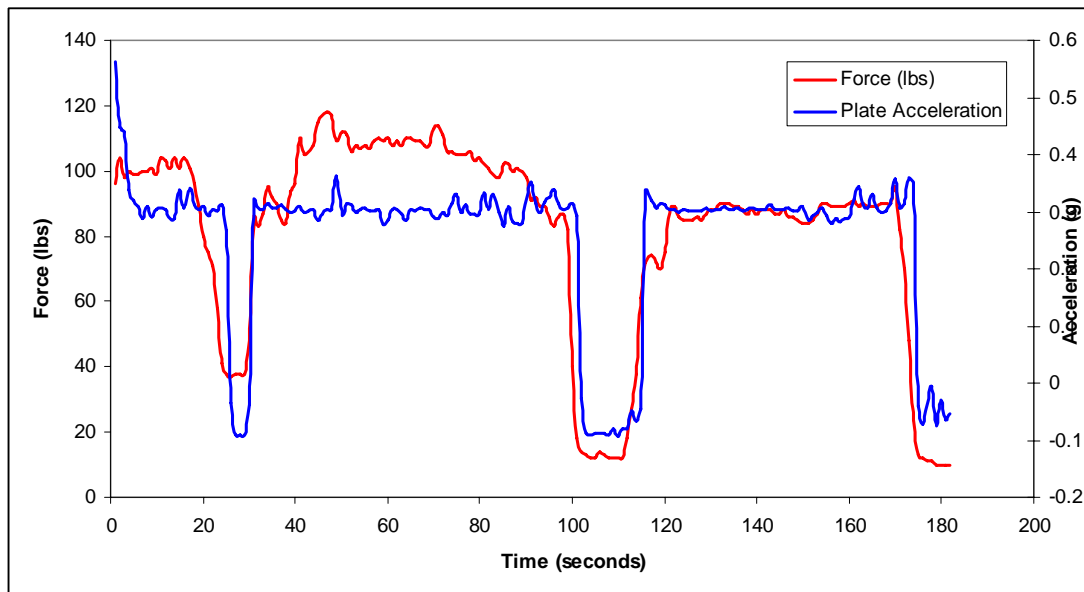
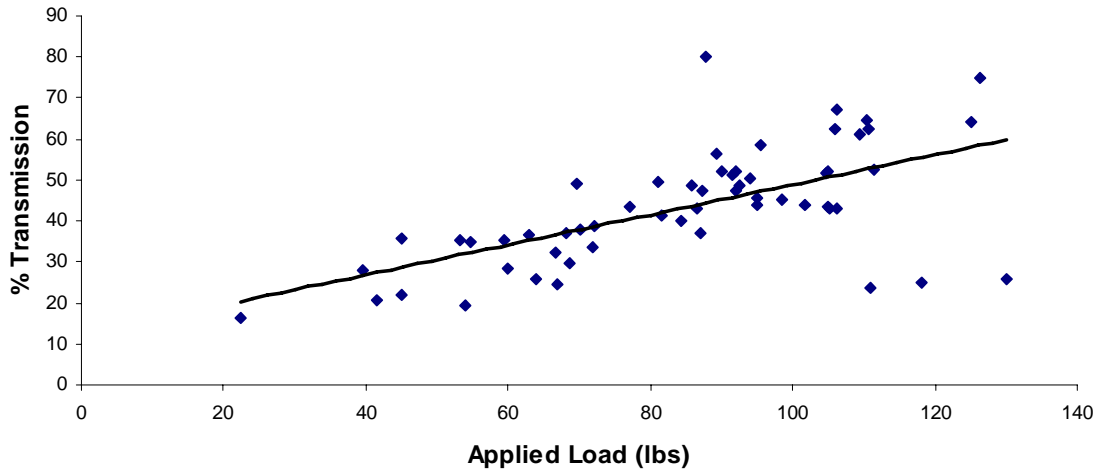


Figure 1b. Data derived from the device indicating, as a function of time, that subtle alterations in peak force (e.g., shifting in the harness system) were readily recognized and accommodated by the sensor system, and 0.3g, peak to peak, of a 30Hz dynamic acceleration were imparted to the subject. Once the harness system fell below 40 lbs of force, the plate shut down.

Transmission was calculated using MATLAB as the ratio of acceleration of the bite bar to the acceleration of the top plate. Load Cell recordings were used to compare the transmission to the applied body weight. Data was compared to data collected at SUNY Stony Brook (SB) to verify significant transmission of vibration. Studies at SUNY SB have shown an increase in transmission with an increase in applied load. At an applied load of 60% of the subject's body

weight, transmission equivalent to 80% of the transmission seen under the effects of gravity could be achieved.

As the applied load is increased, Transmission increases. X-axis shows the applied load in lbs applied to the body. The Y-axis shows the %transmission at the bite-bar. Combined data of 10 subjects shown



The following table describes the C-9 in-flight equipment that was utilized for the experiment.

Table 1. In-Flight Equipment Description

ITEM NAME	QTY	CLASSIFICATION	SIZE (in)	WEIGHT (kg)
VIBE Plate Assembly	1	Class III	21 x 22 x 5	23
VIBE Harness	1	Class III	18 x 20 x 1	3
Long Duration Foot Restraint	1	Class III	42 x 14 x 15	~3
VIBE C-9 Test Fixture	1	Experimental	42 x 31 x 36	33
VIBE Power Cable	1	Experimental	1 x 96 L	~ 1
National Instruments SCXI-1000 Accelerometer Chassis	1	Experimental	7 x 8 x 10	10.0
Dell Laptop Inspiron 600m	1	Experimental	10 X 12X 1.5	2.5
Dell Laptop AC Power Adapter	1	Experimental	5 X 12 X 1.5	0.5
Laptop DAQ Card/Cable	1	Experimental	.5 Dia x 78 L	0.5
Accelerometer Junction Box	1	Experimental	5 X 4 X 3	0.25
Accelerometers Crossbow CXL 10HF3	3	Experimental	1 X 1 X 1	0.15
Camera	1	Canon Digital Camera	5 x 3 x 3	0.95
Double Sided Tape	1 roll	Double sided tape used to secure the accelerometers to the bite bar, VIBE Plate and subject's shin	Standard roll of tape	< .1
Cellophane	1 sheet	Plastic-type material used to cover each wooden bite bar	8.5 x 11	< .01 kg
Bite Bar	5 ea	Wooden paint stirring strip used to mount an accelerometer to determine vibration transmissibility	5 x 1 x .125	0.1
Scissors	1	Small pair of scissors to cut tape and cellophane	5 x 1 x 0.25	0.2
Athletic Tape	1	Standard Ace bandage to secure accelerometer to shin	1.5 x 1.5 x 1 (rolled) 1.5 x 40 x 0.1 (unrolled)	0.075

VIBE Plate Assembly (Figure 2)

Oscillating platform used to provide the 30 Hz/0.3g acceleration/vibrations to the subject's lower extremities and spine in a microgravity environment. Requires a 28 VDC power source and operates at about 5.0 amps steady state when in vibration mode. Assembly includes a touch screen display for a user interface, single power connector, "On/Off" switch and a circuit breaker. Other major components described below that make up the VIBE Plate Assembly include the VIBE Subject Loading Device, VIBE Plate Deployment Device and the VIBE Media Devices.

The VIBE Loading Devices are spring-loaded canisters that are secured to the side of the VIBE Plate assembly and generate the required forces for the subject loading to the VIBE Plate in microgravity. They are capable of generating up to 75lbs of force for each canister.

The VIBE Deployment Device is an attachment device that allows the VIBE Plate to be attached to the LDFR, which is deployed onto a standard Express-type rack seat track. The VIBE Deployment Device also provides the vibration isolation of the VIBE Plate to the ISS or other vehicle.

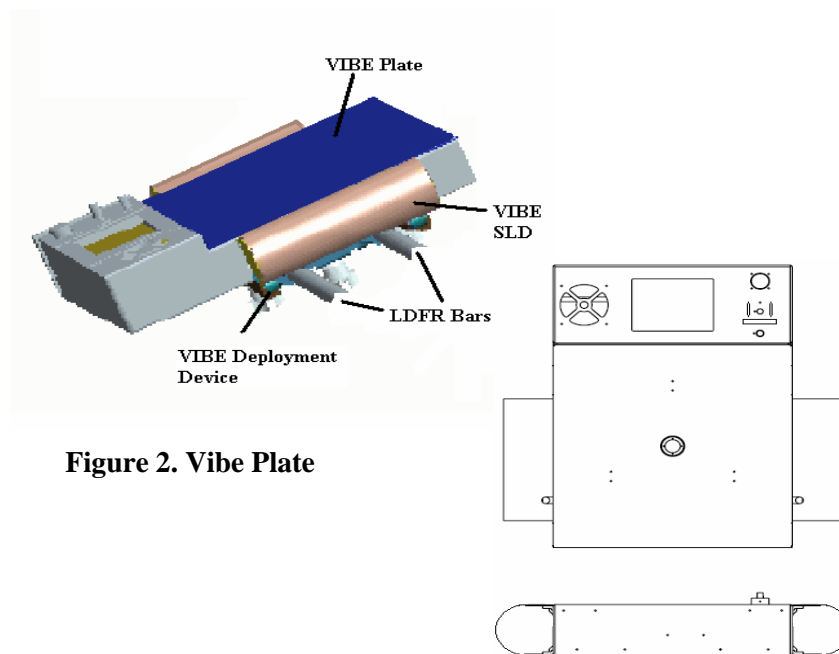


Figure 2. Vibe Plate

VIBE Harness (Figure 3)

The VIBE Harness is a softgoods harness used to provide constant force between the subject and the VIBE Plate Assembly. The harness is worn by each subject and is a one-size fits all design that allows adequate loading through the shoulders comfortably during the 10 minute vibration treatment. There are two chest region clips that can be adjusted for comfort, and underneath the armpits region are two carabiner clips that are used to connect to the VIBE Harness Tether during VIBE operations. The VIBE Harness Tether is a Nomex strap consisting of seven evenly spaced D-rings that allow different loads to be placed on the subject. The opposite end of the tether is a carabiner that clips into the VIBE Loading Device clevis to make the final connections.



Figure 3. VIBE Harness and VIBE Harness Tethers



Figure 4: Long Duration Foot Restraint

The LDFR is an ISS-provided part constructed for specific use to allow crewmembers in orbit to anchor themselves via their feet to a rack face for various tasks. The VIBE experiment team was utilizing the LDFR to deploy the VIBE Plate Assembly in the ISS onto a rack as well as for this application in the C-9.

VIBE C-9 Fixture (Figure 5)

The VIBE C-9 Fixture is a specially designed device that provides a simulated rack face seat track and attachment mechanism to the C-9 floor to deploy the VIBE Plate and test subject within the C-9.



Figure 5: VIBE C-9 Fixture

VIBE Power Cable (no figure needed)

The VIBE Power Cable is a power cable that connects the VIBE Plate and the C-9 utility panel for DC power. The cable has been constructed with appropriate connectors to interface to the VIBE Plate power connector and the C-9 10A connector.

Figure 6 shows the National Instruments SXCI-1000 Chassis and Dell Laptop with cabling. The data acquisition devices utilized for this experiment protocol include the NI SCXI-1000 Chassis with 8-channel accelerometer module and a Dell Laptop. The accelerometers are connected to various positions on the VIBE Plate, VIBE C-9 Fixture, and human test subject to take various acceleration readings during the experiment protocol. The chassis and laptop require 115V AC power to operate the devices.

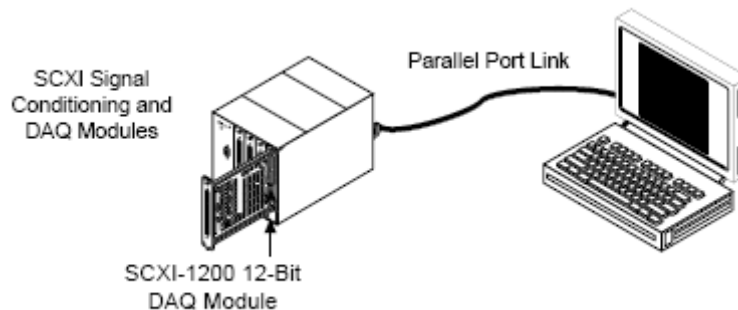


Figure 6. Laptop and SCXI Chassis with Accel DAQ Module

Operational Details (Procedures)

During the flight, the VIBE C-9 fixture equipment and LDFR were installed into their final position. The size of the fixture and its operational concept was such that it was bolted to the C-9's floor space and remained there for the duration of the flight. All the other equipment necessary to conduct the experiment was stowed away in the C-9's common stowage area during takeoff and landing phases of the flight and was deployed once the go ahead was given by the flight director during the in-flight phase. Refer to figure 7 for a model of this layout.

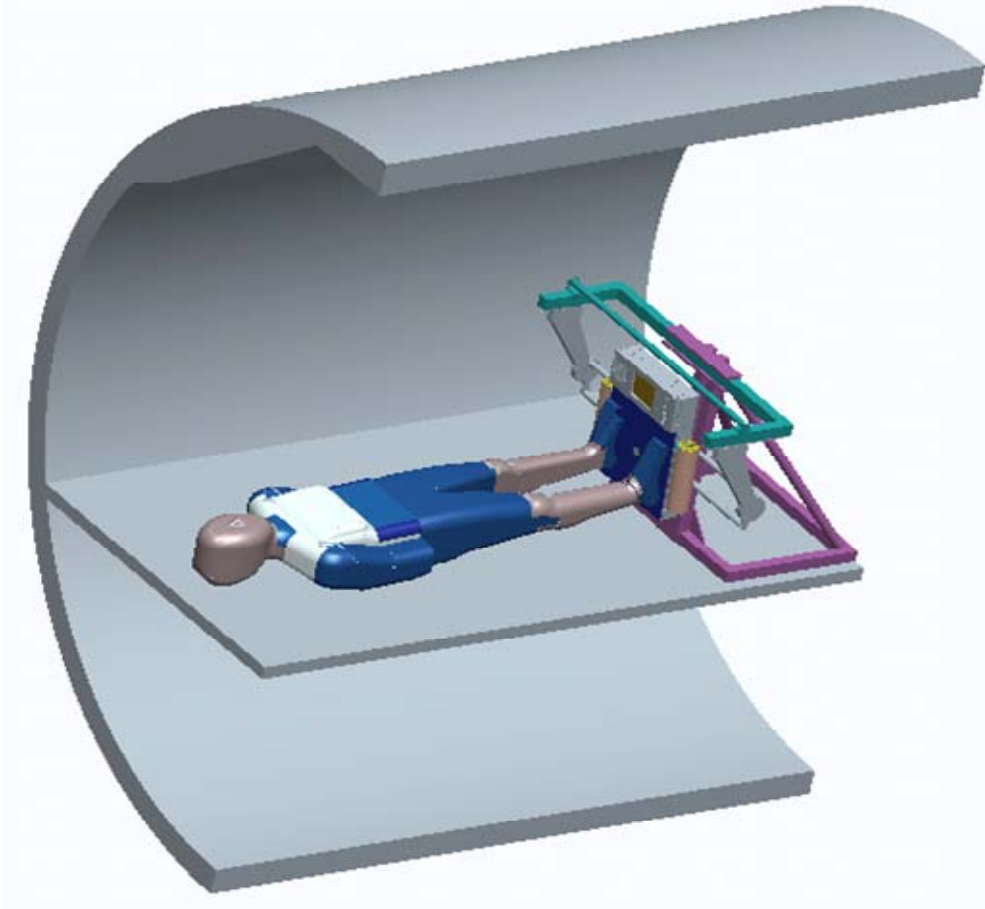


Figure 7. VIBE Experiment deployed sketch in C-9

The VIBE Plate, VIBE Harness, and the data acquisition components including the NI SXCI-1000 chassis, Dell laptop and accelerometer black box were removed from the stowage locations once level flight was reached and the team set up the experiment as needed.

The VIBE Plate itself was first installed onto the LDFR via the VIBE Deployment Device. Once the VIBE Plate was secured to the LDFR, the VIBE plate power cable was connected to the VIBE Plate.

The NI SXCI-1000 chassis and accelerometer black box were strapped to the C-9 floor using standard C-9 straps provided previously, and the laptop was configured with Velcro to attach it to the C-9 floor. The laptop and DAQ devices require AC power, so various power cables were also run from the test equipment to the C-9's standard power multi-outlets.

Once the equipment was all set up, the first subject donned the VIBE harness and prepared for the 0g portion of the flight.

The subject into location once the parabolas began. During takeoff and landing, all personnel were seated at the rear of the plane. Figures 8 and 9 show a layout of the equipment in relation to the C-9 for each scenario.

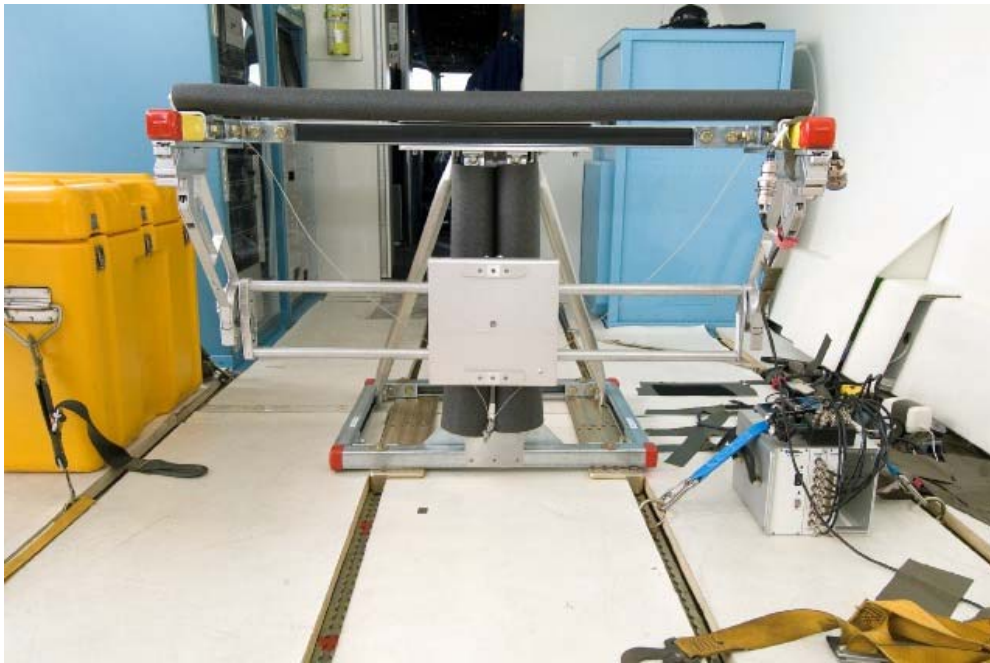


Figure 8: Front view layout of the VIBE C9 fixture and LDFR and deployment device for inflight operations

RESULTS

For each run the subjects were to follow the set of protocols described below:

- a. Ride out a couple of parabolas to “get used to it”
- b. Verify the VIBE Plate, LDFR and VIBE C-9 fixture was secured
- c. Verify the Accelerometer #1 was placed onto the top surface of the plate
- d. Verify the Accelerometer #2 was placed on the bite bar
- e. Verify the Accelerometer #3 was placed at subject’s shin
- f. Subject dons VIBE Harness and configures it for vibration treatment
- g. Just prior to entering the 0g portion of the parabola, the operator sets up the VIBE Plate to begin vibrating. The laptop system and DAQ devices are also set up ready to collect data
- h. Also, just prior to entering the 0g portion of the parabola, the VIBE subject orients him or herself to position the feet onto the VIBE Plate top surface and connect the VLD Strap to the VIBE Harness with assistance from the experiment team. At this point the subject is lying down on the C-9 padded floor. Subject bites down on bite bar with accelerometer attached to it
- i. Once the 0g portion is achieved, the subject extend his or her legs to load on the VIBE Plate to X% body weight (initially targeting 60% and ranging from 50-70%)
- j. During the 0g portion, the data collector begins recording approximately 25 seconds of acceleration data from the various accelerometers or until the 0g portion is coming to an end.



Figure 9. ISO view layout of the entire VIBE System setup during in-flight operations in the C-9.

- k. Coming out of the 0g portion, the subject stops the VIBE Plate vibrations by squatting down to remove load from the VIBE Plate, and the data collector stops the acceleration measurements.
- l. This is then repeated for the various loads and subjects.

The VIBE experiment group had 4 subjects who were tested and one operator/data collector who collected data. The first subject for VIBE was Dr. Clint Rubin, the principal investigator for this BFR experiment.

CONCLUSION

The VIBE equipment worked well and was considered both comfortable and easy to use by the subjects (including one subject who had never used the device before, and was trained, in flight, to use it in approximately 30 seconds). It was clear that there was significant transmissibility, as predicted by the bed rest analog, and that the harness system and the 0.3g, 30Hz signal was well tolerated by all involved. The experiment was considered a success by all parties.

PHOTOGRAPHS

JSC2006E14601 to JSC2006E14660

VIDEO

- Zero G flight week April 11 -14, 2006, Master: DV0554

Videos available from Imagery and Publications Office (GS4), NASA/JSC.

CONTACT INFORMATION

Clinton T. Rubin, Ph.D.
State University of New York at Stony Brook
Dept of Biomedical Engineering
Psychology A Bldg 3rd Floor
Stony Brook, NY 11794-2580
Clinton.Rubin@sunysb.edu
631-632-8521

TITLE

Minimally Invasive Diagnosis and Therapy of Microgravity Medical Contingencies

FLIGHT DATES

April 11-14, 2006

PRINCIPAL INVESTIGATOR

Scott Dulchavsky, Henry Ford Health System

CO-INVESTIGATORS

Shannon Melton, Wyle Laboratories, Inc., Life Sciences Group

Doug Hamilton, Wyle Laboratories, Inc., Life Sciences Group

Ashot Sargsyan, Wyle Laboratories, Inc., Life Sciences Group



GOALS/OBJECTIVES

This flight experiment used the previously developed ultrasound imaging methodology to monitor the diameter of the optic nerve sheath during incremental rise of the intracranial pressure. Data were collected to determine the utility, accuracy, and limitations of the method as a non-invasive alternative for ICP monitoring.

This flight experiment also evaluated diagnostic and therapeutic procedures conducted by Crew Medical Officer (CMO) analogs with remote guidance from medical experts.

Primary Objectives

- Determine if transitions to microgravity cause acute changes in intracranial pressure.
- Determine the degree of correlation between the optic nerve sheath diameter and the intracranial pressure measured invasively in the porcine animal model.
- Determine the accuracy of ultrasound performed by experts versus just-in-time trained CMO analogs in the diagnosis of serious injury or illness while in microgravity.
- Perform ultrasound-guided percutaneous aspiration of fluid (urinary bladder and gallbladder) by just-in-time trained CMO analogs under remote guidance.
- Evaluate the micro-laparoscopy procedures performed by experts versus just-in-time trained CMO in the diagnosis of serious injury or illness while in microgravity.
- Perform percutaneous aspiration of fluid collections (bladder/gallbladder) under microlaparoscopic guidance.
- Determine the alterations in disease presentation, diagnosis, and human factor requirements for use of ultrasound and mini-laparoscopy in microgravity.

INTRODUCTION

The medical care challenges imposed by the unique environment of space require the development of novel diagnostic and treatment strategies for illness and injury of crewmembers. The current concept of operations for medical care on the International Space Station employs non-physician CMO with limited training prior to flight. The CMO is expected to perform many medical procedures should the need for those procedures arise during flight. This experiment evaluated terrestrial clinical methods, which were adapted for both microgravity and inexperienced (minimally skilled) crewmember operators. These diagnostic or therapeutic interventions were performed by a CMO analog who received real-time guidance from a remote expert. These invasive procedures included the use of ultrasound imaging for diagnosis and treatment of many medical disorders that would otherwise require surgery. The experiment evaluated the ability of a CMO, under the real-time guidance of an expert, to insert a needle into various organs for the purpose of stabilizing an acute medical problem. This experiment also evaluated the ability of a CMO, under the real-time guidance of an expert, to perform mini-laparoscopic surgery (a small camera-equipped device is inserted in the abdomen through a small access portal) for diagnosis of illness or injury and for manipulations such as placement of a draining tube into an infected or traumatized organ.

In addition, the optic nerve sheath was monitored with ultrasound to measure potential changes associated with parabolic flight gravity fluctuations, as well as with an artificially elevated ICP. Intracranial pressure was also monitored with a pressure transducer in the ventricle.

METHODS AND MATERIALS

Four C-9 microgravity flights were performed using a porcine model for all procedures.

Hardware

GE Twin Ultrasound (GE Medical Systems, Milwaukee, Wisconsin)

This device is a portable ultrasound system that has been approved for clinical use. The system includes the abdominal (convex), small parts (micro-convex), and small parts (linear) probe.

Eagle 754AP Ventilator (Impact Instrumentation Inc., West Caldwell, New Jersey)

This device was used to maintain breathing parameters throughout the flight. It is a self-contained ventilator-compressor-blender weighing just over 12 pounds, with graphics display, monitors and alarms.

Special Medical Emergency Evacuation Device (Impact Instrumentation, Inc)

The Special Medical Emergency Evacuation Device (SMEED) is a mounting system used to secure medical equipment to a patient litter. SMEED is used principally by the military during ground and aeromedical transport. It was used in this series to secure both therapeutic and diagnostic imaging equipment.

Datex Ohmeda Critical Care Monitor (Welch Allyn Protocol, Inc. Beaverton, Oregon)

The Datex critical care monitor was used to monitor ECG, oxyhemoglobin, pulmonary artery pressure, central venous pressure (CVP), intracranial pressure, and core temperature.

ChillBuster Electric Blanket (ThermoGear, Inc., Tigard, Oregon)

The ChillBuster is a fully portable electric blanket that works via a rechargeable battery or AC power supply.

Storz Microlaparoscope (KARL STORZ, Endoscopy-America, Inc., Culver City, California)

This device is a high-definition laparoscope that is FDA approved for clinical use.

Storz Endoscopy System (KARL STORZ, Endoscopy-America, Inc., Culver City, California)

This system included a camera, fiber optic light source and insufflator that are FDA approved for clinical use. This system interfaces with the microlaparoscope.

Media Rack (Wyle Laboratories, Inc., Life Sciences Group, Houston, Texas)

A flight-rated rack that contains five video recording systems, 3 audio channels and 2 real-time monitors that can be switched between the multiple video sources. All video systems have overlays that display flight time, g-loads, and parabolas. A remote viewing station was set up in a separate area of the plane with two-way audio loops for communication and video from the ultrasound or laparoscope.

VGA2USB Video Capture (Ephiphan, Ottawa, Ontario, Canada)

This device allowed the video capture of the GE Twin Ultrasound from the VGA output.

Camino Multiparameter Pressure Monitor (Integra Life Sciences, Plainsboro, New Jersey)

This device monitored intracranial pressure transducers and interfaced with the Datex CCM.

IVantage Infusion Pump (Delphi Medical Systems, Troy, Michigan)

This is a small pump to provide IV fluids at a constant rate and is FDA approved for clinical use.

Procedures

Intracranial Pressure Measurements

Absolute values of the intracranial pressure were measured with a pressure transducer placed in the parenchyma of the brain through a small port in the parietal bone. A second port was placed on the contralateral side to introduce saline under pressure monitor control. The optic nerve sheath diameter was measured with ultrasound as ICP was increased by intra-parenchymal small volume infusion. A control study was previously conducted to correlate ICP with optic nerve sheath diameter. This study was conducted to observe the normal changes in ICP and optic nerve sheath diameter with microgravity and the additional effect of increased ICP under these conditions.

Ultrasound-guided therapeutics with remote guidance

A minimally trained Crew Medical Officer analog was remotely guided by an ultrasound expert (radiologist) to:

- Identify the gallbladder with ultrasound and then insert a needle for drainage.
- Identify the urinary bladder with ultrasound and insert a needle for drainage.
- Identify free fluid in the abdomen (injected prior to flight) and insert a needle for drainage.

Laparoscopic-guided therapeutics with remote guidance

A minimally trained Crew Medical Officer analog was remotely guided by a laparoscopic expert (surgeon) to:

- Identify the gallbladder with a laparoscope and then insert a needle for drainage.
- Identify the urinary bladder with a laparoscope and insert a needle for drainage.
- Identify free fluid in the abdomen (injected prior to flight) with a laparoscope and insert a needle for drainage.

Hardware Evaluation

- Evaluation of a small IV pump

RESULTS/DISCUSSION

Quality of ultrasound and laparoscopic images collected in microgravity by CMO analog

Preliminary review of ultrasound video by internal sonographers indicates that the imagery is sufficient to formulate a diagnosis of the scanned organ(s). Further analysis is ongoing.

Minimally invasive therapeutics

- The team was successful inserting a needle into all targets with guidance from either both ultrasound or laparoscopy.
- As anticipated, movement of internal organs was observed during the flight. The changing positions required identification of organs during one or two parabolas and the repositioning of the laparoscope or ultrasound and needle placement in one parabola cycle. Although the team was successful in needle placement, they felt that the task would be much simpler in a constant 0g environment.
- Training for these activities was less than four hours. The CMO analogs felt the biggest training issue was understanding how hard and fast it was necessary to push to insert a needle or trochar. Once this task was completed, manipulating the laparoscope under remote guidance was not difficult.
- One animal was extremely difficult to insert the needle under ultrasound guidance. When the laparoscope was placed in the same animal it showed extensive scar tissue in the abdomen from some previous illness. This scar tissue was not visible with ultrasound.

Intracranial Pressure Measurements

Absolute values of the intracranial pressure were measured with a pressure transducer, and expected offsets were observed with transitions from 1g – 0g - 2g. The intracranial pressure was measured using a non-fluid-filled catheter and therefore ICP pressures seen by the transducer did not have any hydrostatic offsets. The arterial pressure and CVP transducers were zeroed to the same hydrostatic level of the ICP transducer tip and therefore calculated central perfusion pressure (CPP) was accurate during microgravity periods. The porcine model does not store a significant amount of blood in the lower extremities compared to humans and therefore blood volume shifts and CVP changes with microgravity were not large. All microgravity-induced

changes in pressure measured by fluid-filled catheters can be explained by loss of hydrostatic offset recorded during the zero-offset calibration procedure.

The optic nerve sheath images were recorded for further refinement of retrospective measurement for correlation with ICP, CVP and CPP. A broadband micro-convex probe was used with the upper frequency limit of 10 MHz. Changes in the shape, structure, and linear dimensions of the optic nerve as imaged by ultrasound were also documented. The preliminary impression is that the optic nerve sheath diameter as measured with ultrasound correlated well with the actual invasively measured intracranial pressure, up to the pressure levels of 60 mmHg.

Hardware Evaluation

- All animals were maintained in the surgical plane of anesthesia throughout the preflight and flight phases of the experiment.
- The IVantage IV pump worked intermittently and seemed to stop working during the 0g part of each parabola. The device recovered during the high-g loads of the pullout each time. However this may have been due to the thickness of the medication that was being delivered with the pump.

CONCLUSIONS

- Overall, the CMO analogues and remote guidance experts agreed that remotely guided ultrasound needle placement and remotely guided laparoscopic needle placement in microgravity is “very doable” with minimally trained operators.
- Optic sheath diameter seems to correlate well with the value of intracranial pressure. Further analysis of data is expected to result in an unambiguous assessment of such measurement as a non-invasive indicator of ICP. While precise quantitative measurement of ICP may not be possible, trend monitoring and semi-quantitative estimation is still a valuable non-invasive capability to assess ICP. Our data confirm anecdotal results of similar nature obtained in small numbers of ICU patients with abnormal intracranial pressure levels. The changes in optic nerve sheath diameter may be a more valuable clinical tool than absolute values for the purpose of monitoring therapy.
- Further analysis of the data is warranted and final results will be published in peer-reviewed journals.

ACKNOWLEDGMENTS

This activity could not have been completed without the help of many people. The investigators would like to acknowledge the following individuals for their efforts:

- Kathleen Garcia, Rick Pettys, Terry Guess, and Ash Moghaddam, Wyle Laboratories, Inc., Life Sciences Group
- Dr. David Kwon, Henry Ford Health System
- Mr. Bill Oddo, Detroit Receiving Hospital
- Dr. Don Deyo and team at the University of Texas Medical Branch

PHOTOGRAPHS

JSC2006E14534 to JSC2006E14570

VIDEO

- None

Videos available from Imagery and Publications Office (GS4), NASA/JSC.

CONTACT INFORMATION

Scott Dulchavsky, MD
Henry Ford Hospital System
2799 W. Grand Boulevard K8
Detroit, Michigan 48202
Sdulchal@hfhs.org
313-916-9903

TITLE

Vestibular Adaptation in Parabolic Flight

FLIGHT DATES

April 11-14, 2006

April 18-21, 2006

PRINCIPAL INVESTIGATOR

Mark Shelhamer, Johns Hopkins University

CO-INVESTIGATORS

Faisal Karmali, Johns Hopkins University

Ondrej Juhasz, Johns Hopkins University



GOAL

To determine the neural mechanisms of human adaptation to parabolic flight.

OBJECTIVES

The purpose of this research study is to examine the ability of human subjects to adapt various behaviors (reflexive eye movements and orientation perception) to different conditions of gravito-inertial force (g level). The resulting information will be of value in determining how the brain processes gravity information, in learning how humans can maintain different adapted states in different g levels simultaneously, and in aiding the design of future space flight programs.

INTRODUCTION

On their first exposure to parabolic flight, many people experience motion sickness. Some subjects have been known to consider at this time not returning flying the following day. Their experience the second day is, however, usually considerably better than that of the first day; motion sickness is much less prevalent. The adaptation process is dramatic and rapid, and some of it appears to occur during the intervening period while not flying. This phenomenon demonstrates aspects of adaptation and consolidation. One question that immediately arises is, does adaptation to parabolic flight involve adaptation to each separate gravity level (context-specific) or is there a more generalized adaptation to the overall flight experience (implying for example a non-g-specific change in sensory weighting)? We are studying this with a series of measurements before, during, and after flight, on sets of first-time flyers and experienced flyers.

This study consists of multiple related experiments to learn more about how the human nervous system adapts to different gravity levels. We are particularly interested in adaptation of vestibular-mediated responses such as orientation perception and reflexive eye movements. These adaptive processes are important because of possible impairments in sensorimotor performance when astronauts undergo transitions between gravity levels. Some of these changes, and the adaptive processes that counteract them, may be similar to vestibular changes in aging and ill people on Earth. In order to investigate these changes, we measure oculomotor and perceptual responses in subjects exposed to various gravity levels, as provided by parabolic flight.

Our most prominent findings to date involve changes in torsional eye position. During the g-level changes of parabolic flight there are changes in torsional eye position (ocular counterrolling: OCR). These changes can be markedly asymmetric [Markham & Diamond 1993, Markham et al. 2000]. This change in torsional alignment may be due to a decompensation of otolith asymmetry in unusual g environments; on Earth, the nervous system presumably compensates for natural asymmetries in otolith organ properties, but in hyper-g and hypo-g this compensation is inappropriate and produces torsional misalignment. A similar disconjugate change has been found during space flight [Diamond & Markham 1998].

METHODS AND MATERIALS

We carried out a mix of sensorimotor and perceptual measures designed to examine a range of physiological responses, from low-level reflexive through high-order perceptual. Each test was carried out in level 1g flight and in both g levels of parabolic flight, early and late in each flight. Experienced flyers are tested for one flight, since they are expected to exhibit almost immediate adaptation. New flyers are tested over the course of three consecutive flights in order to monitor adaptive changes. All subjects fly without benefit of motion-sickness medication. There are six main tests:

1. Ocular counterrolling (torsion) with the head upright and tilted. Torsional position of each eye is measured with a high-resolution digital camera.
2. Translational vestibulo-ocular reflex (TVOR) during transient lateral head motions. Lateral head motions are imposed by the experimenter, and the resulting reflexive eye movements are measured with a head-mounted video system.
3. Pitch angular vestibulo-ocular reflex (AVOR). The oculomotor response to pitch head movements at about 0.1 to 1.0 Hz is measured with a head-mounted video system.

4. Vertical alignment (skew). Vertical alignment of the eyes is assessed with a high-resolution digital camera.
5. Subjective vertical. The subject's sense of "down" (percept of vertical) is assessed in two ways. For subjective visual vertical, the subject sets a small line on a pair of goggles to the perceived vertical. For "postural" vertical, the subject sets a small indicator rod to the subjective vertical while seated.
6. Roll vection. The subject views a large rotating disk, which produces a sensation of self-rotation in a direction opposite to that of disk motion. The head-mounted video system measures torsion and the subject reports the subjective sense of self-rotation (vection) with a joystick and a verbal rating.

RESULTS

Early results center on three of the six measures, in two subjects who had not previously flown in parabolic flight.

The first result involves static torsional (roll) eye position in different g levels. There was a reduction in disconjugate torsion from the beginning to the end of flight 1. This disconjugacy was reduced from flight 1 to flight 2 and had almost completely abated by flight 3. The disconjugacy depends on g level, and this g dependence decreased with experience, but more slowly with the head tilted than upright. These results show that torsional disconjugacy is initially high but is reduced within the first flight, and the adaptation that occurs is recalled at the start of subsequent flights.

The second result involves compensatory eye movements (VOR) during pitching motions of the head. During active sine-like head movements (~0.9 Hz, 20 deg), eye movements were recorded with a head-mounted video system and head movements with a rate sensor. Gain was computed as the total eye excursion divided by head excursion, for each movement. The gain of this pitch VOR during active head movements depended on the instantaneous g level, but this dependence decreased with experience. Relative to pre-flight testing on day 1, gain early in flight 1 was reduced in 0g and increased in 1.8g. This difference between 0g and 1.8g diminished early in flight 2 (subject 1), and early in flight 3 (subject 2). Gain differences between the g levels decreased more slowly with passive head movements. After the first day of flight, the differences between 0g and 1.8g decreased and became statistically insignificant, showing that the system had adapted a proper response to each gravity state.

Perceived roll rotation (vection) was typically less in 1.8g than in 0g, as expected, and this difference, in general, decreased with experience.

Overall, all responses showed a g-level dependence early in flight that decreased with experience. The rate of adaptation varied between the different measures: ocular alignment (torsion) adjusts the most rapidly, followed by the pitch VOR, then vection. Disconjugate torsion rapidly decreased upon exposure to parabolic flight, and adaptation was retained between flights. This reduction occurred in both 0g and 1.8g, suggesting the operation of a central compensation for otolith asymmetry in each g level. Slower adaptation with the head tilted may occur because less time is spent with the head tilted in parabolic flight. Pitch VOR gain initially decreased in 0g and increased in 1.8g, consistent with an otolith contribution to this response. The difference in gain between the g levels decreased with experience and eventually disappeared, showing that the different otolith contributions in the different g levels are correctly processed after

adaptation. Adaptation was also faster for active than for passive pitch movements. Vection showed a marked difference between 0g and 1.8g, as expected from inhibition by the otoliths, and this difference decreased with experience. Upon adaptation, torsion, pitch VOR, and vection are more properly calibrated in each g level, supporting the hypothesis of a context-specific adaptation of each response.

In addition to these results from our primary experiment, we began to evaluate two pieces of equipment that might be of use in future parabolic flight investigations. One is a portable unit for measuring dynamic visual acuity (DVA). A rate sensor measures the instantaneous rotational velocity of the head; when it exceeds a threshold value, a random character is presented on a hand-held device for a brief time, and the subject must identify the character. This is a test of the ability of the subject to use vestibular signals to generate appropriate compensatory eye movements, and is a functional analog to the pitch VOR measures discussed above. The other device is a portable unit for measuring eye position, using a magnetic search coil that sits on the eye. A larger version of this device is used in many clinics and labs, but this smaller unit has great potential for use in other experimental environments such as parabolic flight.

DISCUSSION AND CONCLUSION

Although we have now flown three out of a planned four weeks in this study, the data analysis is still in its early stages. Current analysis suggests that, in accord with the time course of overall adaptation to parabolic flight, the most low-level of the neural responses that we measured – torsion – shows adaptive changes very rapidly. Higher-level integrative responses – pitch AVOR and roll vection – show clear differences between g levels early in flight, becoming smaller with subsequent flights. These results indicate that low-level responses such as ocular alignment and compensation for otolith asymmetry occur very rapidly, while those responses that require integration of afferent information from several physiological sensors adapt more slowly. Furthermore, some of these adaptive effects take place in a context-specific manner, such that the responses are appropriate for each instantaneous gravity level.

REFERENCES

- A. Berthoz, T. Brandt, J. Dichgans, T. Probst, W. Bruzek, T. Vieville (1986) European vestibular experiments on the Spacelab-1 mission: 5. Contribution of the otoliths to the vertical vestibulo-ocular reflex. *Exp Brain Res* 64:272-278.
- S.G. Diamond, C.H. Markham (1998) The effect of space missions on gravity-responsive torsional eye movements. *J Vestib Res* 8:217-231.
- F. Karmali, O. Juhasz, M. Shelhamer (2006) Adaptation due to repeated exposure to parabolic flight, of static torsional alignment and the pitch vestibuloocular reflex. Presented at the 2006 MidWinter Meeting of the Association for Research in Otolaryngology, Feb. 5-9, Baltimore MD.
- J.R. Lackner, P. DiZio (1993) Multisensory, cognitive, and motor influences on human spatial orientation in weightlessness. *J Vestib Res* 3:361-372.
- J.R. Lackner, A. Graybiel, W.H. Johnson, K.E. Money (1987) Asymmetric otolith function and increased susceptibility to motion sickness during exposure to variations in gravito-inertial acceleration level. *Aviat Space Environ Med* 58:652-657.
- C.H. Markham, S.G. Diamond (1993) A predictive test for space motion sickness. *J Vestib Res* 3:289-295.

- C.H. Markham, S.G. Diamond, D.F. Stoller (2000) Parabolic flight reveals independent binocular control of otolith-induced eye torsion. *Arch Ital Biol* 138:73-86.
- D.M. Merfeld, L.H. Zupan, C.A. Gifford (2001) Neural processing of gravito-inertial cues in humans. II. Influence of the semicircular canals during eccentric rotation. *J Neurophysiol* 85:1648–1660.
- D.M. Merfeld, L.H. Zupan (2002) Neural processing of gravito-inertial cues in humans. III. Modeling tilt and translation responses. *J Neurophysiol* 87:819-33.
- M.F. Reschke, L.N. Kornilova, D.L. Harm, J.J. Bloomberg, W.H. Paloski (1997) Neurosensory and sensory-motor function. In: C.L. Huntton, V.V. Antipov, A.I. Grigoriev (eds), *Space Biology and Medicine. Vol. III. Humans in Spaceflight*. Reston VA: AIAA, pp. 135-193.
- M. Shelhamer, DS Zee (2003) Context-specific adaptation and its significance for neurovestibular problems of space flight. *J Vestib Res* 13:345-362.

ACKNOWLEDGMENTS

This work was funded by NIH grant DC006090.

PHOTOGRAPHS

JSC2006E14432 to JSC2006E14451
JSC2006E14661 to JSC2006E14678
JSC2006E15045 to JSC2006E15057
JSC2006E15198 to JSC2006E15211
JSC2006E15521 to JSC2006E15532
JSC2006E15634 to JSC2006E15633

VIDEO

- Zero G flight week April 11 -14, 2006, Master: DV0554
- Zero G flight week April 17 -21, 2006, Master: 720868

Videos available from Imagery and Publications Office (GS4), NASA/JSC.

CONTACT INFORMATION

Mark Shelhamer, Sc.D.
Johns Hopkins University, School of Medicine
210 Pathology Bldg.
600 N. Wolfe St.
Baltimore MD 21287
mjs@dizzy.med.jhu.edu
410-614-6302

TITLE

Microgravity Investigation of Crew Reactions in 0g (Adapt)

FLIGHT DATES

April 18-21, 2006

PRINCIPAL INVESTIGATOR

Dava Newman, Massachusetts Institute of Technology



GOAL

The Adapt experiment focuses on understanding the mechanisms by which astronauts adapt to, move about, and develop motor strategies for differing gravity environments. The overall goal of this research program is to improve astronaut performance and efficiency through the use of rigorous quantitative dynamic analysis, simulation, and experimentation. This goal will be achieved by studying the neural adaptation process that permits astronauts to efficiently perform movements across a spectrum of gravity (i.e., microgravity, moon, Mars, and Earth). The Adapt experiment will quantitatively characterize (e.g., muscle groups used and joint torques required) the skills and movement strategies that veteran astronauts use to move their bodies through altered gravity environments and how the motor control strategies develop over time during long-duration spaceflight missions. A key hypothesis of the Adapt experiment is that a single adaptation process can be identified, that is responsible for the adaptation seen across the entire gravity spectrum.

The Adapt research effort investigates the locomotor skills required to move one's entire body from place to place while in orbit, as well as the ability to reorient oneself. Observing astronaut skills and performance requires a highly accurate data acquisition system. The Adapt sensors and

accompanying kinematic video system will provide a complete picture of the astronauts' control strategy from calculated joint torques that can be computed from the coupled kinetic and kinematic measurements (based on CCD cameras that enable noninvasive motion capture). Knowledge of the joint torques will permit a detailed analysis of the joint and musculoskeletal dynamics employed to execute motions as well as the neural adaptation process in altered gravity. Understanding the adaptation process will facilitate the development of new training techniques that encourage astronauts to develop appropriate movement strategies prior to exposure to the altered gravity environment and during transition to another gravitational environment.

OBJECTIVES

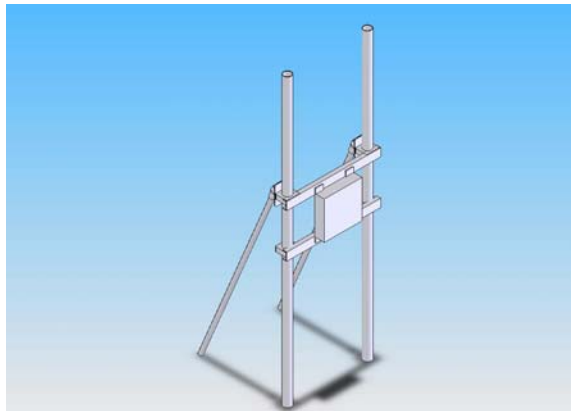
The primary purpose of the C-9 reduced gravity Adapt experiments is to validate the hardware, software, experiment protocol, analysis, and modeling techniques for the Adapt flight experiment planned for the International Space Station (ISS).

METHODS AND MATERIALS

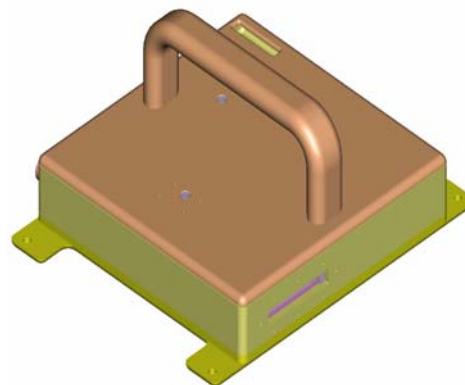
In order to validate the techniques for the experiment planned for the ISS, subjects performed prescribed body motions closely resembling those planned for the Adapt flight experiment using the Adapt sensor restraints. Data were collected using sensors and video cameras.

Equipment

The Adapt setup on the C-9 consisted of three braced mounting structures, each of which had an Adapt sensor assembly attached (Figure 1), and two stand-alone camera poles. The camera poles were placed such that detailed motion data could be obtained in the vicinity of the primary sensor. An additional camera pole was configured such that an added motor-control task was possible. All mounting structures and camera poles were attached to the aircraft floor using the standard mounting bolts. Figure 2 shows an image of the setup from the rear of the aircraft.



(a)



(b)

Figure 1. (a) The braced mounting with sensor attached and (b) a close-up of the sensor details with a hand restraint attachment.



Figure 2. Adapt setup as viewed from the rear of the aircraft.

Laptops were used during the experiment to collect data from each of the sensors. The sensors were zeroed during the first parabola at the beginning of the microgravity segment. More information about the sensors and the data acquisition process can be found in Ferguson et al [1]. The laptops were secured during the parabolas with Velcro and stored in the overhead cargo containers for takeoff and landing. Four digital video cameras were used to document the testing. The video cameras were also set up after takeoff and were stowed prior to landing.

Flight Operations

Four members of the team were on the C-9 each day of flight-testing. One team member was responsible for operating the video cameras; one team member was responsible for operating the sensors; one team member acted as experiment director; and the final member acted as the experiment subject. The subjects wore dark clothing and markers at the key joints to simplify the video analysis.

The body motions performed by the subjects included push-offs and landings, traverses, a motion-accuracy game, and self-rotations. The majority of the motions performed were push-offs and landings from and to the Adapt sensors in order to illustrate the subjects' locomotor control strategy. After several push-offs, the subjects would traverse around the three sensors. The traverse involved moving from the primary (push-off) sensor, to the side sensor, to the landing sensor, and back to the primary sensor. In the motion-accuracy game, the subjects put a hoop on a rod (Figure 3). During the game the size of the hoop was decreased in order to see the effects on the subjects' motor-control methodologies. Throughout all these motion experiments, force and moment data were collected from the Adapt sensors in addition to video data that were recorded using the kinematic video system.



Figure 3. The motion-accuracy game [2].

The ability of a person to self-rotate was also examined during several parabolas. Self-rotation is possible through limb manipulation, which changes the body's moment of inertia [3]. Two variants on rotating about the body's long axis (head to toe) were examined for ease, effectiveness, and stability. The first variant involved a continuous rotary motion. In this case, the arms were continuously rotated in conical motions (the rotation axis of the arms was parallel to the rotation axis of the body) while trying to maintain symmetry in order to minimize the cross-coupling of rotations. In the second variant, a four-part motion involving body-twists was performed. These steps were:

1. In the initial stage, the body is straight, arms down and legs spread to the side.
2. The torso is twisted about the axis of intended rotation. (An internal torque at the waist.)
3. The moment of inertia is increased at the top of the body by spreading the arms and decreased in the lower part of the body by closing the legs.
4. In the final stage, the body is untwisted at the waist and the arms are lowered.

RESULTS/DISCUSSION

Figure 4 shows a typical push-off maneuver performed by one of the subjects. During each parabola, at least one complete motion (push-off, landing, push-off, and landing) could be completed. Having four days of flights, allowed data to be collected on five different subjects. Each motion was repeated several times by the subjects in order to obtain information on their adaptation. The data collected from the sensors and kinematic video system is currently undergoing analysis. Figures 5 and 6 show some typical data (forces, moments, and video data) collected using the Adapt sensors, video systems, and supporting software. These data can be correlated in order to obtain the joint torques [4]. With this information, the muscle groups used and the subjects' control strategies can be better understood, leading to an improved understanding of human adaptation.



Figure 4. An image from a typical experimental motion consisting of a foot push-off, hand landing, hand push-off, and foot landing [2].

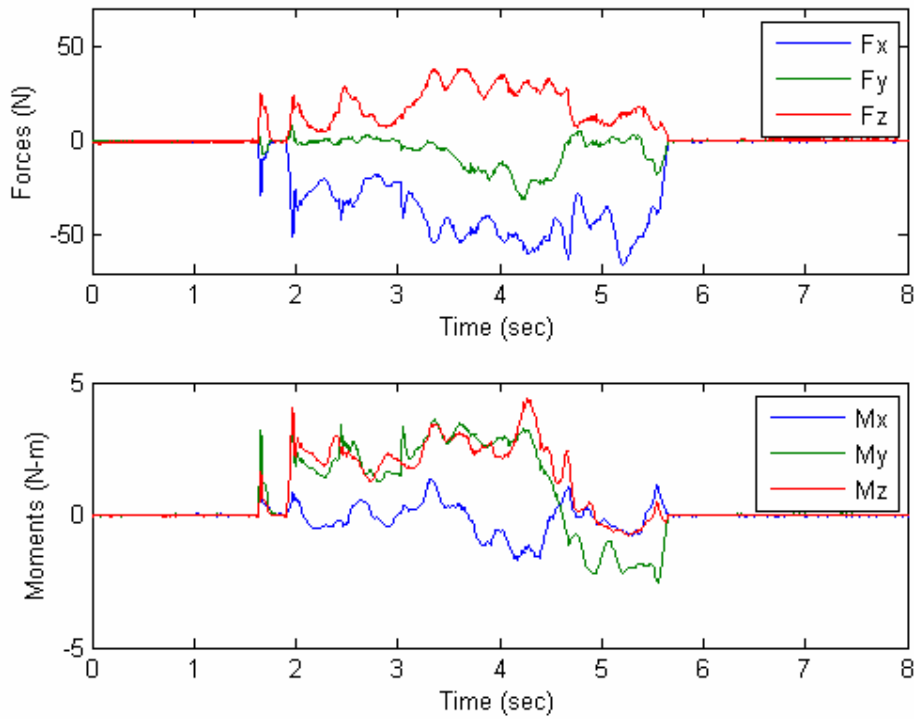


Figure 5. Forces and moments applied to the primary (push-off) sensor over time for a single push-off on Day 2 of flights.



(b)

Figure 6. Frames from the kinematic video data recorded during day one. (Note that the video data shown is not segmented equally over time.)

Important results were also determined from the self-rotation data. While the continuous rotary motion involved fewer steps, it was far more difficult to perform correctly. Subjects had difficulty maintaining a symmetric motion between the arms and reverted to a simpler anti-symmetric motion. There was also significant cross-coupling in rotations and minimal rotation about the intended axis. Using the body-twist strategy provided rotations with minimal cross-coupling and significant net rotations. Figure 7 shows a self-rotation using the body-twist method.



Figure 7. A successful self-rotation using the body-twist strategy [2].

CONCLUSION

The tests that were performed on the C-9 have been important in validating the hardware, software, experimental protocol, analysis, and modeling techniques for the Adapt flight experiment planned for the ISS. The C-9 environment has helped to identify what can be expected during the tests on the ISS, and offered preliminary adaptation information in a microgravity environment. The data collected from these tests are currently being analyzed in order to understand adaptation, locomotion, and reorientation in an altered-gravity environment. The models that are being developed to describe these mechanisms will lead to improved countermeasures and on-orbit diagnostic tools. In addition, these data will facilitate the development of new training techniques that encourage astronauts to develop appropriate movement strategies prior to exposure to the microgravity environment.

REFERENCES

1. Ferguson, Philip A., Krebs, Christopher P., Stirling, Leia A., and Newman, Dava J. "Kinetic and Kinematic Sensing System for the MICRO-G/Adapt International Space Station Experiment." SAS 2006-IEEE Sensors Applications Symposium, Houston, Texas, 7-9 February 2006.
2. NASA Johnson Space Center Photographs. April 18-21, 2006.
3. Kulwicki, P., Schlei, E., and Vergamini, P., "Weightless man: Self-Rotation Techniques," Technical Documentary Report no. AMRL-TDR-62-129, 1962.
4. Ferguson, Philip A. Quantifying and Modeling Adaptive Astronaut Movement: Motion Strategies for Long-Duration Spaceflight Missions. PhD thesis, Massachusetts Institute of Technology, 2006.

PHOTOGRAPHS

JSC2006E15009 to JSC2006E15030

JSC2006E15175 to JSC2006E15197

JSC2006E15483 to JSC2006E15520

JSC2006E15612 to JSC2006E15633

VIDEO

- Zero G flight week April 17 -21, 2006, Master: 720868

Videos available from Imagery and Publications Office (GS4), NASA/JSC.

CONTACT INFORMATION

Dava Newman, Ph.D
Massachusetts Institute of Technology
77 Massachusetts Ave.
Room 33-307
Cambridge, MA 02139
(617) 258-8799
dnewman@mit.edu

TITLE

A Simple Countermeasure for Space Motion Sickness

FLIGHT DATES

April 18-21, 2006

May 23-26, 2006

PRINCIPAL INVESTIGATOR

Millard F. Reschke, NASA/Johnson Space Center

CO-INVESTIGATORS

Jeffrey T. Somers, M. S., Wyle Laboratories, Inc., Life Sciences Group

R. John Leigh, Veterans Affairs Medical Center



GOAL/OBJECTIVES

The primary intent of this study was to determine the efficacy of reducing retinal slip via stroboscopic vision on motion sickness induced by pitch head movements during the μ gravity portion of parabolic flight.

METHODS AND MATERIALS

For this experiment, a total of 10 subjects were assigned to two groups: group A and group B. Each group participated in flying twice in this simple crossover design study that resulted in a total of four flights. Group A were initially exposed to the treatment condition, and group B were initially exposed to the control condition. Treatment condition for the two groups was reversed

on the subsequent flights. One subject did not complete the required flights, resulting in a total of 9 subjects.

Each subject was equipped with Cambridge Research FE-1 LCD goggles, an electrical driver box for the goggles. In the treatment condition, the goggles were set to flash at 4Hz with a 10 msec clear time, and for the remainder of the duty cycle the lenses remained dark. In the control condition, the goggles were set to flash at 0.5 Hz with 10 msec of dark time, and for the remainder of the duty cycle the lenses were clear. The control condition was designed to have no effect on motion sickness, but to prevent the subjects from knowing the difference between the treatment and control conditions. Each subject was also given a pushbutton to initiate the goggles, a neck brace and a headset with a microphone. Each headset was connected to an iPod and each microphone was connected to an individual voice recorder.

Each operator had a microphone that was connected to an individual voice recorder. The operator was equipped with a motion sickness score sheet that was held in place by a clipboard.

In an attempt to attain normalized motion sickness scores, the operators repeatedly trained the subjects on the definition of each motion sickness symptom according to the Pensacola Diagnostic Index (PDI) (Graybiel 1968). If the total motion sickness score based on the PDI reached a level of 8 or higher, the test for that particular subject was terminated (however, symptoms could still accrue until the end of the flight). The subjects were also instructed to give a subjective rating. This rating was based on the subjects' self-rating of motion sickness on a scale of 1-20, where '1' is normal (i.e., no motion sickness).

The subjects remained completely stationary with their eyes closed during the hyper-g pullouts. Upon reaching the microgravity portion of the parabolas (<0.06g), the operators would instruct the subjects to, "Push your button. Open your eyes. Begin." As shown in Figure 1, subjects would then begin making en bloc pitch head and body movements at 0.5 Hz as described by Lackner and Graybiel (1984).



Figure 1. Subjects making pitch head and trunk movements during microgravity

This frequency was guided by the tone provided via the iPod. Once the announcement, “Feet down. Coming out” was made, the operators would instruct the subjects, “Stop. Close your eyes.” The subjects would then sit upright while the operator asked the subjects to report their symptoms. This would be repeated for a total of 35 parabolas or until the subject reached the terminating level of motion sickness (PDI score of 8 or higher) or the subject asked to stop.

RESULTS

The results show that, although the flashing strobe goggles did not completely remove the appearance of motion sickness due to parabolic flights, they did inhibit the appearance of some symptoms and even prolonged the time to onset of becoming motion sick.

Total Parabolas

Five out of nine subjects did not complete the 35 parabolas during the control condition. Of those five subjects, four subjects completed more parabolas during the treatment condition. Three of the nine subjects completed all 35 parabolas for both tests, and one subject completed more parabolas during the control condition. The following chart displays the number of parabolas completed before termination due to motion sickness (i.e., PDI score of 8 or higher). Thirty-five parabolas signify that the subject went the entire test without an early termination.

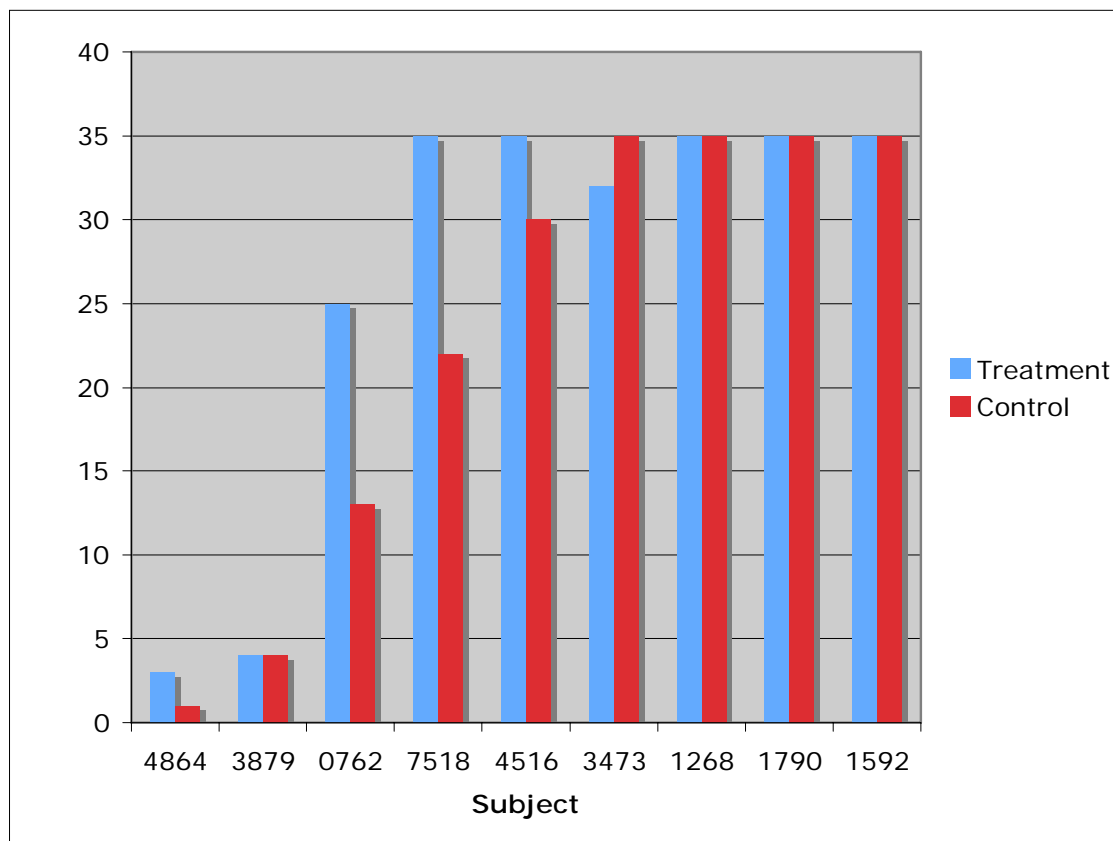


Figure 2. Motion Sickness Tolerance Time.

For each subject and for each condition, shown are the number of parabolas completed before termination due to motion sickness (i.e., PDI score of 8 or higher). Thirty-five parabolas signify that the subject went the entire test without an early termination. Note that three subjects completed all parabolas without terminating testing early.

Final Motion Sickness Scores

As previously mentioned, the subjects' levels of motion sickness were based upon a previously derived set of standards, referred to as the PDI. The following results describe the PDI score at either the time of test termination or the score at the end of the 35th parabola. Of the nine subjects, three subjects finished with a PDI score of 0 for both conditions. Three of the remaining six subjects had a lower final PDI score during the treatment condition, two of the six subjects had the same final PDI score for both conditions, and one subject reported a higher final PDI score during the treatment condition than in the control condition, although this subject did have a maximum PDI of 6 during the control condition that abated before the end of the test.

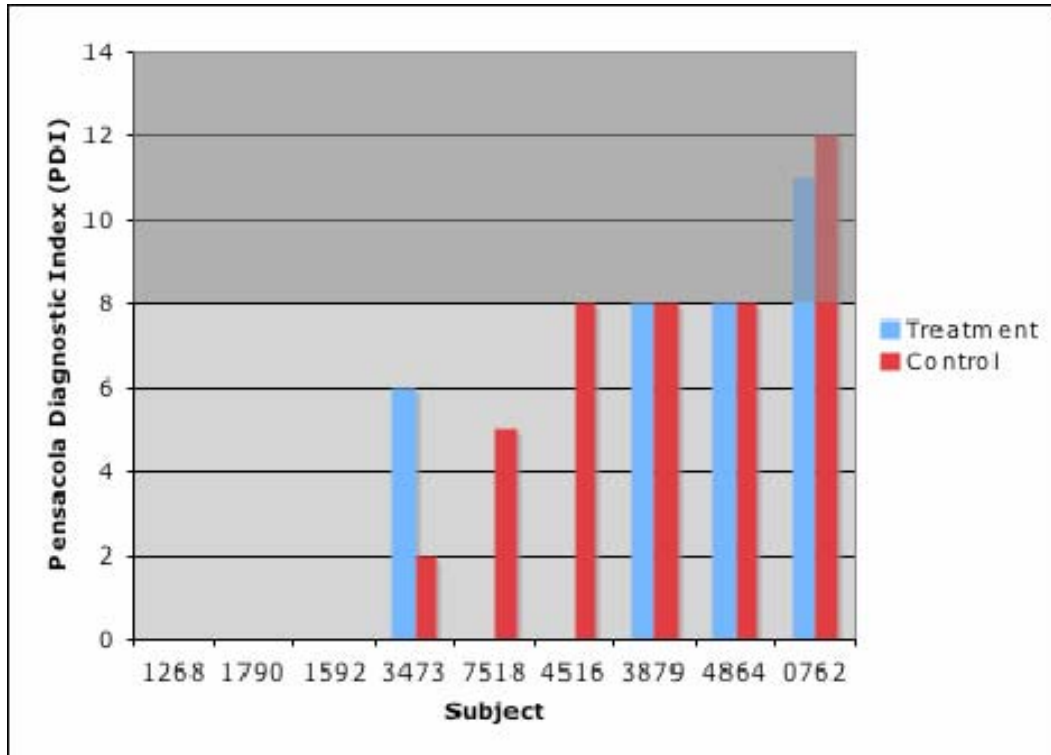


Figure 3. Motion Sickness Scores.

For each subject and for each condition, shown are the final PDI scores for motion sickness. A PDI of 8 or more terminated the test (denoted by the shaded region). Note that 3 subjects had no symptoms in either condition and 3 subjects terminated the test early for both conditions.

DISCUSSION

This experiment was designed to test the efficacy of using 4Hz stroboscopic vision to inhibit or prevent motion sickness symptoms that arise during en bloc head and body movements during microgravity portions of parabolic flight. Since hyper-gravity pullouts are inescapable during these flights and since these pullouts are, in most cases, the most provocative portions of the parabolas, it is impossible to determine how much the hyper-gravity pullouts contributed to the subjects' motion sickness scores. Subjects who were becoming ill often reported that the most provocative part of the parabolas was the transition from microgravity to hyper-g. Nonetheless, the data show that the goggles are effective in delaying and reducing motion sickness during parabolic flights.

The transition from microgravity to hyper-g also led to some ambiguity in reporting motion sickness symptoms. Subjects who were obviously motion sick would report seemingly low levels of symptoms. This was because subjects were instructed to report the symptoms they were experiencing during the microgravity portion of the parabola only, and not their symptoms that they were experiencing at the moment. Since the subjects reported symptoms during the hyper-g portion of the parabola and were, therefore more ill, the reported symptoms may have been less than what they actually experienced at the time they reported them.

CONCLUSION

The results from these flights are very promising concerning the ability of the goggles to reduce motion sickness symptoms in microgravity. Although they did not completely alleviate the onset of motion sickness, the overall trend was that the goggles did reduce the symptom score while allowing the subjects to participate in more parabolas.

Since we have completed testing only nine subjects, it is desirable to fly more subjects in the future to give a more accurate picture of the effectiveness of the goggles. The results obtained from this study do support our previous findings in our other ongoing studies.

REFERENCES

1. Graybiel, A., Wood, C., Miller, E.F. and Cramer, D.B. Diagnostic criteria for grading the severity of acute motion sickness. *Aerospace Med.* 1968, 39,453-455.
2. Lackner, J.R. and Graybiel, A. Elicitation of Motion Sickness by Head movements in the microgravity phase of parabolic flight maneuvers. *Aviat Space Environ Med.* June 1984, 55: 513-20.

PHOTOGRAPHS

JSC2006E15405 to JSC2006E15407
JSC2006E15472 to JSC2006E15477
JSC2006E20503 to JSC2006E20518
JSC2006E20552 to JSC2006E20561

VIDEO

- Zero G flight week April 17-21, 2006, Master: 720868
- Zero G May 22-26, 2006, Master: 720909

Videos available from Imagery and Publications Office (GS4), NASA/JSC.

CONTACT INFORMATION

Millard F. Reschke, Ph.D.
Human Adaptation and Countermeasures Office (SK)
NASA/Johnson Space Center
Houston, TX 77058
Tel: (281) 483-7210
FAX: (281) 244-5734
Email: millard.f.reschke@nasa.gov

Jeffrey T. Somers, M.S.
Wyle Laboratories, Inc., Life Sciences Group
1290 Hercules, Suite 120
Houston, TX 77058
Tel: (281) 483-7485
FAX: (281) 244-5734
Email: jeffrey.t.somers@nasa.gov

R. John Leigh, M.D.
Veterans Affairs Medical Center
10701 East Boulevard
Cleveland OH 44106-1702
Phone: 216-791-3800 ext. 5218
Fax: 216-231-3461

Department of Neurology
University Hospitals
11100 Euclid Avenue
Cleveland OH 44106-5040
Phone: 216-844-3190
Email: rjl4@case.edu

TITLE

Experimental Microfluidic System Interfaced to Cell Culture Bags for Real Time Analysis of Amino Acids

FLIGHT DATES

April 18-19, 2006

PRINCIPAL INVESTIGATOR

Steve Gonda, NASA/Johnson Space Center
Chris Culbertson, Kansas State University

CO-INVESTIGATORS

Greg Roman, Kansas State University
Amanda Meyer, Kansas State University
Sandra Geffert, University of Houston



GOAL

The ultimate goal of this project is to integrate microfluidic devices with NASA's space bioreactor systems. In such a system, the microfluidic device would provide real-time feedback control of the bioreactor by monitoring pH, glucose, and lactate levels in the cell media, and would provide an analytical capability to the bioreactor in extraterrestrial environments for monitoring bioengineered cell products and health changes in cells due to environmental stressors. Such integrated systems could be used as biosentinels both in space and on planet surfaces.

20 μm . This provided a large fluidic resistance to hydrodynamic flow through the microfluidic channels so that pressure caused by the external fluidics did not significantly affect the electrophoretic separations.

The goal of this experiment was to validate the fluidic interface between the microfluidic chip and the external fluidic network including the cell culture bag. To accomplish this goal several different samples were placed in a series of cell culture bags. The bags contained different numbers and concentrations of analytes, but also in the concentration of the analytes. The different samples in each bag would allow us to characterize the fluidic interface and the time it takes for a sample to reach the injector and also allow us to use the quantitative ability of the electrophoretic separations for determining differences in concentration of amino acids and proteins.

Illustrated below is a schematic of the flow-through chip connected to the external fluidics. A series of charge-coupled device (CCD) images were collected, demonstrating the combination of hydrodynamic fluid flow through the wide flow-through channel, with the electrokinetic injection and separation of amino acids into the microfluidic channels. A flow rate of $\sim 250 \mu\text{L}/\text{min}$ could be achieved through the wide flow-through channel. This allowed for rapid realtime analysis of the contents of the cell culture bag. The time it took for the analyte to travel from the cell culture bag to the cross injector was 1-5 min depending on the flow rate from the pump.

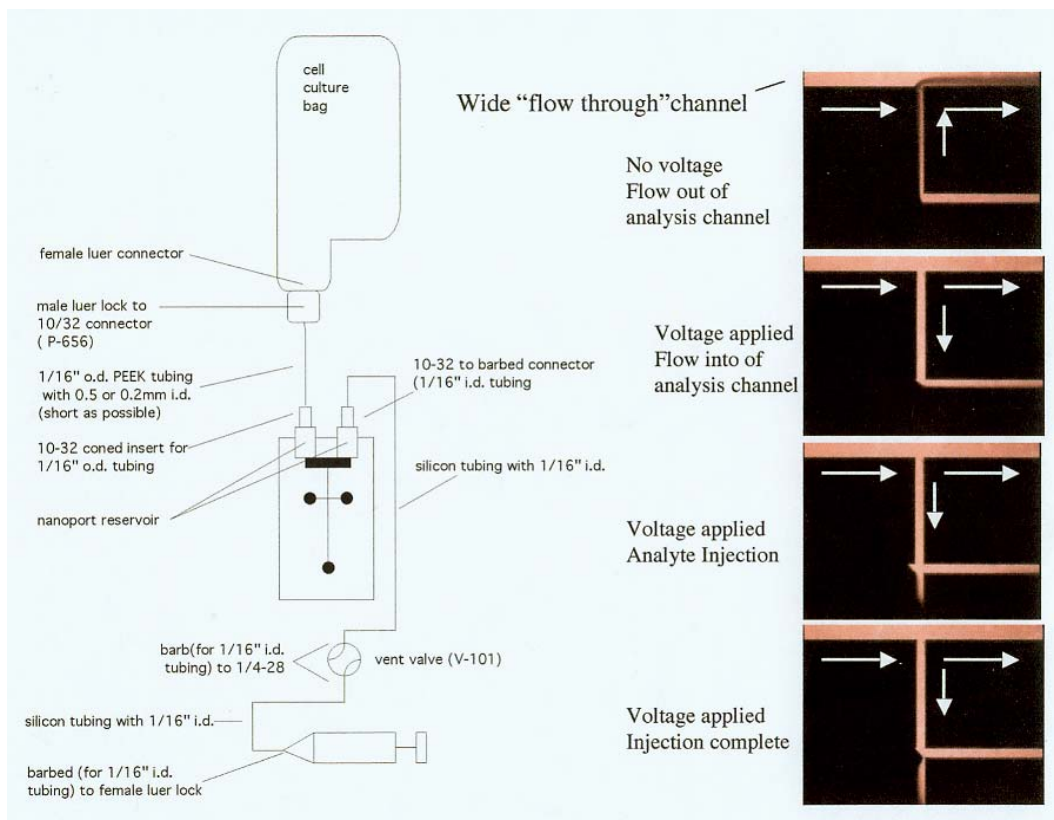


Figure 2. Schematic of cell culture bag-microfluidic device interface.

Sample Preparation: The following samples were mixed separately in three 10 mL cell culture bags using 10 mM sodium tetraborate at a pH of 9.3:

- Sample A: 2 μM of serine-FITC, 2 μM arginine-FITC, 2 μM glutamic acid-FITC, 2 μM histidine-FITC, and 500nm GFP
- Sample B; 1 μM serine-FITC, 1 μM arginine-FITC and 1 μM glutamic acid-FITC

The solutions were stored at 8°C until used. A four-way valve made it possible to connect these bags in parallel with the microfluidic device. Each cell culture bag was sampled for 15 min during flight before switching to another sample.

Chip Preparation and Operation: Chip preparation consisted of flushing a 50/50 (v/v) 1M NaOH/methanol solution through the channels, followed by water and then by run buffer. The electrophoretic separations were carried out in a pH 9.3, 10 mM sodium tetraborate buffer. Gated injections between 0.025 and 0.1 s were performed to introduce the sample into the separation channel. The separation distance was 2 cm and the field strength in the separation channel was ~ 1000 V/cm. Laser light scattering off of the channel walls was used to align the device.

RESULTS/DISCUSSION

On April 18, we successfully made 307 electrophoretic separations of samples from two different cell culture bags interfaced with our microfluidic separation device on NASA's C-9 microgravity research aircraft. We performed the separations over the course of 40 parabolas. The microfluidic system was set up to automatically sample the fluids from the cell culture bags during all phases of the flight. Fluids (borate-buffered aqueous solutions) from the cell bags were peristaltically pumped through the wide channel on the chip as shown in Figure 2. After 30 parabolas we switched the cell culture bag from which we were collecting samples. Figure 3 below shows the separations accomplished from the samples in each cell culture bag. One can distinctly see the change in analyte concentration for Arg, Glu and Ser and the elimination of reGFP and His as the sample from cell culture bag B replaced the sample contained in cell culture bag A. Very little carry-over of Sample A can be seen in the electropherogram of Sample B. The switch between samples at present takes ~ 5 min due to the length of tubing that connects the sample bags with the microfluidic device. This length could be considerably shortened to allow faster switching times if necessary.

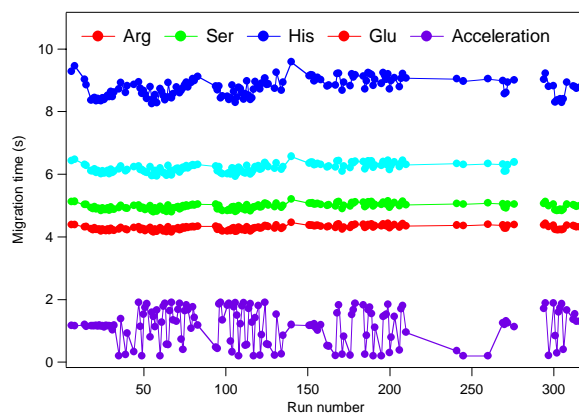


Figure 3. Migration time plotted as a function of run number during the flight

While we are still analyzing the data from all 307 runs, the run-to-run reproducibility looks very good. The relative standard deviation of the migration time for the amino acid analytes varied

from 1.5 to 3.2% over the entire course of the flight as seen in Figure 3. Using Ser as an internal migration marker, we should be able to improve the migration time reproducibility even further, as we have shown previously for microgravity research flights.¹ It is interesting to note that the microfluidic platform was turned 90° from its orientation in previous flights. This seemed to have significantly reduced the hydrodynamic pumping that we saw in earlier flights during the 1.8g portions of the parabolas. With the reduced pumping, the variation in analyte migration times between the 0g and 1.8g portions of the flight was significantly reduced, producing better results.

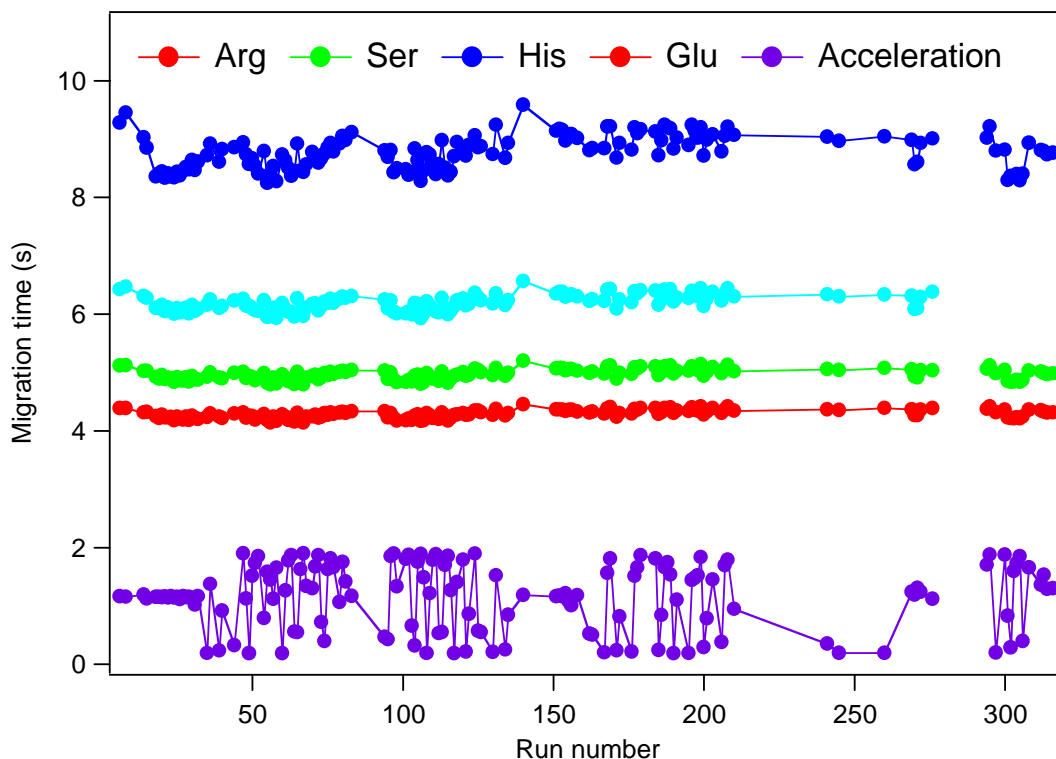


Figure 4. Migration time plotted as a function of run number during the flight

CONCLUSION

We demonstrated a microchip-cell culture interface capable of performing rapid sampling of nanoliter volumes that were subsequently separated and quantified using capillary electrophoresis in reduced- and hyper-gravity environments. The results have validated our delivery method between the external fluidics and the on-chip microfluidics. The optimal flow rate through the flow-through channel was ~ 250 $\mu\text{L}/\text{min}$.

REFERENCES

1. Culbertson, C. T.; Tugnawat, Y.; Meyer, A. R.; Roman, G. T.; Ramsey, J. M.; Gonda, S. R., Microchip Separations in Reduced-Gravity and Hypergravity Environments. *Analytical Chemistry* 2005, 77 (24), 7933-7940.

PHOTOGRAPHS

JSC2006E15004 to JSC2006E15008

JSC2006E15166 to JSC2006E15174

VIDEO

- Zero G flight week April 17-21, 2006, Master: 720868

Videos available from Imagery and Publications Office (GS4), NASA/JSC.

CONTACT INFORMATION

Dr. Christopher Culbertson

E-mail: culbert@ksu.edu

TITLE

Microfluidic Ion Sensor Array

FLIGHT DATES

April 18-21, 2006

PRINCIPAL INVESTIGATOR

D. Marshall Porterfield, Purdue University

CO-INVESTIGATORS

Stan Roux, University of Texas

Steve Wereley, Purdue University



GOAL

Previous experiments that utilized self-referencing microsensors have suggested that polar calcium currents are required for gravimorphogenic development in *Ceratopteris* fern spores (Chatterjee et al., 2000). Further work to fully understand the physiology of the calcium signaling events in this cellular system have not progressed because of inherent limitations in the spatial/temporal resolution of current experimental sensor systems. We developed a microfluidic ion sensor array (MISA) device, which includes integrated sensors, microelectro mechanical structures (MEMS), and microfluidics subsystems on a silicon substrate. The MISA chip will allow us to perform real-time measurements of multidimensional calcium flux patterns around sixteen fern spores using solid-state calcium sensor arrays. The ionophore-based (ETH-5234) sensors have been fabricated and tested by obtaining calibration curves, and by separate solution method interference tests. A novel coupling method, dual-electrode differential coupling, was

devised so that the differentials between two working electrodes could be amplified and digitized directly without the use of a reference electrode. An 18-bit high-speed data acquisition system with customized software has been assembled to acquire data from the MISA device. The MISA system was built to be used in parabolic flight/microgravity based physiological experimentation, to study the role of polar calcium currents in gravity-dependent cellular development.

OBJECTIVES

To test a MISA chip system for direct real-time sensing of trans-cellular calcium currents in single cells, and use this system to study *Ceratopteris* fern spores, and how they respond to altered gravity.

METHODS AND MATERIALS

The design and fabrication of the *in silico* lab-on-a-chip MISA chip (ul Haque et al., 2006) has been previously described but will be briefly reviewed here. The chip has sixteen microfluidic cell-holding-pores, which are 150 by 150 μm each and have 4 Ag/AgCl electrodes leading into them. An SU-8 structural layer was used for insulation and packaging purposes. The *in silico* cell physiology lab is wire bonded on to a custom printed circuit board for easy interface with a state-of-the-art-data acquisition system (DeCarlo et al., 2006). The electrodes are coated with a Ca^{2+} ion-selective membrane based on ETH-5234 ionophore and operated against an Ag/AgCl reference electrode. Initial characterization results have shown Nernst slopes of 30mv/decade that were stable over a number of measurement cycles.

The spores were presoaked in a calcium free medium (Chaterjee et al., 2000) for 2-5 days before the flight experiment. The dormant soaked spores were triggered to germinate by exposure to light approximately 5 hours before the flight. During this time 16 individual cells were placed in the microfluidic chambers on the MISA biochip, and overlaid with a MS agar gel medium. The holding reservoir containing the MISA chip was sealed and the amplifier housing was closed and sealed. The amplifier housing was integrated into the DAQ after takeoff. After powering up, the system offsets were measured and recorded and the data recording mode was set. On Days 1-3 of the flight experiment, we measured top-bottom currents on all parabolas. On Day 4 we alternated between top-bottom, top-side, bottom-side, and side-side.

RESULTS

During day 1 of the flight series, the data system rebooted during the flight. As a result only a partial data set was obtained. Analysis of the system after flight did not yield any problems so no action was taken. On Day 2 the accelerometer data package was not initialized so the data from the MISA device could not be fully correlated with gravitational force. On Days 3 and 4, perfect runs were obtained with 6/16 cells yielding quality results on Day 3, and 7/16 responding on Day 4. Representative data from the accelerometer (Figure 1) and the MISA biochip device (Figure 2) are presented here.

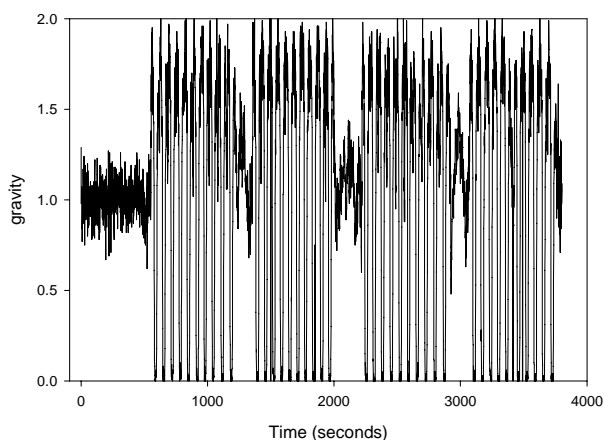


Figure 1. Raw accelerometer data from the flight experiment flown on April 20, 2006. Note the four groups of ten parabolas recorded during the flight of the C-9.

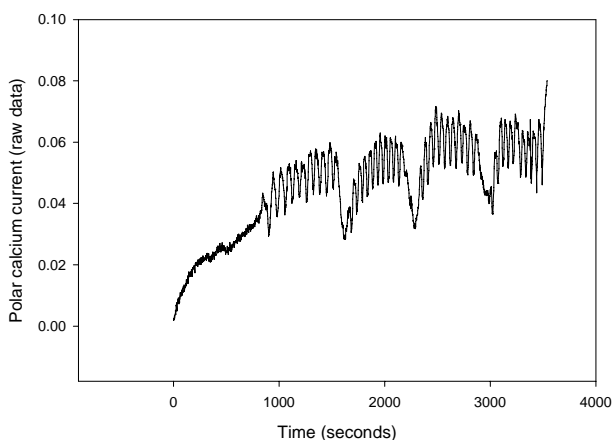


Figure 2. Representative data from an individual cell integrated into the MISA chip during the reduced-gravity flight experiment flown on the C-9 on April 20, 2006.

DISCUSSION

The process of data analysis is still ongoing, but the raw data show that the calcium current did change with gravitational force during the experiment. The polar current increased when the C-9 was in the 1.8g phase of a parabola, and decreased when the C-9 was in the microgravity phase of the parabola.

CONCLUSION

The MISA technology performed as expected during Days 3 and 4 of the flight week. There were some unexplained glitches during Days 1 and 2. While the exact cause of the problems was not identified, they did not resurface, and were ultimately attributed to user error. Despite these setbacks the technical and scientific objectives for the experiment were met. The functional MISA system enabled the direct real-time recording of calcium-dependent electrophysiological cell signaling in response to applied gravitational force. The data that we did record support the hypothesis that the polar calcium current is gravity-dependent, and the magnitude of the measured current is responsive to the amount of gravitational force during the flight.

REFERENCES

1. Chatterjee, A., Porterfield, D.M., Smith P.J.S., Roux S.J. 2000. Gravity-Directed Calcium Current in Germinating Spores of *Ceratopteris Richardii*. *Planta* 210: 607-610.
2. De Carlo, A.R. Rokkam, M. ul Haque, A., Wereley, S.T., Irazoqui, P.P., Wells, H.W., McLamb, W.T., Roux, S.J., Porterfield, D.M., 2006. Development of a Microfluidic Ion Sensor Array (MISA) to Monitor Gravity-Dependent Calcium Fluxes in *Ceratopteris* Spores. *Gravit. and Space Biol. Bull.* (In Press)
3. ul Haque, M. Rokkam, A. R. De Carlo, S.T. Wereley, H.W. Wells, W.T. McLamb, S.J. Roux, P.P Irazoqui, D.M. Porterfield. 2006 Design, Fabrication and Characterization of an In Silico Cell Physiology lab for Bio Sensing Applications. *Journal of Physics Conference Series* 34: 740-746.

PHOTOGRAPHS

JSC2006E14997 to JSC2006E15003
JSC2006E15161 to JSC2006E15165
JSC2006E15478 to JSC2006E15482
JSC2006E15608 to JSC2006E15611

VIDEO

- Zero G flight week April 17 -21, 2006, Master: 720868

Videos available from Imagery and Publications Office (GS4), NASA/JSC.

CONTACT INFORMATION

D. Marshall Porterfield
Purdue University
Department of Agricultural and Biological Engineering
Department of Horticulture and Landscape Architecture
Weldon School of Biomedical Engineering
225 South University Street
West Lafayette, IN 47906-2093
Phone: 765.494.1190

TITLE

Predicting and Assessing Postural Reentry Disturbances

FLIGHT DATES

April 25-28, 2006

PRINCIPAL INVESTIGATOR

James R. Lackner, Brandeis University

Paul DiZio, Brandeis University



OBJECTIVES

In the experiment we conducted during parabolic flights on board the C-9 aircraft April 25-28, 2006, our primary goal was to measure how exposure to spaceflight-like environments of weightlessness (0g) and increased gravity (1.8g) in parabolic flight affect the subjective vertical and perceived angular self-displacement.

Our Aims, corresponding to the two conditions we tested, were two-fold:

Aim 1. Measure blindfolded subject's perception of vertical and of angular self-displacement during naturalistic, recumbent yaw axis rotations (supine subject in a tilting bed) in 0g, 1g, and 1.8g. During recumbent yaw axis rotations in non-0g environments, there are continuous otolithic and somatosensory cues about the vertical and about angular self-displacement. We were interested in how these cues would influence the sense of self-rotation derived from the semi-circular canals, which are the only cue about self-rotation in 0g.

Aim 2. Measure blindfolded subject's perception of self-displacement during naturalistic, yaw axis rotations about a vertical axis in 0g, 1g, and 1.8g. Semi-circular canal signals are the sole cue about self-rotation during rotation about a vertical axis (seated subject in a turning chair), in all force backgrounds in parabolic flight).

A secondary goal was to measure changes in the subjective body midline in the same conditions. A total of eight subjects were tested; all subjects participated after giving informed consent. The summary and preliminary results of these experiments are presented below.

METHODS

Recumbent yaw rotation paradigm. Subjects were blindfolded and tightly restrained in a motorized bed which can tilt left or right from a supine position about the long body axis. The subject wore earplugs and noise-canceling earphones and listened to white noise, to mask the sounds of the aircraft which otherwise would have served as orientation cues. Before each trial, The bed was set to the desired starting angle prior to the 1.8g phase of each parabola, and the blindfolded subject received an instruction to hold a joystick parallel to his/her body midline (the plane dividing the left and right halves of their body). The experimenter triggered a bed movement when he/she judged that a stable 1.8g force had been reached, by viewing accelerometer readout on the computer console. All bed movements were programmed to have Gaussian velocity profiles. The amplitudes of bed movement were 7.5, 15, 22.5, 37.5, 52.5 or 67.5 deg to the right or left, in random order. Displacements were symmetric about a point either 5 or 10 degrees left or right of vertical, so the maximum bed position was 43.75 deg tilted left or right. Bed movement duration ranged from .7 sec to 4.79 sec. When the bed movement was complete the subject heard a computer-generated command to use the joystick to duplicate the spatial displacement he/she had just experienced. Five seconds later they heard a command to point the joystick in a vertical direction. Specifically, they were instructed to “align the joystick parallel to the direction an object would fall”. Five seconds later, they were instructed to align the stick with their apparent body midline. Five seconds later, still in the 1.8g period, the bed moved to the starting position for the next tilt. Shortly after this a transition to 0g occurred, the experimenter triggered the next bed movement, and the computer automatically prompted subjects for the same sequence of judgments as in 1.8g. This was repeated for 20 parabolas per subject. Subjects were tested similarly before flight and in straight and level flight, 1g.

Upright yaw rotation paradigm. Subjects were blindfolded and tightly restrained in a motorized chair which could turn them about a vertical, rostral-caudal axis. The procedure was exactly the same as in the recumbent yaw protocol, except subjects were asked to point the joystick toward a remembered, eye-level landmark in the aircraft instead of to the perceived vertical.

RESULTS

Preliminary analyses of some of the pre-flight, baseline data were completed even before the April week of parabolic flights. A summary of these findings is given below. We have not yet analyzed the in-flight results, but a few general impressions can be provided.

Baseline, 1g performance. There is little or no previous psychophysical investigation of naturalistic head turns. Our data indicate that in 1g, subjects underestimate angular displacements. The error functions level off for larger turn amplitudes. This means the errors are a progressively smaller percentage of the turn amplitude as the physical amplitude becomes larger. Figure 1 illustrates this for one subject during recumbent yaw rotations in 1g, and the pattern was also present for upright yaw. Formal analyses will focus on whether small differences between upright and recumbent yaw in 1g are significant. These patterns were independent of the peak velocity and duration of displacement and the starting and ending tilt angle.

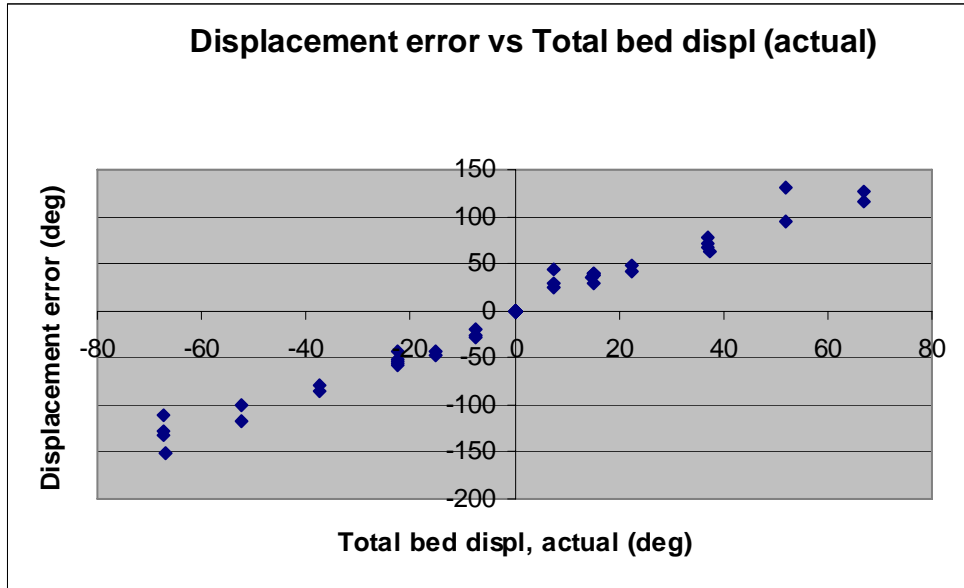


Figure 1

Errors in indication of the subjective vertical also showed a sigmoidal relationship to the amplitude of physical displacement about the recumbent yaw axis. See Figure 2. Subjects underestimated the extent of their tilt relative to vertical. This pattern is consistent with previous data obtained during static tilt experiments ([Bortolami, Pierobon, DiZio & Lackner, 2006](#)).

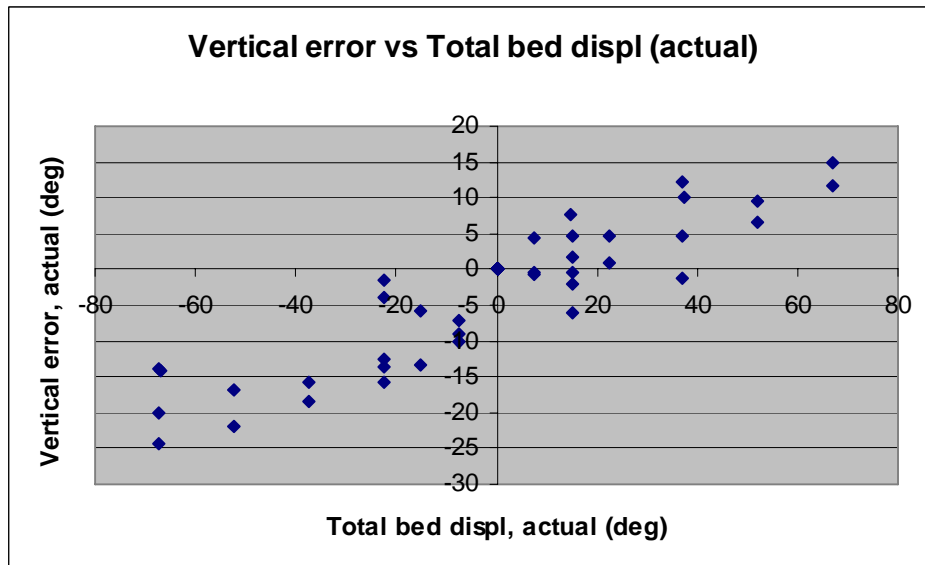


Figure 2

In-flight, 0g and 1.8g performance.

Observations by the experimenters and interviews with the subjects suggested that performance and experiences of the subjective vertical, apparent displacement and apparent midline tasks were similar in 1g and 1.8g. In 0g, uniformly, the apparent vertical settings were aligned with the body midline. The estimates of self-rotation were smaller in 0g than in 1g and 1.8g, for comparable physical displacements. Formal analysis will examine whether this g-related difference is the same for recumbent and upright yaw.

CONCLUSION

These findings indicate that integration of the velocity signal from the semicircular canals is not adequate to produce an accurate sense of angular self-displacement. Any differences in performance on the self-displacement task between the upright and recumbent yaw tasks in 1g will help suggest a contribution of otolith/somatic orientating cues to self-displacement perception. The preliminary observation that the subjective vertical is always aligned with the body midline in 0g suggests a strong somatosensory contribution to the subjective vertical. If the preliminary observation of a reduction of self-displacement in 0g relative to 1g and 1.8g holds up to full scrutiny, it would suggest that a graviceptive input modulates integration of the canal signal.

REFERENCES

Bortolami S.B., Pierobon A., DiZio P., Lackner J.R.. Localization of the subjective vertical during roll, pitch, and yaw body tilt. *Exp Brain Res*, in press, 2006 (EPub available)

ACKNOWLEDGMENTS

Grant Support: NASA Grant NNJO4HJ14G

PHOTOGRAPHS

- None

VIDEO

- None

CONTACT INFORMATION

Dr. James R. Lackner, Director lackner@brandeis.edu
Dr. Paul DiZio, Associate Director dizio@brandeis.edu

Ashton Graybiel Spatial Orientation Laboratory
Brandeis University MS 033
Waltham MA 02454-9110
Tel: 781-736-2033
Fax: 781-736-2031

TITLE

Medical Operations Support Team (MOST): Remote Guidance of Crew Medical Officer (CMO)
Analogues through Space Relevant Medical Sciences

PRINCIPAL INVESTIGATOR

Hal Doerr, Baylor College of Medicine
National Space Biomedical Research Institute

CO-INVESTIGATOR

Victor Hurst IV, Wyle Laboratories, Inc., Life Sciences Group



INTRODUCTION

The MOST has separated its study into two sets of experiments. The background for each set of experiments is as follows:

Clinical Remote Guidance (CRG)

Management of medical events and contingencies aboard the International Space Station (ISS) requires a trio of skill sets: 1) performance of medical tasks using the ISS Health Maintenance System (HMS) equipment, 2) application of clinical acumen, and 3) communication using remote guidance (RG) techniques from ground-based flight controllers to the ISS crew. The performance of medical tasks is provided by an astronaut crew medical officer (CMO), who often is not a physician, while the clinical acumen and remote guidance communication are provided by a board-certified flight surgeon (FS) physician in the Mission Control Center (MCC) at NASA's Johnson Space Center (JSC). The success of this system depends, in part, on the abilities of the CMO to easily recall the skills learned during their 40-80 hours of preflight medical training and the of FS to remotely provide appropriate direction to the CMO being able to ensure that the proper task is being performed to mitigate the medical concern. The need for FS-CMO teams to be competent in using Crew Resource Management (CRM) techniques during such events is also understood. Practice of these skills is necessary for an FS-CMO team to

confidently manage medical events aboard the ISS; however, the ability to practice such skills in concert with one another is limited. Therefore, it is paramount for an FS-CMO team to maximize their learning efficiency during their preflight medical training. As demonstrated by flight simulation improving pilot performance, the use of medical patient simulation may be able to improve an FS-CMO team's performance in managing medical events.

The integration of medical patient simulation at JSC has been ongoing in recent years as demonstrated by the acquisition of two high-fidelity patient simulators. The MOST has supported this effort by helping NASA Space Medicine to integrate these simulators into the Space Medical Training "flow" for Medical Operations, including training for flight surgeons and astronauts. Preliminary medical simulation exercises by the MOST using the medical patient simulators in both ground-based and simulated microgravity environments demonstrated how these simulators can help FS and CMO analogues practice managing space-relevant medical events using ISS HMS equipment; however, it is unclear whether the FS cohort would benefit from such exercises, especially in a simulated microgravity environment. As a result, the MOST developed this preliminary study with guidance from the NASA JSC FS Office to determine 1) whether FS gives consistent instructions to CMO/CMO analogues as they manage a space-relevant medical event in a microgravity environment and 2) whether the performance of both operational and medical tasks by the CMO/CMO analogues in a microgravity environment affects how an FS remotely guides the CMO through a medical event.

Sub-optimal ILMA Insertion

Proper performance of specific clinical skills by a caregiver during medical contingencies is paramount for mitigating serious medical conditions. As an example, airway management techniques are necessary for caregivers who are attempting to establish and maintain a patent airway while treating a patient undergoing respiratory distress. To ensure that these techniques are learned properly by the caregiver, the settings are most often arranged in a configuration that is optimal for both the caregiver and the patient; however, in many situations such settings are sub-optimal, thus causing the caregiver to adapt to these sub-optimal conditions. Such occurrences are no exception aboard the ISS. As a result, the FS and astronaut cohorts must be ready to adapt their optimal airway management techniques for sub-optimal situations. Previous microgravity experiments by the MOST and other investigators have evaluated several techniques for securing airways in sub-optimal positions by non-physician caregivers, including insertion of a supraglottic airway device (Intubating Laryngeal Mask Airway (ILMA)) and performing direct laryngoscopy with insertion of a cuffed endotracheal tube (1, 2). For this study, the MOST selected two ILMA insertion techniques from the previous study to be performed by members of both FS and astronaut cohorts to determine if either technique is sufficient to perform in sub-optimal positions in a microgravity environment.

OBJECTIVES

1. Determine if FSs give consistent instructions to proxy CMOs as they manage a space-relevant medical event in a microgravity environment.
2. Determine if the performance of both operational and medical tasks by a proxy CMO in a microgravity environment affects how an FS remotely guides the proxy CMO through a medical event.
3. Finalize training techniques for sub-optimal insertion of the Intubating Laryngeal Mask Airway (ILMA).

METHODS AND MATERIALS

Human Subjects

On August 18, 2005, the MOST received approval to use humans as participants for this study from the NASA-JSC Committee for the Protection of Human Subjects (CPHS). The proposal was titled “C-9 Medical Operational Support Team (MOST) Protocol ‘Telementoring of Crew Medical Officer (CMO) Analogs through Space Relevant Medical Scenarios.’” The levels of formal medical training for the 14 participants were as follows: 8 physicians, 2 astronaut physicians, 1 emergency medical technical (EMT), 1 astronaut EMT, 1 nurse, and 1 with no formal medical training.

Patient Simulator

An Emergency Care Simulator (ECS; Medical Education Technologies, Inc., Sarasota, FL) was used for all phases of the experiments. The ECS is a modified version of the commercial ECS that is certified for use in the simulated microgravity environment provided by C-9 aircraft.

Patient Simulator Restraint System (PSRS)

The PSRS is a restraint system that mimics the ISS Crew Medical Restraint System (CMRS) and was developed with Wyle Laboratories, Inc., Life Sciences Group (Houston, TX), in part, to assist the MOST with conducting patient simulation experiments in the simulated microgravity environment aboard C-9 aircraft. The system consists of a table made of 80/20 aluminum (constructed by Wyle Laboratories, Inc., Life Sciences Group) combined with a commercial rescue backboard (Iron Duck, Chicopee, MA), a strap restraint system (Iron Duck, Chicopee, MA), a commercial vertical rescue harness (Elk River, Inc., ANSI-rated, Type 1), and a modified flight suit (Soft Goods Team, Wyle Laboratories, Inc., Life Sciences Group). The PSRS secured the CMO and ECS during the Clinical Remote Guidance of the flight while the harness system allowed the ECS to float safely for the team to evaluate the sub-optimal ILMA insertion techniques.

Clinical Remote Guidance (CRG)

Each CRG session consisted of a physician acting as the FS and another participant acting as the CMO. On each flight day, the proctors of the study provided the FS-CMO teams with a background of the medical scenario they were going to manage during the flight. Once in position, the FS and CMO conducted the scenario using ISS HMS equipment only when exposed to the simulated microgravity environment provided by the aircraft. Each CRG session lasted 10 parabolas or approximately 4.5-5 minutes of simulated microgravity. The two medical conditions presented on the ECS to the FS-CMO teams in random order were a tension pneumothorax and a negative pressure pulmonary edema. To minimize variability between RG sessions, the ECS was programmed to present the symptoms of each condition with the same timeline. All data were recorded using audio/video data collection systems provided by Wyle Laboratories, Inc., Life Sciences Group (Reduced Gravity Media Rack) or the NASA-JSC Photography office. All video data were converted to DVD format for retrospective analysis by the MOST investigators.

Sub-optimal ILMA Insertion

Three ILMA insertion techniques (1 optimal, 2 sub-optimal) were performed for this study. Each participant acted as a caregiver and was directed to attempt these techniques following a preflight instruction session on the day of the flight and a demonstration of the technique by an anesthesiologist physician in microgravity aboard the aircraft. The techniques were as follows:

Optimal

Kneel (ECS and participant restrained)
The participant secured him or her at the head of the strapped-down patient and inserted the ILMA per the technique developed by Beck *et al.* (2). Following insertion, the participant inflated the cuff on the ILMA using a 20 cc syringe (Figure 1).



Figure 1

Sub-optimal

Cradle (only participant restrained)
While floating during microgravity, the participant secured his or her feet to the



Figure 2

deck and placed their arm posteriorly across the shoulder blades of the mannequin. As a result, the neck of the mannequin rested in the participant's antecubital space and then the participant placed their hand on the lateral pectoral border of the mannequin's axilla (Figure 2). This tactic provided an adequate sniff position for insertion of the ILMA by the participant. While cradling the head of the floating mannequin, the participant inserted the ILMA into the oral airway of the mannequin. After ILMA insertion, the participant inflated the ILMA cuff using a 20 cc syringe. This technique was originally developed by two astronauts on a previous MOST flight 1.

Trap (mannequin and participant not restrained)

The participant straddled the mannequin's torso while facing the front of the mannequin's head. To secure the mannequin, one leg of the participant was placed over the mannequin's shoulder while the other leg was placed under the mannequin's armpit, opposite of the mannequin's shoulder. With the legs wrapped around the mannequin's torso, the participant cradled the back of the mannequin's head with one hand and used the free hand to insert the ILMA into the mannequin's oral airway (Figure 3). Following insertion, the participant inflated the ILMA cuff using a 20 cc syringe. This technique was developed by the MOST on a previous flight 1.



Figure 3

RESULTS

Clinical Remote Guidance (CRG) (Figure 4)

For the eight trials conducted, all FSs were successful in diagnosing the patient as well as properly remotely guiding the CMO through the medical event; however, the responses elicited from the FS cohort did vary. In the cases where the CMO was an astronaut-physician, the FS was able to give more instructions to the CMO than a with non-astronaut physicians. Observation of flight video along with comments from post-flight debriefs indicated that the performance of both operational and medical tasks by the CMO/CMO analogues in the microgravity environment did not affect how a FS remotely guided that CMO through a medical event.



Figure 4

Sub-optimal ILMA Insertion

Fourteen participants conducted 46 trials of the sub-optimal ILMA insertion techniques. Please note that all 11 physicians attempted all three insertion techniques. Two participants, who were physicians, were unsuccessful performing the ‘Cradle’ technique (see Table 1). Overall, 43 of 46 trials (94%) conducted were properly performed.

Position	# of Trials	Successful	% Successful
Kneel	14	14/14	100 %
Cradle	15	12/15	80%
Trap Doerr	17	17/17	100%
Total	46	43/46	94%

Table 1

DISCUSSION

Clinical Remote Guidance (CRG)

This study demonstrated to flight surgeons and astronauts the challenges of performing diagnostic and treatment protocols in an analogue environment relating to space flight. Feedback from participants indicated that the study was a great introduction to becoming more familiar with the operational constraints and medical treatments aboard the ISS. Their feedback also demonstrated an appreciation of self-evaluation of their knowledge and skill sets as it relates to space medicine, suggesting the need to increase their exposure to this high-fidelity analogue environment and this specific type of training.

Sub-optimal ILMA Insertion

This study demonstrated the use of airway management techniques in sub-optimal conditions relating to space flight. Use of these techniques will provide a crew with options for using the ILMA to manage airway issues aboard the ISS. Although it is understood that the optimal method for patient care during space flight is to have both patient and caregiver restrained, these techniques provide a needed back-up should conditions not present themselves in an ideal manner.

CONCLUSION

Medical simulation exercises and task training, along with training for the sub-optimal ILMA insertion techniques, will be developed by the MOST in concert with the Flight Surgeon and Astronaut Offices as well as Space Medicine Training at NASA JSC.

ACKNOWLEDGMENTS

The MOST would like to acknowledge the NSBRI for its continued support of the MOST Project. In addition, the team also acknowledges Ashkan Moghaddam, Terry Guess and the Advanced Projects Group at Wyle Laboratories, Inc., Life Sciences Group for their robust support with flight preparation and execution. Finally, the MOST also acknowledges the valued support and guidance from the NASA JSC Reduced Gravity Office (RGO) for these as well as previous experiments aboard RGO aircraft.

REFERENCES

1. Doerr HK, Bacal K, Mena GE. Human Patient Simulator Evaluation Flights Evaluation of HPS Function: Evaluation of HPS as a Training Platform. *KC-135 and Other Microgravity Simulation: Summary Report*. NASA/TM-2005-213162, Section 2-15: 97-104. 2005
2. Beck G, Wu J, Pettys M, Ferson D. Functional Performance Validation of Airway and Ventilation Techniques in Microgravity. *KC-135 and other Microgravity Simulation: Summary Report*. CR-208936, pp 24-34. 2003

PHOTOGRAPHS

JSC2006E16984 to JSC2006E117039

VIDEO

- Zero G flight week April 24-28, 2006, Master: 720873

Videos available from Imagery and Publications Office (GS4), NASA/JSC.

CONTACT INFORMATION

Hal Doerr, M.D.

Director, Houston Center for Advanced Patient Simulation (HCAPS)

Department of Anesthesiology

1 Baylor Plaza

Houston, TX 77030

hdoerr@houston.rr.com

TITLE

The Effects of Microgravity on the Binding Kinetics of Two Lipid Binding Proteins

FLIGHT DATES

May 9-12, 2006

PRINCIPAL INVESTIGATOR

Vince LiCata, Louisiana State University

CO-INVESTIGATORS

Andy Wowor, Louisiana State University

John Jackson, Louisiana State University



GOAL

To determine if microgravity alters protein kinetics and equilibria.

OBJECTIVES

To test microgravity effects on two rapid protein + lipid kinetic reactions.

METHODS AND MATERIALS

Materials

Bovine serum albumin (BSA) was obtained from Sigma Chemical Co. (St. Louis, MO), and used without further purification. ANS (1.8 anilino naphthalene) was obtained from Molecular Probes (Eugene, OR). Adipocyte lipid binding protein (ALBP) was purified in house using previously

published procedures (Schoeffler, et al., 2003). All other standard reagents were purchased from Sigma.

Over the course of several parabolic microgravity flights, we measured:

1) Dependence on ligand concentration of the kinetics of binding of 1.8 anilino naphthalene sulfonate (ANS) to BSA. Mixing of ANS and BSA was accomplished using a modified stopped-flow fluorometer. The concentration of ANS was altered manually, with 2-4 parabolas were used for measurements with each ANS concentration. The entire binding reaction was complete within 100 milliseconds after mixing. Up to 5 separate mixing reactions were monitored during each 20-second parabola. Each reaction was non-linearly analyzed to obtain an apparent rate constant τ (tau). Values of τ at different concentrations of ANS were plotted to determine association and dissociation (on and off) rates for the reaction.

2) Ligand concentration dependence experiments were also performed for the binding of ANS to the ALBP. This reaction is also complete within 100 ms of mixing. The same procedures described for the BSA + ANS reaction above were followed for the ALBP + ANS reaction.

For the ALBP + ANS reaction, a full concentration series was collected at 6 different solution viscosities. Viscosity of the solution was altered by adding sucrose. Concentration series were collected at 0, 10, 15, 20, 25, and 30% sucrose.

Data Analysis

Kinetic traces were fit to single exponential equations (Equation 1). In all cases tested, a double exponential fit did not improve the fit.

$$Y = Y_0 + A_1 e^{-(x-x_0)/\tau} \quad (\text{Equation 1})$$

All reactions were performed under pseudo-first order conditions. The rate of a pseudo-first-order reaction is determined by monitoring the k_{obs} or $1/\tau$ with respect to concentration of a variable reactant (Cantor & Schimmel, 1980; Hammes, 2000). The first-order rate (k_{obs}) is proportional to the slope of this relationship (Equation 2). A plot of k_{obs} vs. [ligand] yields a straight line, with a y-intercept of zero under perfect first order conditions. However, because there is some back reaction (reverse reaction), the y-intercept will not be zero, but will be a measure of the back reaction rate. Observed rate constants at each concentration of ligand are fit to Equation 2 to determine the forward and reverse rate constants (k_F and k_R).

$$k_{obs} = 1/\tau = k_F [A]_0 + k_R \quad (\text{Equation 2})$$

Because the reactions are initiated by mixing pure solutions of the two components, the back reaction is minimal relative to the forward reaction, and is thus much less well determined in the experiment.

RESULTS

All reactions were measured both during the microgravity portion of each parabola, and during the 1.7g portion of each parabola. The 1.7g measurements served as the control measurements in flight. All reactions were also measured at 1g either in the laboratory or on the C-9 while it was parked in the hangar at JSC.

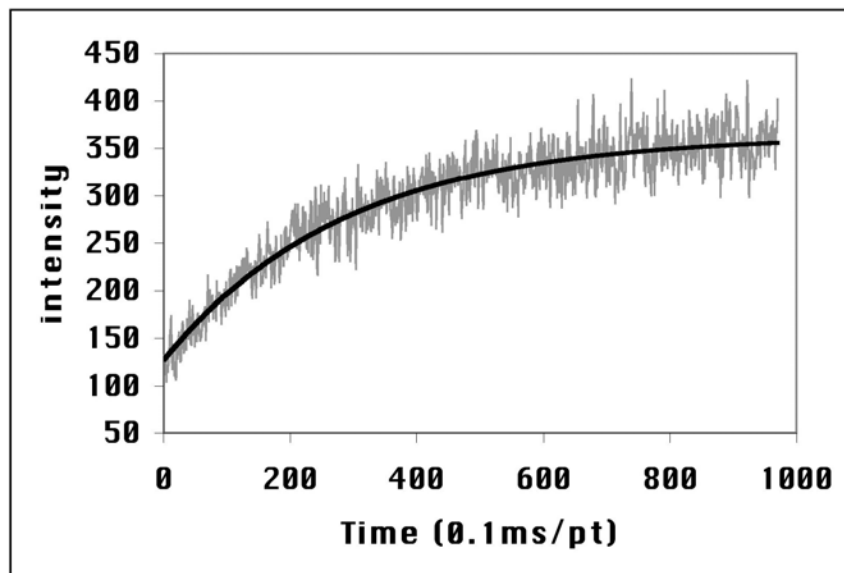


Figure 1. Representative kinetic data collected on board C-9 flights. An average of 5 independent shots of $3\mu\text{M}$ ALBP + $3\mu\text{M}$ ANS is shown. The line through the data shows the best-fit exponential (Equation 1), from which the apparent rate constant is determined.

A full series of kinetic reactions similar to that shown in Figure 1 was collected at 6 different ligand (ANS) concentrations for each protein. Then, a full 6 ligand concentration dependence data set was collected at several different viscosity values. Each of these series was collected in microgravity (top of the parabola) and in macrogravity (bottom of the parabola). Figure 2 shows the difference between the viscosity dependencies of ALBP + ANS in microgravity vs. macrogravity.

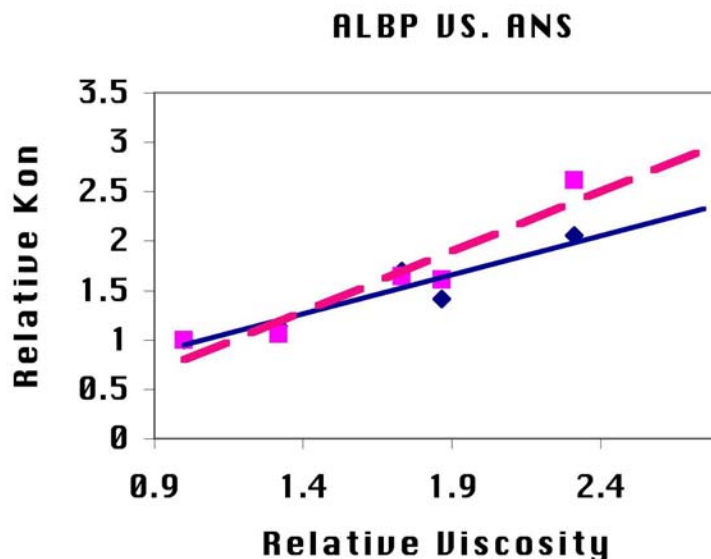


Figure 2. Relative forward rate constants (k_{on} or k_F) versus relative solution viscosity in microgravity (solid line) and macrogravity (dashed line).

The data of Figure 2 indicate a possible change in the association kinetics for ALBP + ANS in microgravity versus macrogravity. Herein we find a viscosity dependence of 1.2 in macrogravity versus a viscosity dependence of 0.8 in microgravity (the slopes of the two lines in Figure 2). This difference indicates that the association of ALBP and ANS is more sensitive to alterations in viscosity in macrogravity than in microgravity. Full statistical analysis of this data is still in progress.

DISCUSSION AND CONCLUSIONS

The goal of this flight series was to determine if microgravity alters the reaction rates for very rapid biological reactions. The reactions examined reached equilibrium within 100ms. Small apparent effects of microgravity were observed, generally making the reactions appear to be less sensitive to the relative viscosity of the reaction environment. Further statistical analysis of the results is necessary to confirm these conclusions.

REFERENCES

1. Schoeffler, A.J., Ruiz, C.R., Joubert, A.M., Yang, X., and LiCata, V.J., 2003, Salt modulates the stability and lipid binding affinity of the adipocyte lipid binding protein, *J. Biol. Chem.* 278, 33268-33275.
2. Cantor, C. R. and Schimmel, P. R. (1980) *Biophysical Chemistry, Part III, The Behavior of Biological Macromolecules*. W. H. Freeman and Company. San Francisco, CA. USA.
3. Hammes, G. G. (2000) *Thermodynamics and Kinetics for the Biological Sciences*. A. J. Wiley and Sons. New York, NY. USA.

PHOTOGRAPHS

JSC2006E17784 to JSC2006E17785
JSC2006E17792
JSC2006E17799 to JSC2006E17801
JSC2006E17808 to JSC2006E17812
JSC2006E17816 to JSC2006E17817
JSC2006E17929

JSC2006E17936
JSC2006E17947 to JSC2006E17953
JSC2006E17960
JSC2006E17962 to JSC2006E17965
JSC2006E18106 to JSC2006E18114
JSC2006E18189 to JSC2006E18203

VIDEO

- Zero G May 8 – May 12, 2006, Master: 720902

Videos available from Imagery and Publications Office (GS4), NASA/JSC.

CONTACT INFORMATION

Vince LiCata, Ph.D.
Department of Biological Sciences
Louisiana State University
Baton Rouge, LA 70803
Phone: (225) 578-5233
FAX: (225) 578-2597
email: licata@lsu.edu

TITLE

An Advanced Portable Ion Analyzer for Water Quality Monitoring and Control

FLIGHT DATES

May 9-10, 2006

PRINCIPAL INVESTIGATOR

Tony Ragucci, Lynntech, Inc.

CO-INVESTIGATOR

Francisco Maldonado, Lynntech, Inc



GOAL

The goal of this experiment is to determine the ability of Lynntech's Mesofluidic Phase Separator to successfully function in a 0g environment.

OBJECTIVES

The primary objective of this research is to test Lynntech's Mesofluidic Phase Separator in a 0g environment under various gas and liquid flow rates. Recorded data of ambient conditions and video of the phase separator was analyzed to determine the success rate of phase separation. A data table of results that characterizes the phase separator was produced which summarizes device function under relevant flight conditions.



Figure 1. Lynntech's Mesofluidic Phase Separator as installed for flight testing.

METHODS AND MATERIALS

Lynntech, Inc. designed and constructed a microgravity-compatible experimental platform for Lynntech's Mesofluidic Phase Separator (Figure 1). In order to separate gas and liquid, the phase separator uses an expanded polytetrafluoroethylene (ePTFE) tube, bent into a small spiral configuration. The ePTFE tubing has a pore structure that allows gas to pass through its wall but restricts water from passing through. Because of internal pressure in the tubing, the small inner diameter in the tubing, and a spiral path that the tubing follows, gas bubbles are driven toward the ePTFE wall and out of the tubing. The gas is then collected in an outer chamber of the device and can be directed toward a collection bag. The dimensions of the phase separator are 5.4cm x 2.0cm diameter. It weighs 11.7 grams and is completely passive.

As seen in Figure 2, the structure of the platform is constructed from 80/20 extruded aluminum, which was chosen for its light weight and structural properties. The top section secures the laptop used to monitor the system in place. The bottom section houses the control board, one phase separator, two peristaltic pumps, a MiniDV video camera, a 700mL deionized water reservoir, a waste water reservoir, a 700mL dry nitrogen gas reservoir, and a gas recovery reservoir. In order to protect all the electronic equipment, two barriers have been implemented to prevent any

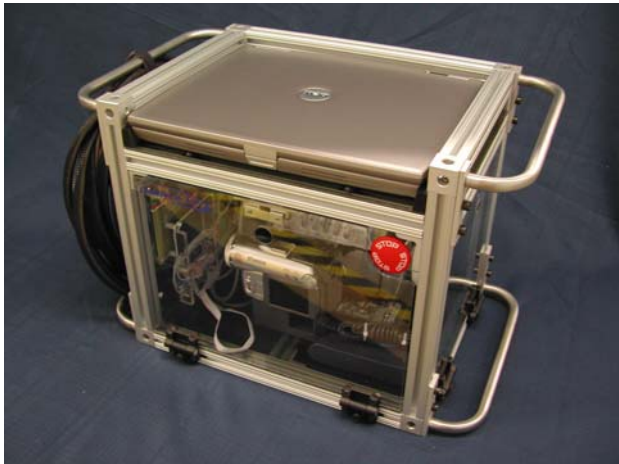


Figure 2. Lynntech, Inc. Flight Box

damage to the system in the case of a water leak. As a primary containment, the water is sealed within a 700mL capacity polyethylene (0.8 mm thick) bag equipped with a bulkhead fitting. As a secondary containment, all liquid and gas reservoirs are sealed inside a 3 liter jug with grommets to seal around the tubes at their points of exit. As a safety measure, there is an emergency shutoff switch mounted on the front of the system that will cut off power to all components should the need arise.

To record data from the flight test, both the MiniDV camera and the laptop are used for data acquisition. The camera is focused on the fluid composition of both outlet lines and the

inlet mixture of gas and liquid provided by computer-controlled peristaltic pumps. The camera records a miniature liquid crystal display that displays the g_x , g_y , and g_z accelerometer signals from the plane, the inlet flow rate of gas and liquid, and the elapsed experimental time.

Simultaneously, the laptop records the accelerometer signal, flow rates, time, pressure, temperature and relative humidity at a rate of ten data points per second. During 40 parabolic flights, an array of gas-to-liquid inlet mixtures is run to characterize the performance of the phase separator.

RESULTS

An array of 36 flow rates was tested on each of the two flights. Figure 3 shows the flight box during a 0g test run. During each parabola, the flight box was in 0g, on average, for 22 seconds. The parabolas were flown in sets of ten. In Figures 4-6, the first parabola of each set is numbered.

The results obtained indicated that the phase separator operated as designed. While 100% phase separation was not achieved at all liquid/gas ratios, the lower range in which the ion analyzer operates was 100% efficient, meaning that no gas bubbles were detected in the liquid outlet line of the phase separator and, conversely, no liquid was detected in the gas outlet of the phase separator. The following figures 4-8 and tables 1-2 are separated by day, and represent the Z acceleration, temperature, pressure and relative humidity as a function of time.



Figure 3. Lynntech's experimental setup in 0g

Due to electrical difficulties in communicating the accelerometer signals from the plane to the flight box, the scaling factor for the X, Y, and Z accelerations were lost. However, the data were scaled after the flight was complete, based on separate measurements from the plane. The data shown have been scaled, therefore, to represent approximately accurate values. This data also provide an indicator for when the 0g parabolas begin and end.

As seen in Figure 4, the temperature steadily decreased during the 2-hour flight on Day 1.

From the beginning of the first parabola to the end of the last parabola, the temperature dropped 10°C.

Figure 5 shows that the pressure stayed relatively constant throughout the entire flight. The pressure remained within the range of 10.23 – 12.04 psi. Figure 6 shows the relative humidity gradually decreasing from 29.63% - 21.09% over the course of the flight. Table 1 represents the matrix of gas and liquid flow rates that were tested on Day 1. For each flow rate, the range of ambient temperature, pressure, and humidity range is listed, as well as the percent of phase separation attained. To determine the percentage of total gas removal, the video recording of the outlet tubes was carefully analyzed for bubbles in the outlet liquid line. Any bubbles present were measured, using the background scale, and their volume was proportionally deducted from the total volume of gas sent though the phase separator during the 0g portion of that particular testing parabola.

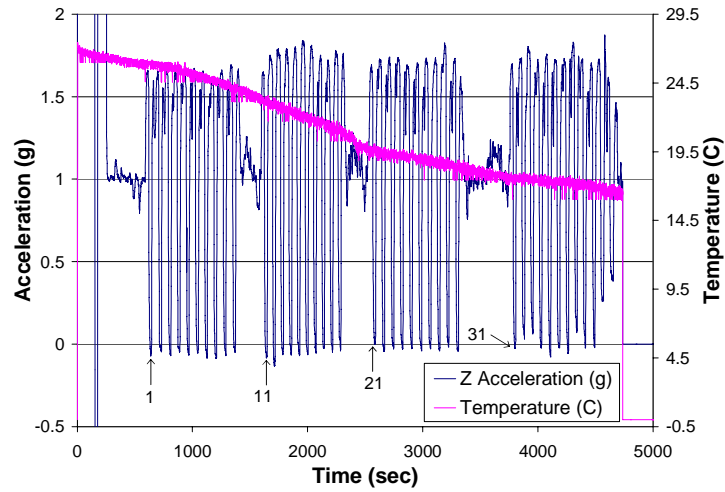


Figure 4. Day 1. Temperature and Z Acceleration vs. Time

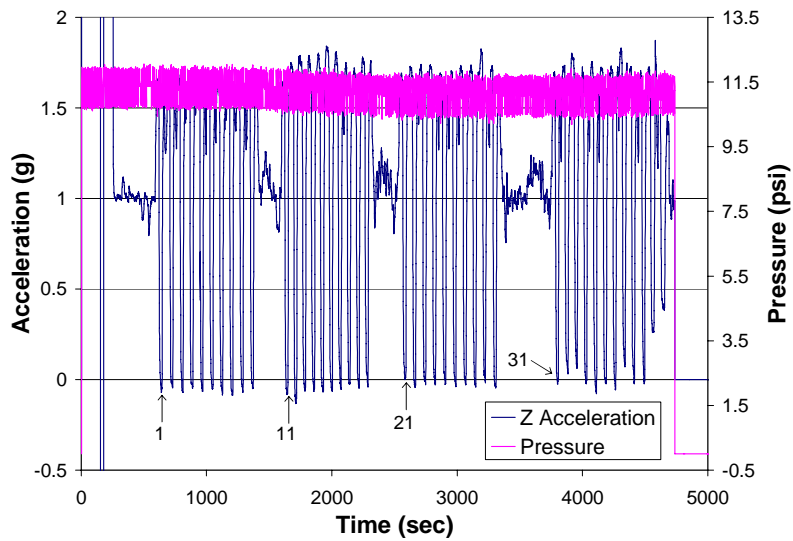


Figure 5. Day 1. Pressure and Z Acceleration vs. Time

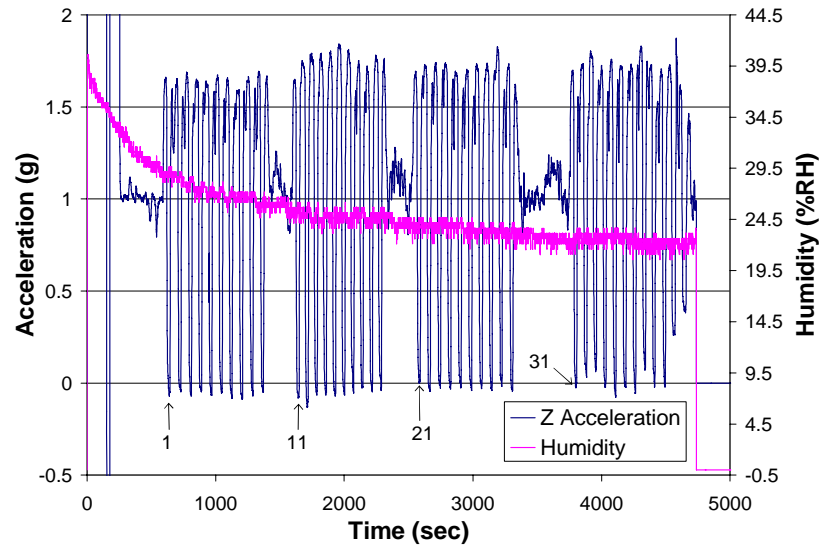


Figure 6. Day 1. Humidity and Z Acceleration vs. Time

Table 1. Day 1 Results

2500	Temperature: 16.58-17.30 °C Pressure: 10.46-11.78 psi Humidity: 21.60 - 22.63% Phase Separation 100%	Temperature: 16.04-17.52 °C Pressure: 10.47-11.75 psi Humidity: 21.60 - 23.13% Phase Separation 100%	Temperature: 17.04-17.71 °C Pressure: 10.45-11.73 psi Humidity: 22.63 - 23.13% Phase Separation 100%	Temperature: 17.03-17.92 °C Pressure: 10.45-11.75 psi Humidity: 22.11 - 23.64% Phase Separation 100%	Temperature: 18.29-19.06 °C Pressure: 10.36-11.71 psi Humidity: 22.63 - 24.15% Phase Separation 99.9854%	Temperature: 18.89-19.66 °C Pressure: 1 0.44-11.72 psi Humidity: 23.64 - 24.15% Phase Separation 99.9751%
1600	Temperature: 16.55-17.61 °C Pressure: 10.52-11.67 psi Humidity: 21.6 - 23.64% Phase Separation 100%	Temperature: 16.86-17.74 °C Pressure: 10.54-11.76 psi Humidity: 22.11 - 23.64% Phase Separation 100%	Temperature: 16.98-18.0 °C Pressure: 10.47-11.76 psi Humidity: 22.11 - 23.13% Phase Separation 100%	Temperature: 18.24-19.23 °C Pressure: 10.43-11.70 psi Humidity: 22.63 - 24.15% Phase Separation 100%	Temperature: 18.71-19.67 °C Pressure: 1 0.4-11.75 psi Humidity: 23.13 - 24.66% Phase Separation 99.9886%	Temperature: 21.18-22.19 °C Pressure: 10.5-11.8 psi Humidity: 24.66 - 25.16% Phase Separation 99.9874%
1000	Temperature: 17.03-17.82 °C Pressure: 10.42-11.68 psi Humidity: 21.60 - 23.64% Phase Separation 100%	Temperature: 17.11-17.82 °C Pressure: 10.47-11.69 psi Humidity: 21.09 - 23.13% Phase Separation 100%	Temperature: 18.32-19.28 °C Pressure: 10.43-11.83 psi Humidity: 23.13 - 24.15% Phase Separation 100%	Temperature: 18.89-19.80 °C Pressure: 10.46-11.76 psi Humidity: 23.64 - 24.15% Phase Separation 100%	Temperature: 21.72-22.36 °C Pressure: 0.52-11.89 psi Humidity: 24.15 - 25.16% Phase Separation 99.9924%	Temperature: 22.63-23.38 °C Pressure: 10.56-11.87 psi Humidity: 24.66 - 26.16% Phase Separation 99.9798%
630	Temperature: 17.44-18.88 °C Pressure: 10.23-11.71 psi Humidity: 22.63 - 24.15% Phase Separation 100%	Temperature: 18.33-19.34 °C Pressure: 10.44-11.83 psi Humidity: 21.60 - 24.15% Phase Separation 100%	Temperature: 19.08-20.07 °C Pressure: 10.49-11.73 psi Humidity: 23.13 - 24.66% Phase Separation 100%	Temperature: 21.73-22.68 °C Pressure: 10.54-11.92 psi Humidity: 23.64 - 25.66% Phase Separation 100%	Temperature: 22.69-23.56 °C Pressure: 1 0.57-11.98 psi Humidity: 25.16 - 26.66% Phase Separation 99.9287%	Temperature: 24.34-24.93 °C Pressure: 10.21-12.05 psi Humidity: 26.16 - 27.16% Phase Separation 99.9822%

400	Temperature: 18.87-19.63 °C Pressure: 10.4-11.84 psi Humidity: 23.64 - 24.66% Phase Separation 100%	Temperature: 20.29-21.68 °C Pressure: 10.47-11.79 psi Humidity: 23.64 - 25.16% Phase Separation 100%	Temperature: 22.14-23.04 °C Pressure: 10.58-11.76 psi Humidity: 24.66 - 25.16% Phase Separation 100%	Temperature: 23.14-24.5 °C Pressure: 10.71-12.02 psi Humidity: 25.16 - 26.66% Phase Separation 100%	Temperature: 24.5-25.16 °C Pressure: 10.6-11.97 psi Humidity: 26.16 - 27.66% Phase Separation 100%	Temperature: 24.93-25.58 °C Pressure: 10.69-11.99 psi Humidity: 26.66 - 27.66% Phase Separation 100%
250	Temperature: 21.14-22.03°C Pressure: 10.61-11.79 psi Humidity: 24.66 - 25.66% Phase Separation 100%	Temperature: 21.73-23.08 °C Pressure: 10.47-11.89 psi Humidity: 24.15 - 25.66% Phase Separation 100%	Temperature: 24.01-24.69 °C Pressure: 10.66-11.95 psi Humidity: 26.16 - 27.16% Phase Separation 100%	Temperature: 24.58-25.25 °C Pressure: 10.66-11.98 psi Humidity: 26.66 - 27.66% Phase Separation 100%	Temperature: 24.58-25.75 °C Pressure: 10.65-11.95 psi Humidity: 26.66 - 27.66% Phase Separation 100%	Temperature: 25.4-25.93 °C Pressure: 10.7-11.98 psi Humidity: 27.16 - 28.65% Phase Separation 100%
Gas ▲ Liquid ► ($\mu\text{L}/\text{min}$)	250	400	630	1000	1600	2500

The following graphs and table represent the data collected on Day 2. As seen in Figure 7, the temperature steadily decreased during the 2-hour flight. From the beginning of the first parabola to the end of the last parabola, the temperature dropped 10.09°C, similar to the temperature drop on Day 1. Figure 8 shows that the pressure fluctuated within a constant range throughout the entire flight. The pressure remained within the range of 10.19 – 11.85 psi. Figure 10 shows that the relative humidity remained in a somewhat constant range through the first one and a half parabolas, at which point it began to gradually decrease. Overall, the humidity ranged from 27.66% - 21.60% over the course of the flight. Table 2 summarizes the matrix of gas and liquid flow rate testing results that were obtained and the phase separation success on Day 2.

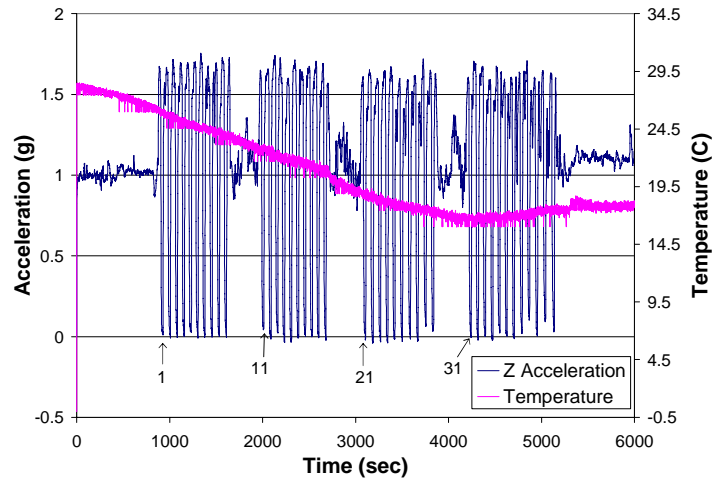


Figure 7. Day 2. Temperature and Z Acceleration vs. Time

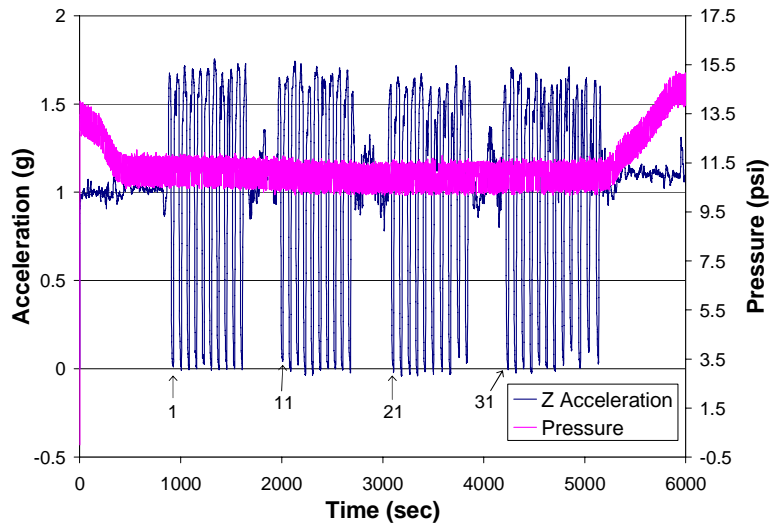


Figure 8. Day 2. Pressure and Z Acceleration vs. Time

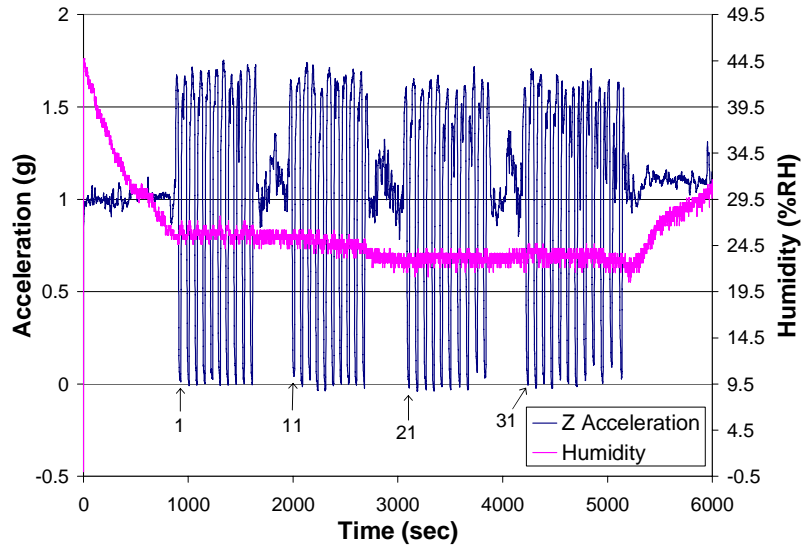


Figure 9. Day 2. Humidity and Z Acceleration vs. Time

Figure 10. Day 2. Humidity and Z Acceleration vs. Time

Table 2. Day 2 Results

2500	Temperature: 16.35-17.34 °C Pressure: 10.38- 11.51 psi Humidity: 23.13-24.15% Phase Separation 100%	Temperature: 16.04-17.08 °C Pressure: 10.37-11.59 psi Humidity: 22.11-24.15% Phase Separation 100%	Temperature: 16.04-17.19 °C Pressure: 10.33-11.67 psi Humidity: 22.11-24.66% Phase Separation 99.9996%	Temperature: 16.86-17.69 °C Pressure: 10.23-11.67 psi Humidity: 22.63-24.15% Phase Separation 99.9932%	Temperature: 17.44-18.31 °C Pressure: 10.19-11.69 psi Humidity: 22.11-24.15% Phase Separation 100%	Temperature: 18.35-19.28 °C Pressure: 10.32-11.60 psi Humidity: 21.60-23.64% Phase Separation 100%
	1600	Temperature: 16.04-17.20 °C Pressure: 10.35- 11.54 psi Humidity: 22.63-24.15% Phase Separation 100%	Temperature: 16.24-17.21 °C Pressure: 10.23-11.56 psi Humidity: 23.64-24.66% Phase Separation 100%	Temperature: 17.11-17.86 °C Pressure: 10.20- 11.55 psi Humidity: 22.11- 24.15% Phase Separation 100%	Temperature: 17.45-18.42 °C Pressure: 10.28- 11.51 psi Humidity: 22.11- 24.15% Phase Separation 99.9956%	Temperature: 20.38-21.32 °C Pressure: 10.23-11.61 psi Humidity: 23.64-25.16% Phase Separation 99.9918%
1000	Temperature: 16.57-17.08 °C Pressure: 10.38-11.54 psi Humidity: 22.62-24.65% Phase Separation 100%	Temperature: 17.09-18.02 °C Pressure: 10.20- 11.65 psi Humidity: 22.11- 24.15% Phase Separation 100%	Temperature: 17.69-18.61 °C Pressure: 10.25- 11.54 psi Humidity: 22.11- 23.64% Phase Separation 100%	Temperature: 20.49-21.43 °C Pressure: 10.30- 11.59 psi Humidity: 23.13- 25.16% Phase Separation 100%	Temperature: 21.38-22.38 °C Pressure: 10.32-11.59 psi Humidity: 23.64-26.16% Phase Separation 99.087%	Temperature: 23.14-24.28 °C Pressure: 10.45-11.70 psi Humidity: 25.16-26.66% Phase Separation 99.923%

630	Temperature: 17.40-18.13 °C Pressure: 10.29-11.78 psi Humidity: 22.63-24.15% Phase Separation 100%	Temperature: 17.45-18.97 °C Pressure: 10.25-11.52 psi Humidity: 22.11-24.15% Phase Separation 100%	Temperature: 20.87-21.72 °C Pressure: 10.25-11.58 psi Humidity: 23.13-25.66% Phase Separation 99.9716%	Temperature: 21.86-22.67 °C Pressure: 10.45-11.64 psi Humidity: 24.15-26.16% Phase Separation 100%	Temperature: 23.14-24.56 °C Pressure: 10.46-11.73 psi Humidity: 25.16-27.16% Phase Separation 100%	Temperature: 24.36-25.06 °C Pressure: 10.57-11.78 psi Humidity: 25.66-27.66% Phase Separation 100%
400	Temperature: 18.06-19.31 °C Pressure: 10.24-11.61 psi Humidity: 21.60-23.64% Phase Separation 100%	Temperature: 20.29-21.84 °C Pressure: 10.37-11.58 psi Humidity: 23.64-25.66% Phase Separation 100%	Temperature: 21.72-22.93 °C Pressure: 10.45-11.70 psi Humidity: 25.16-26.16% Phase Separation 100%	Temperature: 24.17-24.81 °C Pressure: 10.51-11.80 psi Humidity: 24.15-26.16% Phase Separation 100%	Temperature: 24.57-25.15 °C Pressure: 10.64-11.77 psi Humidity: 25.16-26.66% Phase Separation 100%	Temperature: 25.12-25.76 °C Pressure: 10.47-11.79 psi Humidity: 25.16-26.67% Phase Separation 100%
250	Temperature: 21.31-22.18 °C Pressure: 10.27-11.53 psi Humidity: 24.15-26.16% Phase Separation 100%	Temperature: 22.19-23.13 °C Pressure: 10.44-11.76 psi Humidity: 25.16-26.16% Phase Separation 100%	Temperature: 24.33-24.96 °C Pressure: 10.56-11.74 psi Humidity: 25.16-26.66% Phase Separation 100%	Temperature: 24.57-25.49 °C Pressure: 10.65-11.81 psi Humidity: 25.16-26.66% Phase Separation 100%	Temperature: 24.57-25.99 °C Pressure: 10.55-11.85 °C Humidity: 25.16-27.16% Phase Separation 100%	Temperature: 25.69-26.13 °C Pressure: 10.60-11.83 psi Humidity: 24.66-26.66% Phase Separation 100%
<i>Gas</i> ▲ <i>Liquid</i> ► <i>(μL/min)</i>	250	400	630	1000	1600	2500

DISCUSSION

The flight testing method devised to evaluate the device was effective and appropriate for evaluation purposes. The flight box was raised from the deck of the plane when the 0g portion of the flight began and was left in suspension for the duration of a flight parabola. Minor orientation and position corrections were required during this period to prevent the box from contacting a wall or drifting too far from its station. The disturbance introduced by these corrections was minor, however. Additionally, vibrations produced by the two peristaltic pumps, the drive motor for the MiniDV camera, and the fan and hard drive from the laptop computer may have also affected the measurement. However, the amplitude of these vibrations was below the level detectable by hand on the panel where the phase separators were mounted.

The phase separator removed more than 99% of all gas from the liquid stream at all flow rates tested and all liquid from the gas stream at all flow rates tested. The ambient conditions under which this occurred ranged in temperature from 16°C to 26°C, in pressure from 10.2 to 11.9 psia, and in relative humidity from 22% to 29% over two test flights. However, none of these ambient conditions appeared to have as significant an effect on the efficiency of the phase separator as flow rate did.

Due to the wide range of flow rates tested, both in liquid and gas, and the relatively small number of device failures recorded, it is difficult to make a statistically significant conclusion regarding the exact effect that flow rate, either of liquid or gas, has on the phase separator. However, it does seem clear that higher flow rates of both liquid and gas are more prone to phase separation failure. This may be due to the lack of available time for small, entrained bubbles to reach the wall of the ePTFE tubing to be expelled from the liquid. It is likely that a longer ePTFE tubing length in the phase separator would ameliorate this problem. However, increasing the length of this tubing would also increase the flow volume in the overall instrument, and could increase the rate of water loss due to evaporation through the wall of the ePTFE tubing. As measured independently in previous, ground-based research, however, this water loss rate is small and can be stopped by closing off the gas outlet of the phase separator with a valve. Gas in the internal volume of the phase separator housing becomes saturated with water vapor and no further water loss is experienced beyond that point.

CONCLUSION

Based on the results achieved, the phase separator performed quite successfully in the flight tests performed. In the mesofluidic system that the phase separator is designed to operate in, the typical fluid flow rate is approximately 250 $\mu\text{L}/\text{min}$. In the tests, no failure in phase separation was detected for any flow rate less than 630 $\mu\text{L}/\text{min}$, or approximately 2.5 times the nominal flow rate of the device. Additionally, during typical operation, the gas flow rate in the inlet stream will likely be much lower than the liquid flow rate. In the configurations where the phase separation was incomplete during this flight test, the gas flow rate was typically as high as or higher than the liquid flow rate. This condition is less likely to be encountered in the ion analyzer system that the separator was designed for. Lastly, the degree of failure detected for higher flow rates was quite small. In every case tested, more than 99% of the inlet gas was removed from the outlet stream and in most cases a considerably higher percentage was removed. Therefore, this device may be utilized at higher flow rates in other applications where the requirements for gas removal are less strict than in ion chromatography. Overall, the results achieved were highly

beneficial for the project as a whole and confirmed that the passive, small-footprint, mesofluidic phase separator design operates successfully in a 0g environment at relevant flow rates.

ACKNOWLEDGEMENT

This work is based on work from Contract No. NNJO4HE02A Issued by NASA Lyndon B. Johnson Space Center

PHOTOGRAPHS

JSC2006E17627
JSC2006E17777 to JSC2006E17783
JSC2006E17796 to JSC2006E17796
JSC2006E17802 to JSC2006E17807
JSC2006E17813
JSC2006E17929 to JSC2006E17930
JSC2006E17940 to JSC2006E17942
JSC2006E17938 to SC2006E17946
JSC2006E17954 to JSC2006E17958
JSC2006E17961
JSC2006E17966 to JSC2006E17969

VIDEO

- Zero G May 8 – May 12, 2006, Master: 720902

Videos available from Imagery and Publications Office (GS4), NASA/JSC.

CONTACT INFORMATION

Tony Ragucci
Sensor Program Coordinator / Research Scientist
Lynntech, Inc.
1313 Research Parkway
College Station, TX 77845
(979) 693-0017
tony.ragucci@lynntech.com

TITLE

Prototype Flight Cytometer

FLIGHT DATES

May 11-12, 2006

June 15-16, 2006

PRINCIPAL INVESTIGATOR

Brian Crucian, Wyle Laboratories, Inc., Life Sciences Group

Terry Guess, Wyle Laboratories, Inc., Life Sciences Group

Mayra Nelman-Gonzalez, Wyle Laboratories, Inc., Life Sciences Group

Clarence Sams, NASA/Johnson Space Center



GOAL

The primary experiment for these flights was a microgravity evaluation of the recent engineering changes to the Prototype Flight Cytometer. This instrument is being developed by the JSC Immunology Laboratory to provide medical support during exploration-class space missions.

OBJECTIVES

A spaceflight-compatible flow cytometer would be useful for diagnosing astronaut illness during long-duration space flight and for conducting in-flight research to evaluate the effects of microgravity on human physiology. Currently, there is no capability to generate real-time hematology/immunology data on orbit.

Standard commercially available flow cytometers are large, complex instruments that use high-energy lasers and require liters of liquid “sheath” fluid to operate. They also generate a significant amount of liquid biohazardous waste and require significant training to operate. Cytometers use the fluid mechanical property of “hydrodynamic focusing” to place stained blood cells in single file (laminar flow) as they pass through a laser beam for scanning and evaluation. Many spaceflight experiments have demonstrated that fluid physics is dramatically altered in microgravity (1) and previous studies have shown that sheath fluid-based hydrodynamic focusing may also be altered during microgravity (2). For these reasons it is likely that any spaceflight-compatible design for a flow cytometer would abandon the sheath fluid requirement. The elimination of sheath fluid would remove the problem of weight associated with large volumes of liquids as well as the large volume of liquid waste generated. It would also create the need for a method to create laminar particle flow distinct from the standard sheath fluid-based method.

The Prototype Flight Cytometer (PFC) developed by the JSC Immunology Laboratory is based on a recently developed commercial flow cytometer with significant new engineering modifications. The PFC possesses a novel flow cell design that creates single-particle laser scanning and evaluation without the need for sheath fluid-based hydrodynamic focusing. The instrument is also miniaturized and lightweight, uses a low energy diode laser, has a small number of moving parts and does not generate significant liquid waste. Operationally, the PFC function is similar to that of a standard bench-top laboratory flow cytometer, aspirating liquid particle samples and generating histogram or dot-plot data in standard “FCS” file format.

NASA has awarded a CDDF grant to the JSC Immunology Laboratory to (1) engineer a prototype flight instrument based on the framework of the commercial cytometer; (2) perform ground-based and microgravity validation of the instrument (3) design and validate a set of medical assays compatible with the prototype instrument (4) design and validate a microgravity compatible cell staining device for sample processing that can interface with the instrument. To date, this instrument represents the only fully functioning microgravity-compatible flow cytometer. The results from this project were recently published in a 2005 issue of *Cytometry* (3) and presented to the scientific community at the annual meeting of the International Society of Analytical Cytology (ISAC) in Quebec Canada, May 2006 (4).



METHODS AND MATERIALS

Blood donors. Whole blood samples were obtained from adult donors into EDTA anticoagulant vacutainers. This includes the C-9 flight evaluations and all developmental work performed in preparation for the experiment. The subjects had been screened by the NASA JSC Test Subject Facility for most major infectious diseases and were found to be in good health. Institutional Review Board (NASA-JSC) approval was obtained for this study and written informed consent was obtained from all subjects.

Cell Staining. A complete 2-color antibody panel was formulated to resolve most major leukocyte subsets while remaining within the limitations of the instrument. The cell populations resolved included leukocyte subsets, T cells, B cells, NK cells, T cell subsets and activated T cells. Cell surface markers were stained before flight. For the bead-based cytometry samples, either fluorescent calibration microspheres or linearity fluorescent microspheres were used.

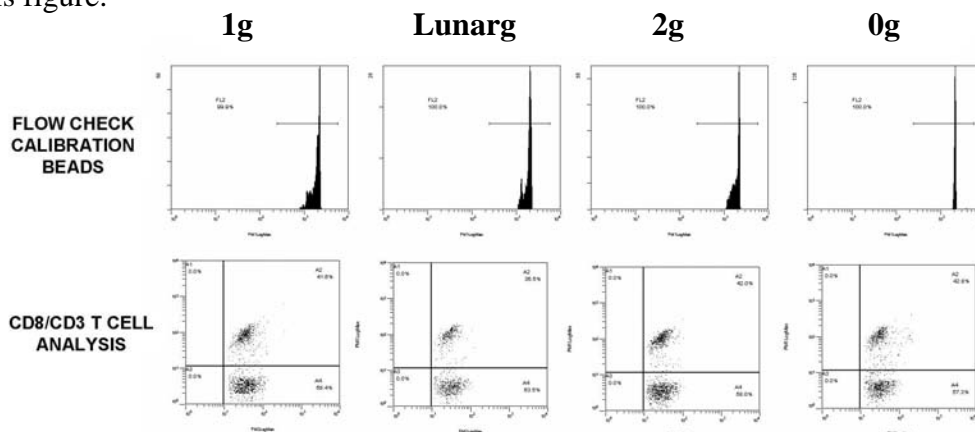
Flow cytometry analysis. All blood cell samples were stained and stored in WBSD-2 devices, designed to interface with the sampling ports on the PFC. To ensure data collection occurred during microgravity only, samples were mixed and affixed to the sampling probe and the instrument was primed prior to the initiation of the microgravity (2g, lunar, etc) phase. Priming took place during the appropriate period prior to the parabolas. Data collection was initiated and ended as the C-9 entered and exited the appropriate phase of the parabola.

FY06 ENGINEERING CHANGES TO CYTOMETER

- The unit was significantly reduced in size. Electronic boards were moved and unused internal volume was reduced.
- Custom-designed sample ports that interface with the WBSD-2 devices were installed on the instrument face. The WBSD-2 devices are designed to stain whole blood cells, lyse the red blood cells, and fix the stained white blood cells during spaceflight. They are completely microgravity-compatible and were validated during a series of 2004 KC-135 reduced gravity flights.
- The heavy steel casing was replaced with a lightweight rack-size aluminum casing.
- The laptop control system (sub-optimal for reduced gravity operations) was replaced with a touchscreen-based computer control system. This makes the Prototype Flight Cytometer significantly easier to use during reduced-gravity conditions.

RESULTS

The reduced-gravity evaluations performed in May and June of 2006 demonstrated that the latest version of the PFC continued to function extremely well during reduced gravity conditions. The most recent engineering changes had not altered or reduced this capability. During these flights, all three users indicated that the touch-screen instrument computer control was a significant improvement for reduced-gravity operations. In addition, the lightweight portable aspects of the instrument were proven, as the PFC was stored in the overhead aircraft storage bins prior to in-air deployment and utilization. Representative dot-plot data from these C-9 flights demonstrating PFC capability during 0g, lunar gravity, 2g (hypergravity), and 1g (control data) are presented in this figure:



DISCUSSION

The flow cytometer is an extremely versatile laboratory instrument with a broad spectrum of uses in both clinical medicine and basic science research. It is therefore highly desirable to develop a spaceflight-compatible cytometer for use on the International Space Station and for medical support during exploration-class space missions. The PFC's medical capability, level of miniaturization, use of a low-energy diode laser, and elimination of the sheath fluid uniquely meet the existing prerequisites for use during spaceflight. Having proven functionality during 0g, the PFC may be well suited to be the prototype from which a medical instrument for on-orbit operations is designed.

CONCLUSION

Significant engineering changes to the Prototype Flight Cytometer were made and instrument performance during reduced gravity was successfully verified.

REFERENCES

1. NASA-Marshall Space Flight Center (1997). Microgravity Research Division: Microgravity Fluid Physics Discipline Brochure. Available online at <http://mgnews.msfc.nasa.gov/db/fluid-phys.pdf> (PDF document) or <http://mgnews.msfc.nasa.gov/db/fluids/fluids.html> (HTML document).
2. Crucian, B., Norman, J., Brentz, J., Pietrzyk, R. and Sams, C. Laboratory outreach: student assessment of flow cytometer fluidics in zero-gravity. *Laboratory Medicine* 31(10):569-572, 2000.
3. Crucian, B., and Sams, C. Microgravity evaluation of a potential spaceflight-compatible flow cytometer. *Cytometry*, 66(1):1-9, 2005
4. Crucian, B., and Sams, C. Development of a Prototype Flight Cytometer for medical support during exploration class space missions. *International Society for Analytical Cytology* meeting, Quebec, Canada, 2006.

PHOTOGRAPHS

JSC2006E18060 to JSC2006E18105
JSC2006E23168 to JSC2006E23206
JSC2006E23961 to JSC2006E23994

VIDEO

- Zero G May 8 – May 12, 2006, Master: 720902
- Zero G June 16 – 23, 2006 flights, Master: 721249

Videos available from Imagery and Publications Office (GS4), NASA/JSC.

CONTACT INFORMATION

Brian Crucian, Ph.D.
Wyle Laboratories, Inc., Life Sciences Group
1290 Hercules Suite 120
Houston, TX 77058
281-483-7061
brian.crucian1@jsc.nasa.gov

TITLE

Evaluation of Hardware for Sampling of Water onboard ISS for Subsequent Microbial Testing

FLIGHT DATES

May 11-12, 2006

June 14-15, 2006

PRINCIPAL INVESTIGATORS

Mayra Nelman-Gonzalez, Wyle Laboratories, Inc., Life Sciences Group

Wing Wong, Wyle Laboratories, Inc., Life Sciences Group

CO-INVESTIGATORS

Brian Crucian, Wyle Laboratories, Inc., Life Sciences Group

Terry Guess, Wyle Laboratories, Inc., Life Sciences Group

Clarence Sams, NASA Johnson Space Center

Duane Pierson, NASA Johnson Space Center

Mark Ott, NASA Johnson Space Center



GOAL

The purpose of this experiment was to perform a microgravity evaluation of some engineering changes to the water collection/sampling hardware used on the International Space Station (ISS) for microbial testing of water samples.

OBJECTIVES

Prototype hardware for the crew health care system (CHeCS) Water Microbiology Kit for ISS was evaluated on this C-9 flight. This hardware is specifically designed for the in-flight detection of bacteria in water stored on the ISS at the new acceptability limit. This is one parameter used to mitigate risk to crew health. While sampling water onboard ISS, the inadvertent capture of air bubbles has been a problem. This evaluation tested protocols developed by engineers to modify the hardware and protocols to eliminate the problem related to the air bubbles. This is critical since the new acceptability limit has reduced volume sampling requirements increasing the requirement to eliminate potential air bubble trapping.



Water sampling device in use onboard ISS

Three distinct hardware components were evaluated. The first involved determining the appropriate procedure to eliminate air bubbles during water sampling. Procedures were also tested for the elimination of air bubbles that may accidentally be aspirated into the sampling syringe on orbit.



Phase 2 of the testing involved the direct sampling of water onto a Microbial Capture Device (MCD) which is used during on-orbit sampling for bacterial count determination. Several aspects were addressed during this evaluation. These included, methodology for exclusion of air bubbles, the sample volume requirement for filling the samples filter devoid of air bubbles, the transit of water sample through the filter, and determination of the syringe pressure required to move the sample volume into the filter and then through the syringe.

Phase 3 of the testing involved direct sampling of water first from a water sampling syringe onto an MCD, then into the aspiration syringe. This evaluation involved determination of whether a hardware modification from the second evaluation (specifically the removal of a venting filter to eliminate pressure problems) would pose problems with transit of the sample into and through the MCD.

All three evaluations were conducted onboard the C-9 throughout multiple parabolas and were recorded using video and photographic imagery. The results will be provided to the CHeCS

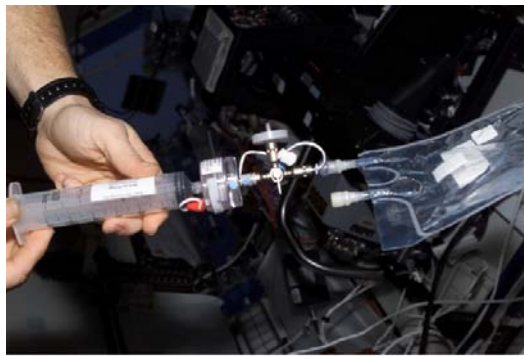
System engineers to determine which modifications are feasible for use on future ISS Expeditions.

MATERIALS AND METHODS

Modified water collection hardware and full water sample bags were used during the evaluation. The participants performed each step of the water sampling protocol during the microgravity phase of parabolic flight. Digital video of each step in the protocol was captured and examined by the JSC engineers.

RESULTS

The evaluations on the May and June flights provided clear insight into the questions being addressed. First, removal of air bubbles from the bag prior to sampling could be accomplished so that no impact was observed on the required sampling volume. Various techniques were evaluated for displacement of air bubbles at the exit ports before sampling. Different options were determined to be functional for removing of these bubbles from the exit ports and these options were transmitted to the principle investigators. Problems were encountered when proper seals were not formed between the various hardware pieces. On Day 2 of the first set of flights, special attention was paid to assure that all seals were properly formed. This mitigated any problems encountered during the first day. Actual flight hardware is permanently bonded to ensure proper seals throughout the hardware. This ensures that crewmembers do not encounter unforeseen problems with air bubbles being introduced or improper sampling.



The second set of questions involved the transfer of a sample through an MCD from one syringe directly into another. This sampling device was problematic due to pressure problems that formed during the process. This resulted in an inability to pass all the required volume through the designated MCD. After the first flights, alterations were made design to mitigate the pressure problems encountered with this apparatus. The modification involved a change in the transfer method and the addition of a venting air filtration device to relieve the pressure formed during transfer of the water sample from the first syringe into the MCD, and then transfer of the sample in the MCD into the second syringe.

The second flights demonstrated that the new configuration eliminated the pressure problems encountered with the original hardware. The testing team was able to successfully transfer the entire required sample through the MCD and into the second MCD with minimal pressure problems.

DISCUSSION

Currently the Microbiology Laboratory is working on a redesign of the CHeCS water Microbiology Kit for the ISS. The prototype that is being developed will allow the in-flight detection of bacteria at the new acceptability limit, which is one parameter used to mitigate risk to crew health. The evaluation performed during the recent reduced-gravity evaluations focused on water properties and bubble formation with syringes and filters that are used during flight. These flights allowed us to test all necessary parameters for successfully carrying out the required water sampling activities. More importantly, they provided us with insight into an

unforeseen problem, and this resulted in a redesign of the hardware. This redesign was successful in achieving the required endpoint for sampling and the knowledge gained will be directly applied to the in-flight hardware. The knowledge provided by using the reduced-gravity program for pre-testing actual flight hardware was invaluable for the development and design of experiments and hardware for in-flight activities. In this case, the redesign of the CHeCS water Microbiology Kit will assure the principal investigator team that proper sampling can be carried out by crewmembers, which is crucial for ensuring that all necessary standards are upheld to mitigate risk to crew health with regard to the potable water system on ISS.

CONCLUSION

The reduced-gravity program has provided this team with the ability to test engineering changes to the CHeCS Water Microbiology Kit for the ISS. These tests allowed necessary modification to be made and ensured that proper sampling could be accomplished with the newly configured hardware.

REFERENCES

International Space Station Medical Operations Requirements Documents (ISS MORD) SSP 50260 Revision B

PHOTOGRAPHS

JSC2006E18060 to JSC2006E18105
JSC2006E23168 to JSC2006E23206
JSC2006E23961 to JSC2006E23994

VIDEO

- Zero G May 8 – May 12, 2006, Master: 720902
- Zero G June 16 – 23, 2006 flights, Master: 721249

Videos available from Imagery and Publications Office (GS4), NASA/JSC.

CONTACT INFORMATION

Mayra Nelman-Gonzalez
Wyle Laboratories, Inc., Life Sciences Group
1290 Hercules Suite 120
Houston, TX 77058
281-483-7192
mayra.a.nelman@nasa.gov

TITLE

Microgravity Effects on Plant Boundary Layers

FLIGHT DATES

May 23-26, 2006

PRINCIPAL INVESTIGATOR

Gary Stutte, Dynamac Corporation
Oscar Monje, Dynamac Corporation



OBJECTIVE

The goal of this series of experiments was to determine the effects of microgravity on the developmental boundary layers in roots and leaves and to determine the effects of air flow on boundary layer development. It is hypothesized that microgravity induces larger boundary layers around plant organs because of the absence of buoyancy-driven convection. These larger boundary layers may affect normal metabolic function because they may reduce the fluxes of heat and metabolically active gases (e.g., oxygen, water vapor, and CO₂). These experiments were to test whether a change in boundary layer is associated with microgravity, quantify the change if it exists, and determine influence of air velocity on boundary layer thickness under different g conditions.

METHODS AND MATERIALS

Experiment Description

The following experiments were performed as part of the Microgravity Effects on Plant Boundary Layers project on the C-9:

1. Rates of temperature change in microgravity of monocot (wheat) and dicot (radish) plant leaves at different velocities of forced convection were measured.
2. Rates of temperature change in microgravity of monocot (wheat) and a dicot (radish) plant leaves with different thermal loads (light intensity) were measured.
3. Localization of thermal gradients within the canopy of a monocot (wheat) and dicot (radish) were measured with an infrared thermal imager.

The results from this experiment provided insight into how microgravity-induced changes in boundary layers affect mass and heat transport from different types of plant canopies to the bulk air.

Similar experiments have flown three times aboard the KC-135 aircraft, first as a part of the ISS PESTO experiment in 2000, and twice as a Fluid Physics-Plant Growth Experiment on a combined flight of Advanced Life Sciences and Fundamental Biology experiments in early 2004.

Hardware Description

Oscar Monje, Ph.D., was the technical lead for these experiments and designed the payload hardware package. He has been responsible for postflight analysis of data.

The experiment hardware consists of an aluminum base plate with a small rack that contains the plant chambers, fan, accelerometer, data logger, light and video equipment. The base plate was bolted to the floor prior to takeoff and has the accelerometer, data logger, fan, and light attached. The video equipment and plant chambers were set up upon reaching level flight and were re-stowed prior to landing. An infrared thermal camera was set up 0.6 m from the test plants. The camera was deployed during takeoff and restowed prior to landing. Operators used straps for restraint during the parabolas.



Figure 1. Oscar Monje secures the payload in the C-9.

The aluminum base plate provides structural support for crash landing and has flown numerous times aboard the KC-135. Figure 1 shows the experiment configuration on the aluminum base plate.

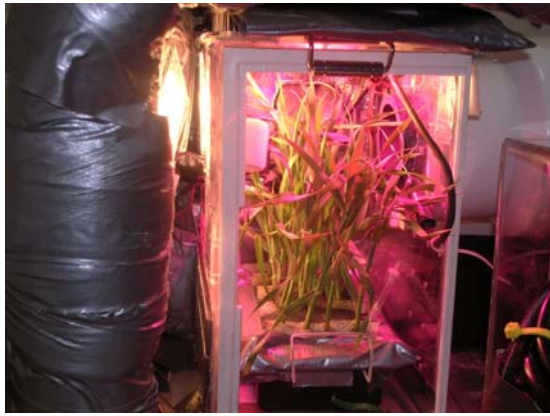


Figure 2. Apogee wheat placed in test stand. The canopy is positioned so that air is forced through the canopy.

The wheat plants were maintained in the test stand using Velcro and positioned so that the wind tunnel forced air through the canopy. This configuration is shown in Figure 2.

The radish plants were maintained in the test stand using Velcro and positioned so that the wind tunnel forced air across the top of the canopy. This configuration is shown in Figure 3.

Flight Profiles

The experiments were conducted over a period of 4 flight days. On each day, a minimum of 4 sets of 10 μg parabolas was obtained. Each set of 10 parabolas was at a different wind speed. The under-canopy temperatures obtained in the first 5 parabolas of each set with a high (white light and red light) thermal source and in the second 5 parabolas of each set with a low (red light) thermal source. Data from radish plants was obtained on flight days 1 and 2, and data from wheat was obtained on flight days 3 and 4. The flight profile of a set of 10 parabolas and a map of the flight path are provided for reference in Appendix A.

RESULTS

Microgravity effects on boundary layer development of monocot and dicot leaves.

Changes in resistance of the boundary layer surrounding plant organs will affect leaf transpiration and the resulting evaporative cooling of the leaf surface. Measuring the heating rates of plant canopies under different g conditions (1g, micro-g, and 2g) should allow changes in boundary layer resistance to be estimated. Hypothesized increases in the boundary layer resistance under reduced gravity conditions should disappear as air velocity increases and induces convective mixing. These assumptions were tested by measuring changes in leaf temperature at different levels of forced convection (wind speed) and thermal load (light intensity) during parabolic flights. Two canopy configurations were used: a planophile canopy of the dicot, radish, and an erectophile canopy of the monocot dwarf wheat.

The g force was measured with an accelerometer, the airflow with a hot wire anemometer, air temperature with thermocouples, and canopy temperature with infrared thermometers. Canopy temperature difference ($T_{\text{leaf}} - T_{\text{air}}$) was recorded during the micro-g and 1g segments at various wind speeds. Light levels were measured with a photosynthetically active radiation (PAR) sensor.

All data were logged on a Campbell Datalogger during each day of the flight, and then downloaded to Instagraph software for analysis. A typical display of data collected during the C-9 flight is shown in Figure 4.



Figure 3, Cherry Bomb Hybrid II radish placed in test stand. The canopy is positioned so that air is forced across the canopy.

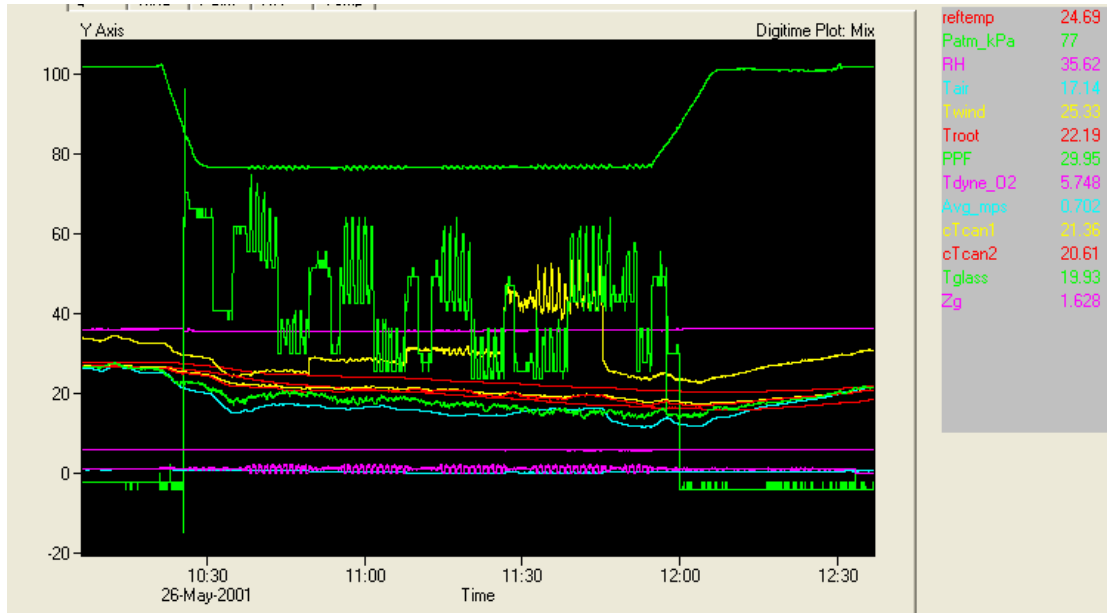


Figure 4. Instagram display of payload sensor data obtained on 26 May, 2006.

The experimental hardware performed well during the parabolic flights.

The boundary layer, as measured by temperature difference, was greater under μg conditions than either 1g or 2g conditions. The effects of increasing air velocity on the boundary layer were less in microgravity than in 1g for both wet and dry surfaces. These data are consistent with the hypothesis that boundary layers in microgravity are greater than they are under 1g. The effects of microgravity on boundary layer increases could be mitigated by increasing air velocity to 0.4 m/s over the surface.

Infrared thermal (IRT) imaging allows the changes in canopy temperature to be localized and quantified during the flight. Reference temperatures were obtained during the 1g periods before the plants experienced any μg parabolas, during the turn-around period following each set of 10 parabolas, and at the end of the parabola set prior to landing at each light setting. Ground controls will also be performed in controlled environment chambers in the Space Life Sciences Laboratory at Kennedy Space Center, Florida.

Initial analysis of the IR images indicates a definite change in canopy temperature in response to g condition, thermal load, and wind speed. The analysis of the interactions between these variables is still being analyzed. However, a typical picture of the canopies of wheat is shown in Figure 5.

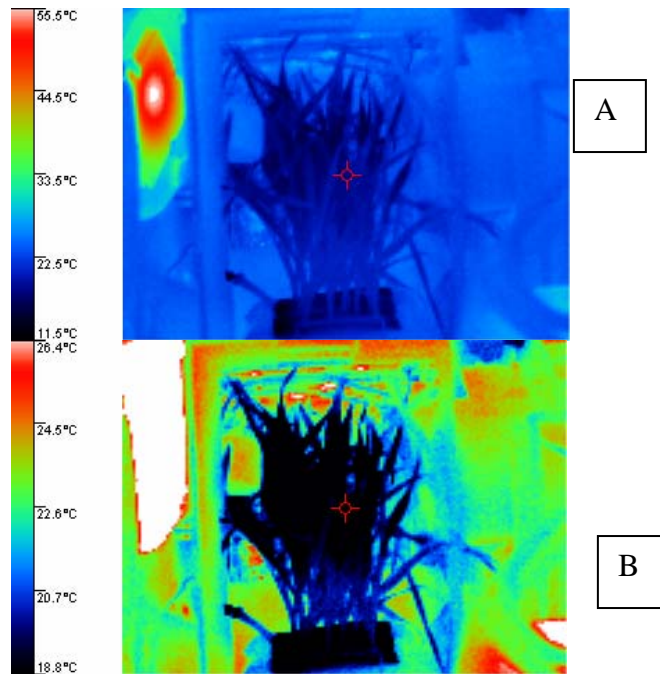
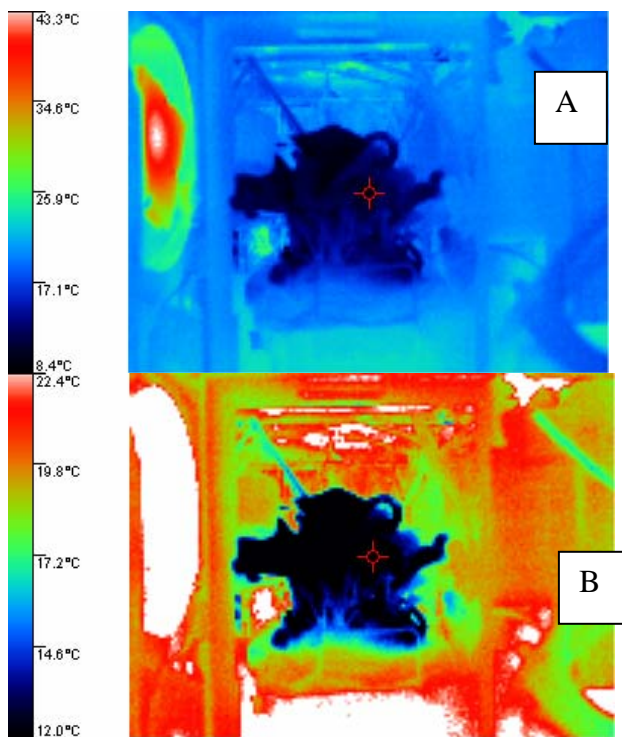


Figure 5. Typical pictures of the canopies of wheat. In A, the temperature profile of the test chamber is seen. In B, the scale has been adjusted so that the canopy can be highlighted for subsequent analysis.



Reconfiguration of the IR temperature sensors to exclude all hardware components, coupled with use of the IRT imaging, is allowing the effects of the *g* environment on development of boundary

layers to be determined, and the wind tunnel experiment has provided data necessary for the design of air handling systems in plant chambers being considered for spaceflight application.

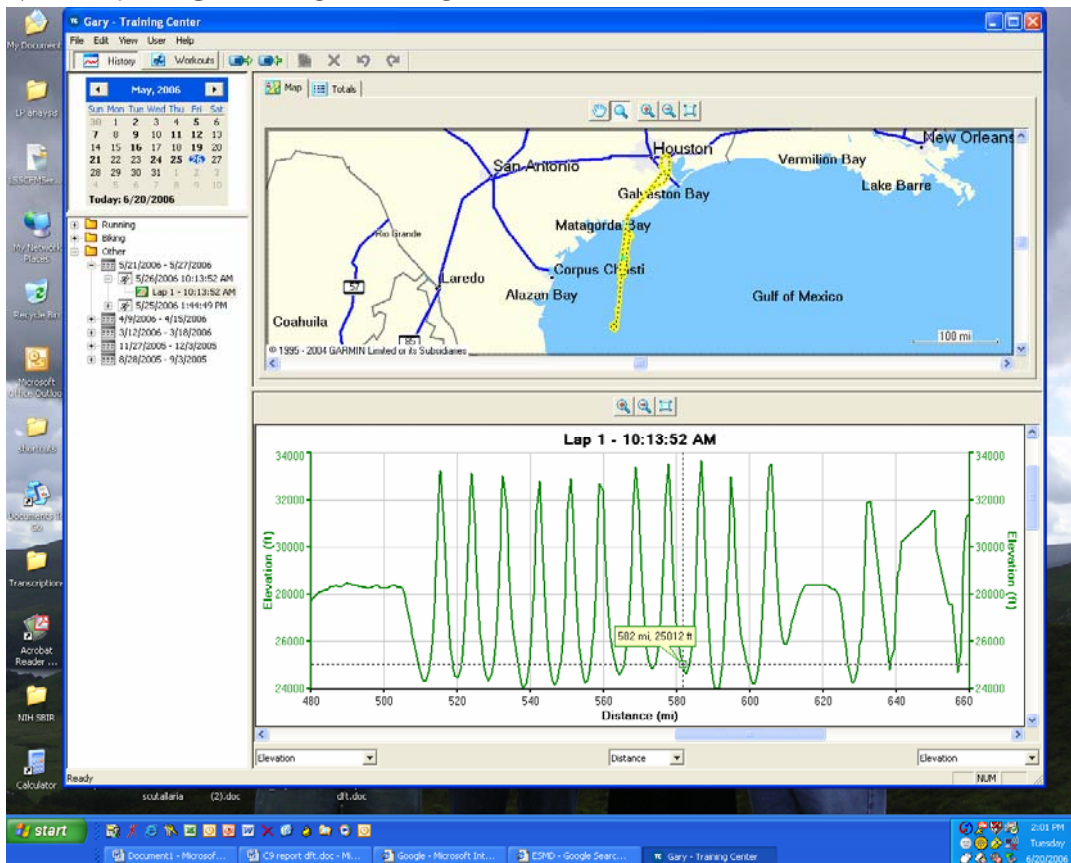
Fractional g testing

During the second, third, and fourth day of the campaign, a request for 0.16 (lunar gravity) and 0.33 (Mars gravity) parabolas was made in order to determine the effects of fractional g on the development, and subsequent mitigation, of canopy boundary layers. These requests were approved and preliminary data under fractional g were obtained. On day 2 (24 May, 2006) data from two lunar (0.16g) and two Martian (0.33g) parabolas were obtained. On day 3 (25 May, 2006) data from four lunar (0.16g) and four Martian (0.33g) parabolas were obtained. On day 4 (26 May, 2006) data from four lunar (0.16g) and one Martian (0.33g) parabolas were obtained.

The data collection parameters were identical to those described above.

During these parabolas, the data suggest that the differential g forces resulted in a proportional effect on boundary layer development around the leaf and in the root zone. These data are very preliminary; however, the results are intriguing for future parabolic flight testing under fractional g conditions.

APPENDIX A. FLIGHT PROFILE FOR FD 4



GPS (Garmin Forerunner 501) display of flight path of C-9 on 26 May, 2006, over the Gulf of Mexico and the corresponding elevation profile for parabolas 30-42.

ACKNOWLEDGMENT

Funding for this work was provided through an NASA Research Announcement grant (NNK04EB08A) from NASA's Advanced Technology Development Program within the Exploration Systems Mission Directorate.

PHOTOGRAPHS

JSC2006E19848 to JSC2006E19855
JSC2006E20530 to JSC2006E20538
JSC2006E20588 to JSC2006E20599

VIDEO

- Zero G May 22-26, 2006, Master: 720909

Videos available from Imagery and Publications Office (GS4), NASA/JSC.

CONTACT INFORMATION

Gary Stutte, Ph.D.
Dynamac Corporation
Bldg M6-1025, SLS Lab 201C
Kennedy Space Center, FL 32899
321-862-3493

TITLE

Medical Operations C-9 Familiarization Flight

FLIGHT DATES

May 23, 2006

PRINCIPAL INVESTIGATOR

Jessica Hughlett, Wyle Laboratories, Inc., Life Sciences Group

CO-INVESTIGATORS

Keith Brandt, NASA/Johnson Space Center

Tyler Carruth, Wyle Laboratories, Inc., Life Sciences Group

Shannon Moynihan, University of Texas Medical Branch

Jennifer Struble, Wyle Laboratories, Inc., Life Sciences Group



OBJECTIVE

Provide familiarization of 0g for new Medical Operations Branch personnel (medical doctors, biomedical flight controllers, and system/crew trainers). This familiarization is designed to expose the students to issues associated with development of procedures used during space flight

and make them more effective when working with astronauts. This research project is part of the Space Flight program and is designed to provide the trainees with a better understanding of the effects of weightlessness on medical procedures, medical hardware, and medical training.

INTRODUCTION

Medical personnel frequently interact with space flight crew to provide training on medical procedures and real-time support of activities while on orbit. The microgravity environment makes many simple procedures challenging. Training medical personnel on the procedures in a microgravity environment can improve the quality of training and support by first-hand experience.

METHODS AND MATERIALS

Parabolic flight provides repeated short-duration exposures to microgravity conditions. A C-9 aircraft operated by NASA Aircraft Operations Division was utilized to provide 40 parabolas for this training.

Instruments

Three workstations were provided on the C-9 aircraft. Personnel rotated through the stations.

Cardiopulmonary Resuscitation (CPR). A full-body CPR mannequin restrained by the Crew Medical Restraint System (CMRS).

Airway. Intubation stations with standard direct-visualized endotracheal intubation and Intubating Laryngeal Mask Airway (ILMA) were available using pallets similar to those available to on-orbit crews. An Intubating head mannequin with open torso was secured to the floor of the aircraft. A Macintosh blade and cuffed endotracheal (ET) tubes were available as well as ILMAs. Equipment was contained in pallets similar to those on SOMS and CHeCKS kits.

Intravenous (IV) therapy. An IV practice arm on an elevated table was used to practice obtaining IV access and administering IV medications.

Procedures

Cardiopulmonary Resuscitation (CPR). Two team members worked together over 20 parabolas to evaluate three different techniques. Inverted (rescuer feet on ceiling), straddling, and side positioning using CMRS restraint strap positions were evaluated.

Airway. Each investigator had 10 parabolas to evaluate standard and ILMA intubation. The positioning and technique were left to the investigator.

Intravenous (IV) therapy. A 500 ml IV fluid bag with standard tubing and angiocath was utilized by each investigator for 10 parabolas. After establishing IV access and securing the angiocath, the investigator simulated injecting medications through the IV port.

RESULTS

CPR. The inverted position subjectively gave the best quality of compressions. It was, however, the most awkward position from which to deliver rescue breaths. The straddle position was very stable, but did not allow for adequate strength of compression. The lateral position was the best for combining compressions and ventilations.

Airway. ILMA insertion was very simple to accomplish in almost any rescuer position. Endotracheal intubation was much more difficult to accomplish due to positioning. It was even more difficult due to failure of the laryngoscope battery.

IV. The microgravity environment did not provide any additional challenges compared to 1g practice, provided both the patient and rescuer are restrained.

DISCUSSION

CPR. If two or more rescuers are available, the inverted compression position for a rescuer would appear to be the best technique. It allows stronger compressions and gets that crewmember out of the way of other tasks. A second rescuer hovering near the head could provide rescue breaths. If only one rescuer is available, then the latter position with the CMRS restraint strap would give the best CPR results. Care must be taken to keep some tension on the restraint strap especially while repositioning for breaths to keep the strap from becoming displaced from the hips.

Airway. The ILMA is a much simpler and expeditious airway to place. If a more secure airway is needed, passing the ET tube through the ILMA would be the best plan, especially since most crew is not experienced in visualized endotracheal intubation.

IV. Anecdotal reports from experienced physician astronauts who have started IVs on orbit would suggest that the procedure on real patients in flight is much more difficult, just as starting IVs on patients is more difficult than on the arm in the 1g environment.

All tests were affected by parabolic flight not giving a stable 0g environment. Positioning was not stable as there were vertical and lateral offsets that would not be present in flight.

CONCLUSION

The three sets of tasks were representative of emergency actions that the crew might have to take on orbit. Allowing Medical Operations personnel to practice these techniques in microgravity can make all investigators feel they are better equipped to train and advise the crew in the performance of these techniques. This experience is invaluable. Being able to tell the crew the optimal way to set up and perform procedures may be necessary and having had the experience will make these descriptions that much easier to understand and to follow.

PHOTOGRAPHS

JSC2006E19840 to JSC2006E19847
JSC2006E19855 to JSC2006E19870

VIDEO

- Zero G May 22 -26, 2006, Master: 720909

Videos available from Imagery and Publications Office (GS4), NASA/JSC.

CONTACT INFORMATION

Ms. Jessica Hughlett
Wyle Laboratories, Inc., Life Sciences Group
1290 Hercules Suite 120
Houston, TX 77058
281-212-1283
jessica.l.hughlett1@jsc.nasa.gov

TITLE

Evaluation of the Effectiveness of Overhead Suspension Reduced-Gravity Analogs in a Microgravity Environment

FLIGHT DATES

June 13-16, 2006

PRINCIPAL INVESTIGATOR

Donald Hagan, NASA/Johnson Space Center

CO-INVESTIGATORS

John DeWitt, Bergaila Engineering Services

Jason Bentley, Wyle Laboratories, Inc., Life Sciences Group



GOAL

The purpose of this experiment was to measure the ground reaction forces and joint motions during locomotion in lunar gravity and weightlessness. The objective was to determine if experiment results found using ground-based overhead suspension systems are similar to those found in true microgravity and lunar gravity environments.

INTRODUCTION

Recently, there has been considerable focus on locomotion in microgravitational and lunar gravitational environments. These studies were done to better understand the biomechanical differences between locomotion in reduced gravity and normal gravity. Because of the need for multiple subjects and multiple sessions per subject, overhead suspension has been used as an analog to reduced gravity.

During overhead suspension trials, subjects don a harness that lifts them from their torso or pelvis. An appropriate magnitude of upward force is then applied to the subject to simulate the effects of reduced gravity on their body weight. This method is especially useful when studying locomotion in lunar or Martian environments because less than 100% of the body weight is relieved.

Two separate experiments are currently being conducted at NASA Johnson Space Center to investigate locomotion. In one experiment, individuals walk and run in simulated lunar gravity while joint motions and ground reaction forces are measured. In another, subjects complete exercise trials with and without additional mass to determine how added mass affects ground reaction forces and joint torques. In the latter experiment, an overhead suspension unit is used to maintain constant body weight, allowing investigation of how inertial forces affect locomotion.

Since each of these investigations has space flight implications, but they are being performed in a normal gravity environment, it is of interest to understand how well the overhead suspension method results compare to those obtained in true lunar or microgravity. Without such knowledge, interpretation of the ground-based results becomes subject to limitations of how accurately the overhead suspension analog recreates the reduced-gravity environment. The purpose of this investigation was to collect locomotion data during lunar and microgravity to compare with those collected using overhead suspension.

METHODS AND MATERIALS

Eight subjects (5M, 3F) completed locomotion trials in lunar and microgravity onboard the C-9 aircraft. Vertical GRF data were collected during each trial with a force treadmill (Kistler Gaitway, Amherst, NY) at 480 Hz for 25 sec. The 3-D positions of retroreflective markers attached to the subjects' left side with double-sided hypoallergenic adhesive tape (lateral neck, hip, knee, ankle, posterior heel, and toe) were found using a six-camera motion capture system (SMART Elite system, BTS Engineering, Padova, Italy). The motion capture system was calibrated each day prior to aircraft takeoff. Each flight consisted of 30 lunar parabolas and 30 microgravity parabolas. Lunar parabolas always preceded microgravity trials.

Lunar gravity trials

During lunar trials, the objective was to determine the walk-run transition speed for each subject. Walk-run transition speeds for some of the subjects during overhead suspension have already been determined; for the remaining subjects, overhead suspension trials will occur at a later date.

Subjects walked and ran freely on the treadmill (see Figure 11). Two subjects were tested during each flight. Prior to any data collection, a parabola was used to reset the force plates within the treadmill while in lunar gravity; thus, up to fourteen parabolas remained to determine walk-run transition speeds. During initial trials, the subjects walked at speeds between 1.1 and 1.3 mph to



Figure 11. Typical lunar test setup with subject and spotter. The subject walked freely on the treadmill for all trials.

allow adaptation to the lunar-g environment. As the subjects became more comfortable, treadmill speed was varied between speeds of 1.3 and 5.0 mph. The speed was held constant within each parabola. The subject's gait style (walk vs. run) was noted for each trial.

Prior to flight, the length of the subjects' legs from the floor to greater trochanter was recorded. The Froude number is the ratio of centripetal force to gravitational force ($Fr = v^2/gl$, where v = locomotion velocity, g = acceleration due to gravity, l = leg length) (Kram et al., 1996). Under Earth gravity conditions, humans change from a walk to run at a Froude number of approximately 0.5 (Hreljac, 1995). The predicted walk-run transition speed for each subject was computed as the speed corresponding to $Fr = 0.5$ with $g = 1.63 \text{ m/s}^2$ (lunar gravity).

During flight, treadmill speed was varied from trial to trial between faster walking speeds and slower running speeds until a narrow range was identified that contained the approximate walk-run transition speed. Speed was modified via trial and error; no two subjects completed exactly the same sequence. The subjects were prompted for verbal feedback between trials. The speed at which walk-run transition occurred was estimated as the mean of the highest walking speed and lowest running speed.

Four subjects in this study had their walk-run transition speeds determined while they were unloaded with an overhead suspension system. These trials occurred during a parallel investigation. Walk-run transition speed was found as the speed at which the subjects could not maintain a walk without increased effort, and subjectively preferred to run. These data were used to compare lunar gravity results with overhead suspension results.

Microgravity Trials

Subjects walked at 3 mph or ran at 7 mph while loaded with bungees in series with one carabiner clip (bungee configuration A) or bungees only (bungee configuration B) and wearing the new Treadmill with Vibration Isolation and Stabilization (TVIS) harness. Bilateral load cells were placed in line with the bungee/clip system. The load cells were approximately 6 inches long, which is the length of two carabiner clips. Therefore the actual bungee/clip configurations used for each subject were bungee + 2 clips and bungee + 3 clips.

Based on load prediction charts, the configurations were estimated to provide approximately 115 to 125 lbs of loading. The actual load varied between subjects and was dependent upon leg length. During the added mass (AM) trials, subjects wore a weighted vest over the TVIS harness (see Figure 2). The vest had dual pockets on the fore and aft sides that allowed up to 80 - 1.1 kg weights to be added as desired. Two added mass conditions were completed. During the light condition, 19.8 kg was added (nine 1.1-kg weights on either side of the vest), and during the heavy condition, 39.6 kg was added (19.8 kg on either side of the vest).



Figure 2. Typical setup during microgravity trials. On left, subject is performing locomotion with TVIS vest and bungee loading in nominal configuration. At right, the subject has donned the weighted vest over the TVIS harness.

Subjects completed 10 locomotion trials as shown in Table 1. Trials without extra mass were always performed prior to those with extra mass. The first subject always completed AM condition 1 trials before AM condition 2. The second subject completed AM condition 2 first. This reduced the number of vest reconfigurations necessary during the flight.

Table 1. Data collection schedule during a typical flight. A parabola was used prior to data collection to reset the force plates within the treadmill. Bungee A = bungee + 1 clip; Bungee B = bungee only.

Parabola	Subject	Speed (mph)	Bungee Configuration	AM condition
1	A	Zero FP		
2		3	A	None
3		7	A	None
4		3	B	None
5		7	B	None
6		Add Weighted Vest		
7		3	A	Light
8		7	A	Light
9		3	B	Light
10		7	B	Light
11		Modify Vest		
12		3	B	Heavy
13		7	B	Heavy
14		Extra		
15		Extra		
Break/Turnaround				

Contact time (CT), stride time (ST), stride length (SL) and GRF data were processed using custom software programmed in MATLAB v7.1. GRF variables included peak impact force (PIF), loading rate (LR), peak propulsive force (PPF), and impulse (Imp). For each trial, the mean of each variable was computed using all recorded footfalls. Repeated measures analysis of variance (ANOVA) was used to determine if dependent variables were influenced by the vest in bungee configuration A. Paired t-tests were used to determine if the vest had an effect in bungee configuration B. Significance was defined as $p < .05$.

RESULTS

Lunar gravity trials

Subjects completed up to 15 trials of locomotion in lunar gravity. Although objective measures were not taken, it was obvious to observers that each subject had difficulty walking during early trials, but adapted to the environment as successive trials occurred. Most subjects were able to stay on the treadmill without help; however, subjects often had to momentarily reach for a spotter during trials to maintain stability.

Table 2 shows the predicted lunar and overhead suspension walk-run transition speeds for each subject. At the time of writing this report, subject 5-8 had not completed tests on the overhead suspension system. Subject leg lengths are also presented.

Table 2. Predicted, actual lunar and actual overhead suspension walk-run transition speeds and corresponding Froude numbers.

Subject	Leg Length (m)	Predicted Transition Speed (m/s)	C-9		Overhead Suspension		% Diff (Lunar - Pogo)
			Transition Speed (m/s)	Froude Number	Transition Speed (m/s)	Froude Number	
1	0.92	0.86	1.47	1.45	1.53	1.56	7
2	0.86	0.84	1.32	1.24	1.34	1.28	3
3	0.93	0.87	1.56	1.61	1.21	0.97	-40
4	0.94	0.88	1.21	0.95	1.29	1.09	15
5	0.89	0.85	1.29	1.15			
6	0.95	0.88	1.70	1.85			
7	0.89	0.85	1.74	2.09			
8	0.91	0.86	1.07	0.77			

Although walk-run transition speeds as predicted with a Froude number equal to 0.5 ranged from 0.64-0.86 m/s, the walk-run transition speeds found during this investigation were much higher, ranging from 1.07-1.74 m/s. For those subjects who completed trials on both the C-9 and overhead suspension system, differences varied across subjects. However, in both conditions, the Froude numbers corresponding to the transition velocity were much greater than 0.5.

Microgravity Trials

CT, ST, and SL means are presented for each gait type (see Table 3 and Figure 3). During walking trials, there was a significant vest effect for both bungee configurations for each variable; CT, ST and SL increased with increasing vest mass. None of the variables were affected by vest mass during running.

Table 3. Mean CT, ST and SL for microgravity trials with and without the weighted vest during walking and running. *indicates a significant vest effect in bungee configuration A; +indicates a significant vest effect in bungee configuration B.

	Gait Type	Bungee Configuration A			Bungee Configuration B	
		No Vest	Light Vest	Heavy Vest	No Vest	Light Vest
Contact Time (s)	Walking ⁺	0.63	0.66	0.68	0.62	0.65
	Running	0.26	0.25	0.27	0.25	0.25
Stride Time (s)	Walking* ⁺	1.16	1.19	1.23	1.13	1.20
	Running	0.79	0.81	0.81	0.81	0.81
Stride Length (m)	Walking* ⁺	1.57	1.63	1.68	1.55	1.63
	Running	2.52	2.59	2.57	2.63	2.57

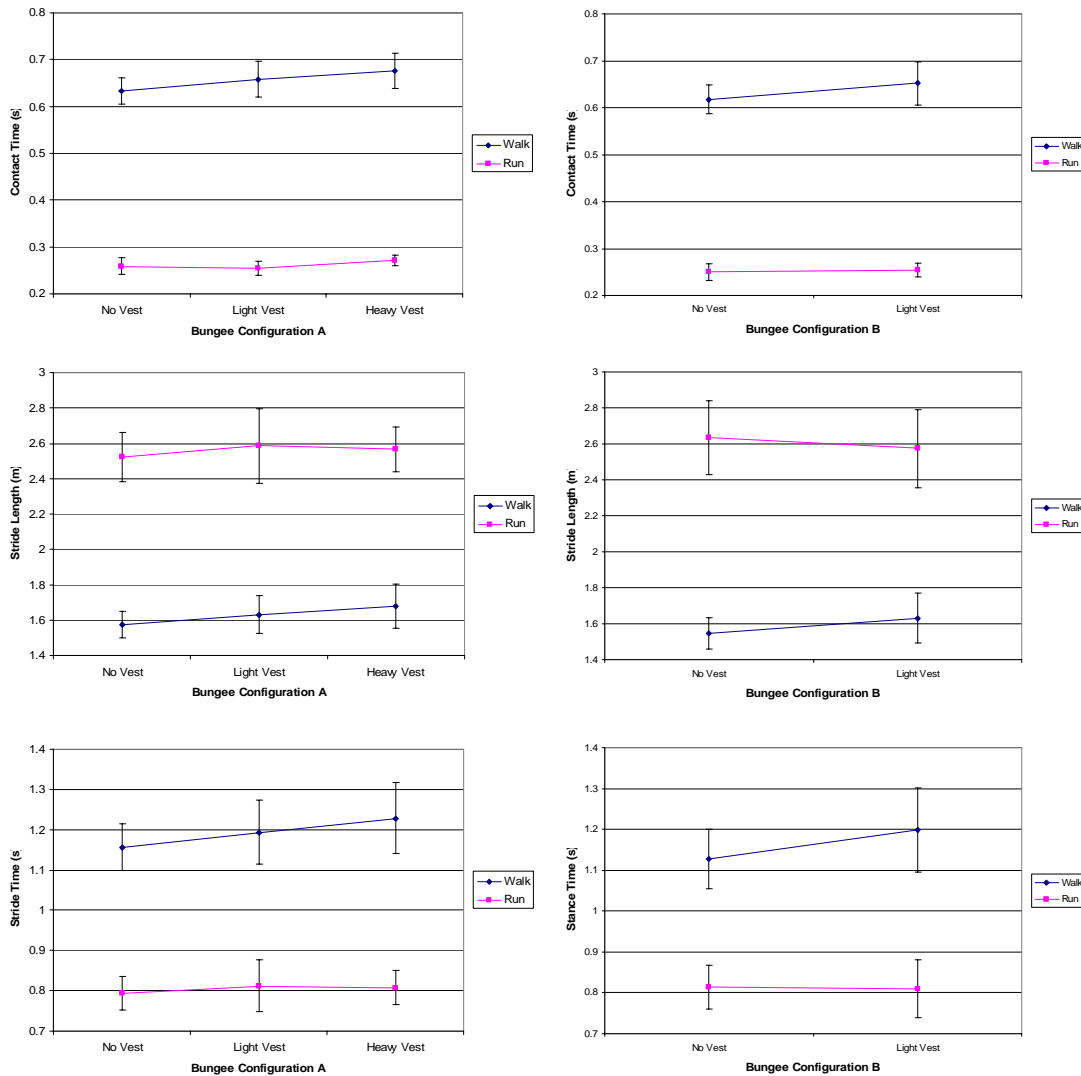


Figure 3. Contact time, stride time and stride length for each bungee configuration with and without the weighted vest.

GRF means are presented in Table 4 and Figure 4. There was a significant main effect of vest use on PIF and LR in bungee configuration B during running. PIF and LR decreased with use of the vest. There was no effect of the vest on any of the variables during walking or running in bungee configuration A.

Table 4. Mean PIF, LR, PPF and Imp for microgravity trials with and without the weighted vest during walking and running. *indicates a significant vest effect in bungee configuration A; ⁺indicates a significant vest effect in bungee configuration B.

	Gait Type	Bungee Configuration A			Bungee Configuration B	
		No Vest	Light Vest	Heavy Vest	No Vest	Light Vest
PIF (BW)	Walking	0.74	0.75	0.79	0.66	0.63
	Running ⁺	1.06	0.95	1.01	0.98	0.80
LR (BW s ⁻¹)	Walking	6.42	7.02	7.00	6.62	6.24
	Running ⁺	32.62	29.34	34.71	32.37	23.89
PPF (BW)	Walking	0.58	0.56	0.59	0.49	0.45
	Running	1.33	1.30	1.24	1.12	1.15
Imp (BW msec)	Walking	311.75	308.78	342.04	247.42	243.73
	Running	209.64	202.06	209.98	174.15	175.11

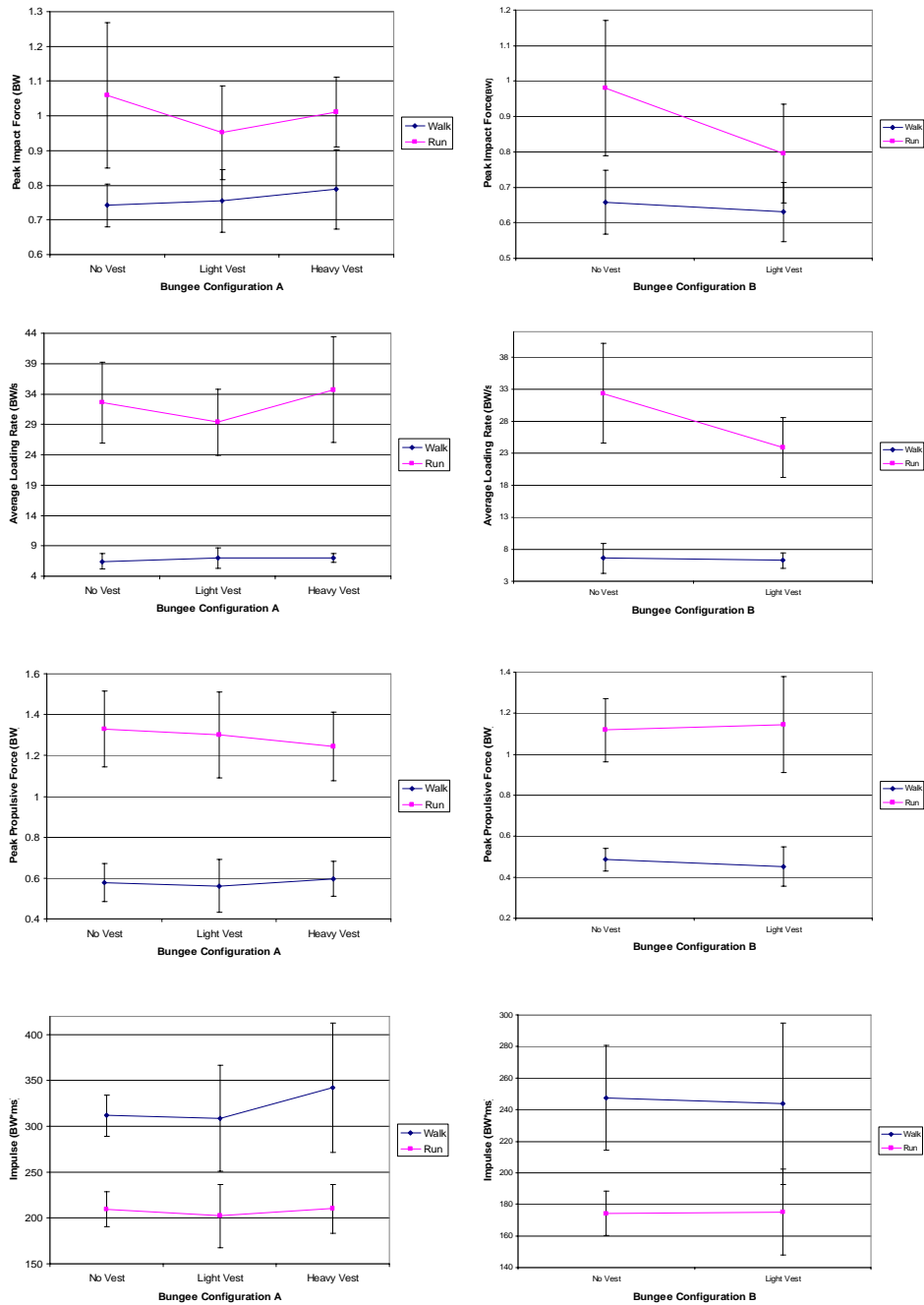


Figure 4. GRF variable means for each bungee configuration with and without the weighted vest.

DISCUSSION

Lunar Gravity Trials

During lunar gravity, if the theory of dynamic similarity holds (Donelan & Kram, 1997), the walk-run transition speed should occur at velocities at or near $Froude = 0.5$. Kram et al (1997) investigated the effect of reduced gravity using an overhead suspension system on walk-run transition speed and found that near lunar gravity, transition speeds were between 0.97 and 1.18 m/s, with corresponding Froude numbers of 0.83-1.13. They attributed the difference between the actual and predicted speeds to be caused by the fact that in the suspension system, the legs

and arms are not un-weighted. Their swinging acts to effectively increase the gravitational level experienced by the subject. They implied that in a true lunar gravity environment, the walk-run transition speed would occur at $Fr = .5$, because the limbs would be unloaded.

Our findings do not support this hypothesis. We found that transition speeds were actually nearer to those obtained during overhead suspension trials than as predicted by the dynamic similarity hypothesis. It appears that the theory of dynamic similarity does not hold at gravity levels near those on the moon. Furthermore, it appears that overhead suspension may be a more valid analog to lunar gravity than had been earlier suggested.

These findings, however, must be accepted with caution. It was obvious that the subjects had difficulty ambulating in the novel gravitational environment. While adaptation occurred during the trials, it is possible that more adaptation was still necessary, and that exposure to the lunar environment for a longer period may result in a different walk-run transition speed. However, while it is possible to run at almost any speed, it is only possible to walk for a specific range of speeds. It was obvious that the subjects continued to comfortably walk at speeds greater than predicted.

One additional finding that is worthy of further study is that if the inverted pendulum model of walking applies in lunar gravity, running must occur at a Froude number = 1.0 (Alexander, 1977). Our results suggest that walking did occur at Froude numbers greater than 1.0, which implies that the inverted pendulum model does not apply in lunar gravity. It is unclear at the present time why this occurs.

Microgravity Trials

When exercising in microgravity, subjects tended to increase contact time, stride time, and stride length when walking with a weighted vest. There were no apparent kinematic changes during running. The increase in all three parameters during walking suggests that as extra mass is placed on the torso, longer time is spent in contact with the treadmill, and longer strides are taken. It is unclear if the increased stride time is a result of the increase in contact time only, or if an increase in swing time also occurs. The increase in stride length could be a result of the foot traveling farther on the tread belt during the increased contact time. It is probable that a modification of joint angles at the ankle, knee and/or hip accompanies the increased timing throughout the stride.

In a ground-based study, using an overhead suspension system that is occurring in parallel to this investigation, the addition of mass without adding weight resulted in an increase in contact time during walking and an increase in both contact time and stride time during running. As mass was added, subjects increased the amount of time their foot was in contact with the ground (running only) and the time for each stride (both walking and running). Although speeds were the same in both investigations, the relative loading was different as subjects were not loaded to full body weight on the C-9. However, it does appear that kinematics is affected by an increase in mass in both environments.

It was surprising to find no effect of the added mass on almost any of the ground reaction force variables. For those that there were affected (PIF and LR), the use of the vest actually decreased the ground reaction forces. This was counter to what was expected because we thought that the additional inertial mass would require increased force to maintain the appropriate locomotive pattern for successful walking or running.

During the overhead suspension investigation, PIF and LR increased during walking and decreased during running with the addition of mass. PPF decreased during walking but did not change during running. Imp increased during running. The decrease of PIF and LR in microgravity compared to the increase during overhead suspension as mass increased is puzzling. It appears that the addition of mass causes a GRF change, but that change is environment-dependent.

It is possible that the central nervous system (CNS) adapts to the addition of mass by modifying locomotive kinematics. There may be a tuning to a desired ground reaction force that is used by the CNS to determine the optimal coordination patterns to complete the gait desired. Gait is modified in order to maintain a given GRF for a specific speed/external load combination.

It is also possible that the addition of inertial mass to the body affects the external load applied by specific bungee/carabiner clip combination. The increased inertial mass must be accelerated back to the treadmill, and rather than the subject providing greater musculoskeletal forces to propel the extra mass, there is actually a decreased need for force because the acceleration is decreased.

It should be mentioned that during the ground-based study, AM conditions were in percent body weight, which allowed for a systematic mass increase across subjects. In the C-9 experiment, testing conditions made it unfeasible to test subjects in the same manner. The change-out of the vest was too difficult given that modifications would need to be made during and between periods of microgravity. It is very possible that this preliminary analysis needs to be completed in a different manner to obtain more comparable data.

CONCLUSIONS

Our findings suggest that during lunar gravity, gait transition speeds are similar to those found when using an overhead suspension device. Adaptation locomotion in the unfamiliar environment may have affected gait transition speed. During microgravity, the use of a weighted vest during locomotive exercise, when loaded with external loads of less than 70% body weight, do not appear to affect ground reaction forces, but do affect kinematics. It is unclear how these interactions may affect the musculoskeletal benefits of locomotive exercise. Further study is warranted in both of these areas.

REFERENCES

1. Kram R, Domingo A, Ferris DP. (1997). Effect of reduced gravity on the preferred walk-run transition speed. *The Journal of Experimental Biology*, 200:821-6.
2. Hreljac A. (1995). Effects of physical characteristics of the gait transition speed during human locomotion. *Human Movement Science*, 14:205-216.
3. Donelan JM, Kram R. (1997). The effect of reduced gravity on the kinematics of human walking: a test of the dynamic similarity hypothesis for locomotion. *The Journal of Experimental Biology*, 200:3193-201.
4. Alexander R McN. (1977). Mechanics and scaling of terrestrial locomotion. In *Scale Effects in Animal Locomotion* (ed. TJ Pedley), 93-110. New York: Academic Press.

PHOTOGRAPHS

JSC2006E22857 to JSC2006E23015

JSC2006E23207 to JSC2006E23360

JSC2006E23998 to JSC2006E24091

VIDEO:

- Zero G June 16 – 23, 2006 flights, Master: 721249

Videos available from Imagery and Publications Office (GS4), NASA/JSC.

CONTACT INFORMATION:

John Dewitt, MS

c/o Wyle Laboratories, Inc., Life Sciences Group

1290 Hercules Suite 120

Houston, TX 77058

281-483-8939

john.k.dewitt@nasa.gov

TITLE

Aerosol Deposition in Fractional Gravity:
Risk Mitigation for Martian and Lunar Habitats

FLIGHT DATES

June 13-16, 2006

PRINCIPAL INVESTIGATOR

G. Kim Prisk, University of California-San Diego

CO-INVESTIGATORS:

Chantal Darquenne, University of California-San Diego

I. Mark Olfert, University of California-San Diego



GOAL

The inhalation and deposition of small particles in the lungs is a health concern here on Earth, and future space travelers risk detrimental health consequences from particle inhalation. Because gravity affects the deposition of particles in the lung, in microgravity, or in the reduced gravity of the moon and Mars, inhaled particles are left in suspension in the airways, and can be transported deeper in the lung where they reach the sensitive alveolar region. It is believed that much of the dust on the moon and Mars is highly reactive, which may exacerbate its potential for lung damage. Because it is electrostatically charged, it sticks to spacesuits and could be tracked into habitats and subsequently inhaled.

OBJECTIVE

The deposition of aerosols from the environment in the lung presents a health risk. For particles larger than 0.5 micron, such deposition is strongly influenced by gravitational sedimentation. In microgravity, deposition by gravitational sedimentation is absent, and as a consequence, airway particle concentrations are higher than in 1g, enhancing aerosol transport to the alveolar region of the lung. The presence of previously unaccounted-for complex mixing patterns in the periphery of the lung, combined with high alveolar aerosol concentrations, results in high deposition in this sensitive region of the lung in microgravity. Similar effects are expected in the fractional gravity environments of the moon and Mars.

The dust on the surface of Mars is highly oxidative, due to the UV environment on the surface. Mars dust is also electrostatically charged, and so will tend to stick to the outside of spacesuits, and be tracked into habitats. The lung, with its huge exposed surface area, is highly vulnerable to adverse effects resulting from exposure to Mars dust.

We propose a multi-faceted approach involving human and animal experiments, combined with sophisticated modeling, to provide a path to assessing the health risk of dust exposure in habitats on both the moon and Mars, addressing Risk #7 in the Bioastronautics Critical Path Roadmap. Such an assessment has profound implications on the degree of engineering (and thus cost) that will be required to limit the risk of such exposure to the inhabitants of these habitats. We will address the following hypotheses and objectives:

1. That total aerosol deposition in the human lung in fractional gravity will be greater than-predicted by existing models (as is the case in microgravity), and that in these circumstances a greater than-predicted alveolar deposition will result. Using the NASA Microgravity Research Aircraft, we will non-invasively measure both the total and regional deposition of inert particles (0.5 to 2 micron) in humans in fractional g corresponding to that on the surface of the moon and Mars.
2. That aerosol deposition in the lungs of spontaneously breathing rats in fractional-g will be more peripheral (closer to the alveoli) than in 1g. We will expose spontaneously breathing rats to fluorescent- and magnetically-labeled particles of varying sizes (between 0.5 and 2µm) in 1g, and in fractional g corresponding to surface of the Moon and Mars, and measure the specific sites of regional deposition in the lungs using both fluorescent confocal microscopy, and magnetic resonance imaging techniques.
3. We will couple existing sophisticated computational fluid dynamics (CFD) models of the upper airways of humans to our model of the alveolar region of the lung, to predict aerosol deposition under conditions matching those of the experiments performed in humans. In rats we will use detailed 3D images of the rat bronchial tree to develop an upper-airway CFD model, which, used in conjunction with an appropriately scaled alveolar model, will predict aerosol deposition under conditions matching those of the experiments performed in rats.

METHODS AND MATERIALS

Human Studies in Fractional G

In the past we have measured both total and regional aerosol deposition in humans in 1g and in µg (see Preliminary Data). The results of those studies highlighted the non-linear nature of aerosol deposition of small (~ 1µm) particles as a function of g level (2). Thus, in order to accurately determine particle deposition in fractional g, direct measurements are required.

Total Deposition

Protocol overview. We measured total deposition of 0.5- and 1- μm particles in the lungs of subjects in 1g, and at fractional g levels corresponding to the surface of the Moon and Mars (termed 1/6g and 1/3g for the sake of convenience). Total deposition was measured during controlled tidal breathing, and as was the case in our previous studies in microgravity (2) we selected data during stable g-level periods after allowing sufficient time at that g level for deposition to stabilize (2-3 breaths). We studied 6 subjects.

Equipment. Deposition data will be collected by using the equipment which is similar to that used in a previous study (2). The subject breathes from a reservoir through a non-rebreathing valve. Aerosol concentration and flow rate are measured at the mouth using a photometer and a pneumotachograph, respectively. A diffusion dryer is located between the photometer and the mouthpiece. The system is heated to body temperature to prevent water condensation. Data are recorded on a laptop PC equipped with a data acquisition subsystem.

Central and Alveolar Deposition (SA1b)

Protocol overview. The protocol was the same as that used in our previous studies of bolus deposition and dispersion (1, 3, 4). The subject performed the standardized maneuver described in Preliminary Studies, and a 70 ml bolus was inserted in the inspiration at one of the preselected penetration volumes (V_p) using the equipment shown in the Facilities and Equipment section. During the subsequent expiration, the exhaled bolus was recorded.

We measured deposition, dispersion (change in bolus half-width), and bolus mode shift. We could designate a volume below end inspiration for the bolus (the penetration volume, V_p), and measured aerosol bolus parameters at each of 3 V_p (200, 500 and 1200 ml). We used two particle sizes (0.5, 1 μm) at 1g, in 1/6g. As was the case before, measurements were performed in triplicate in a total of 6 subjects.

Equipment. The equipment was the same as that used for previous studies and uses the same photometer and pneumotachograph system used in the total deposition studies. In brief, a pneumatically controlled sliding valve allows the subject to breathe either filtered room air, or allows inspiration through a tube pre-filled with a bolus of aerosol. By actuating the sliding valve at the appropriate point during inspiration, the bolus can be delivered at any desired penetration volume with an accuracy of ± 100 ml. A full description can be found in previous publications (3).

Rat Studies in Fractional g

We propose to determine the degree of deposition and the location of inhaled particles in the lungs of spontaneously-breathing rats, and to compare the deposition patterns in 1g and in fractional-g levels corresponding to the surface of the Moon and Mars. Our hypothesis is that in the fractional-g environments, total deposition may be somewhat reduced, but those particles that do deposit will do so more peripherally. In humans, more peripheral deposition results in particles avoiding the mucociliary system and in the case of oxidative particles could increase oxidative damage to the lung.

After performing these studies in rats, we can use anatomical and state-of-the-art imaging techniques to determine the exact site and degree of deposition, providing otherwise unavailable validation for the CFD models. We expect to be able to experimentally demonstrate alterations in the heterogeneity of particle deposition between g levels.

Protocol. We exposed spontaneously-breathing, restrained rats to fluorescent-labeled and MRI-labeled particles during periods of fractional g corresponding to the surface of the Moon and Mars on the NASA Microgravity Research Aircraft. During 1g and during the hyper-g phase of parabolic flight, the animals breathed filtered air, and while the aircraft was in fractional g they were exposed to particle-laden air for head-only particle exposure for a cumulative exposure period of ~20 minutes. At the completion of the flight the animals were euthanized, and the lungs preserved. The lungs will be returned to San Diego for MR imaging of particle location, and for slicing and confocal microscopy of fluorescent particle location (see below). We used three different particle sizes (0.5, 1, and 2 μm), matching those used in the human studies (see above). We required 2 flights per size and g-level (10 rats per condition) for a total of 12 flights.

Exposure techniques. Five rats (adult male Wistar, with a body weight in the range 200-250g) were simultaneously restrained in head-out plastic cones (9) in individual sealed plethysmograph chambers. When the animal breathes, changes in box pressure occur as inspired air is warmed and humidified in the respiratory tract, allowing the calculation of tidal volume and breathing frequency (5; 6). An identical reference chamber was used and differential pressure between the plethysmograph and the reference chamber was measured (8). This eliminated difficulties associated with changes in cabin pressure in the aircraft. The chambers were ventilated continuously by drawing either filtered cabin air or particle-laden air through them at ~250 ml/min (9).

The inlet path for the ventilation is such that it impinges directly onto the nose region of the restrained rats. This arrangement allows us to rapidly switch the inlet flow between filtered (particle-free) air and particle-laden air drawn from a reservoir into which particles in suspension were aerosolized during the period of hypergravity immediately preceding the fractional-g parabola. During 1g and during the hyper-g phase of parabolic flight, the animals breathed filtered air, and while the aircraft was in fractional g they were exposed to particle-laden air for head-only particle exposure. The fractional g time available to us in the aircraft was ~35-40 seconds for 1/6g and ~45-50 seconds for 1/3g, giving a cumulative exposure period of ~20 minutes, assuming 30 seconds (which will be recorded) of fractional g exposure time could be utilized per parabola. Control studies on the ground (1g) were performed after the fractional-g studies, allowing us to match the timing of the exposures to that which occurred during the flights (a delayed synchronous control approach). Importantly in the context of this proposal, Pinkerton et al. (7) showed that in 1g exposure times of 15 to 30 minutes, deposition of 1.0 μm microspheres throughout the bronchial tree and alveoli of spontaneously breathing rats was demonstrated.

At the completion of the flight, the animals were anesthetized by intra-peritoneal injection of pentobarbital, and the trachea was cannulated, and connected to a pressure source to permit setting of intratracheal pressure. The caudal vena cava was cannulated and the carotid arteries and veins cut to permit perfusion fixation. Physiological buffered saline was first infused for 5 minutes to clear blood from the lungs, followed by fixative for 15 minutes as described by Pinkerton (7). Intra-tracheal pressure was maintained at 9 mmHg, providing a lung volume approximating functional residual capacity.

For these flights a 2-chamber prototype plethysmograph with no rat was flown as an engineering evaluation. An animal ventilator provided realistic signals for assessment of noise levels in the aircraft environment.

RESULTS/DISCUSSION/CONCLUSION

Results are not yet available. Preliminary inspection of the data shows good-quality signals. Total and fractional deposition in 1/6 g data were collected on 3 subjects. The prototype rat plethysmograph appears to work well. Further ground testing is underway.

REFERENCES

1. Darquenne C., Paiva M. and Prisk G.K. Effect of gravity on aerosol dispersion and deposition in the human lung after periods of breath-holding. *J Appl Physiol* 89: 1787-1792, 2000.
2. Darquenne C., Paiva M., West J.B. and Prisk G.K. Effect of microgravity and hypergravity on deposition of 0.5- to 3- μ m-diameter aerosol in the human lung. *J Appl Physiol* 83: 2029-2036, 1997.
3. Darquenne C., West J.B., and Prisk G.K. Deposition and dispersion of 1 μ m aerosol boluses in the human lung: Effect of micro- and hypergravity. *J Appl Physiol* 85: 1252-1259, 1998.
4. Darquenne C., West J.B., and Prisk G.K. Dispersion of 0.5-2 mm aerosol in micro- and hypergravity as a probe of convective inhomogeneity in the human lung. *J Appl Physiol* 86: 1402-1409, 1999.
5. Jacky J.P. A plethysmograph for long-term measurements of ventilation in unrestrained animals. *J Appl Physiol* 45: 644-647, 1978.
6. Jacky J.P. Barometric measurement of tidal volume: effects of pattern and nasal temperature. *J Appl Physiol* 49: 81-86, 1980.
7. Pinkerton K.E., Gallen J.T., Mercer R.R., Wong V.C., Plopper C.G., and Tarkington B.K. Aerosolized fluorescent microspheres detected in the lung using confocal scanning laser microscopy. *Microscopy Research and Technique* 26: 437-443, 1993.
8. Steinbrook R.A., Feldman H.A., Fencel V., Forte V.A., Gabel R.A., Leith D.E., and Weinberger SE. Naloxone does not affect ventilatory responses to hypoxia and hypercapnia in rats. *Life Sci* 34: 881-887, 1984.
9. Sweeney T.D., Leith D.E., and Brain J.D. Restraining hamsters alters their breathing pattern. *J Appl Physiol* 70: 1271-1276, 1991.

PHOTOGRAPHS

JSC2006E22821 to JSC2006E22829
JSC2006E22946 to JSC2006E22958
JSC2006E23044 to JSC2006E23090
JSC2006E23883 to JSC2006E23917

VIDEO

- Zero G June 16 – 23, 2006 flights, Master: 721249

Videos available from Imagery and Publications Office (GS4), NASA/JSC.

CONTACT INFORMATION

G. Kim Prisk, PhD, DSc
Department of Medicine -0931
University of California, San Diego
9500 Gilman Drive
La Jolla, CA 92093-0931
kprisk@ucsd.edu

TITLE

Critical Care Skills in Microgravity: Validation and Application of Skill Assessment Toolkit

FLIGHT DATES

June 13–16, 2006

PRINCIPAL INVESTIGATOR

Ronald C. Merrill, Virginia Commonwealth University

CO-INVESTIGATORS

Azhar Rafiq, Virginia Commonwealth University



OBJECTIVES

The health provider in exploration space missions cannot evacuate a patient to Earth. Contingency plans for medical intervention must be designed for autonomy. This study measured the effect of microgravity on performance of fine motor skills such as basic surgical skills.

METHODS AND MATERIALS

Eight subjects with medical and non-medical backgrounds were evaluated during microgravity and lunar gravitational forces during flight aboard NASA's C-9B. We evaluated their skill in tying surgical knots on simulated silicone skin surface using standard techniques. LabView software was developed to archive forces at laparoscopic tool handles during knot tying on a silicone skin interface. Studies were controlled for Scop-dex medication and aircraft environment. Additionally, critical care basic skills were evaluated for airway management. Forces applied in achieving tight mask seal were tested.

RESULTS

All participants completed the tests successfully. The data trends indicate that the force applied to the instruments for task completion during flight was greater than in ground control sessions. This correlated with a decrease in knot quality. In airway management less dexterity was observed, with greater forces applied to achieve tighter mask seals.

DISCUSSION/CONCLUSION

Specific metrics of critical care task performance are essential in developing education modules for providers of medical care during exploration-class missions.

PHOTOGRAPHS

JSC2006E22831 to JSC2006E22856

JSC2006E22959 to JSC2006E22987

JSC2006E23091 to JSC2006E23167

JSC2006E23918 to JSC2006E23960

VIDEO:

- Zero g June 13 – 16, 2006 flights, Master: 721249

Videos available from Imagery and Publications Office (GS4), NASA/JSC.

CONTACT INFORMATION

Ronald C. Merrell, MD, FACS
Medical Informatics and Technology Applications Consortium
NASA Research Partnership Center
Department of Surgery
Virginia Commonwealth University
Richmond, VA 23298
1-800-827-1020
rcmerrel@hsc.vcu.edu

TITLE

Rapid Development of Colorimetric Solid Phase Extraction Technology for Water Quality Monitoring: Evaluation of C-SPE and De-bubbling Methods in Microgravity

FLIGHT DATES

June 21-23, 2006

PRINCIPAL INVESTIGATOR

Marc Porter, Iowa State University

CO-INVESTIGATORS

Torin McCoy, NASA Johnson Space Center

April Hazen-Bosveld, Bob Lipert, John Nordling, and Chien Jiu Shih;
Iowa State University

Jim Alverson, Dan Gazda, Jeff Rutz, John Straub, and John Schultz,
Wyle Laboratories, Inc. Life Sciences Group



GOAL

Verify the functionality of colorimetric solid phase extraction (CSPE) test methods in microgravity and assess the performance of manual bubble removal strategies.

OBJECTIVES

1. Demonstrate agreement between ground and flight data from silver CSPE analyses
2. Evaluate the performance of CSPE iodine analysis with negligible depletion in microgravity
3. Evaluate the performance of CSPE pH measurements by color matching in microgravity
4. Evaluate the performance of bubble-removal strategies
5. Investigate sources of error in CSPE measurements
6. Continue the development of training protocols for new users

INTRODUCTION

Iowa State University and Wyle Laboratories are partnered in an on-going research project focused on developing in-flight water quality monitoring hardware based on colorimetric solid-phase extraction (CSPE). The project is currently in its second funding cycle with the goal of advancing CSPE from a technology readiness level (TRL) of 3-4 to a TRL of 6-7. Initially, much of the work centered on the development of CSPE methods to measure silver(I)¹, iodine, and iodide² in spacecraft water samples. As the project has progressed, the focus has been shifted to refinement of the existing CSPE methods, optimization of fluid handling in microgravity, and instrumental improvements. Support for this work is provided by an NRA grant (NRA 03-OBPR-01-01-0038-0059) through the Advanced Environmental Monitoring and Control (AEMC) program.

Early KC-135 flights served to identify several challenges associated with performing CSPE analyses in microgravity. The most notable challenge was accurate determination of sample volumes, due to the presence of air bubbles in water samples that were collected during the flight.³ Later flights circumvented this issue and attempted to isolate the effects of microgravity on the CSPE methods by using pre-filled sample syringes.⁴ The data from these experiments clearly illustrated the ability of CSPE to quantify the biocidal species silver(I) and iodine in microgravity. Excellent agreement was observed between iodine analyses conducted on the ground and those performed in flight. The ground and flight results for silver(I) showed a strong correlation, although there appeared to be a slight positive offset in the silver(I) flight data.

This series of microgravity experiments continued the work from previous flights by attempting to understand and eliminate the offset between the flight and ground determinations of silver(I) by CSPE. The flights also provided the opportunity to evaluate two new variations of CSPE and to test manual bubble-mitigation strategies. The new variations of CSPE tested were color-matching analysis, which was demonstrated by measuring the pH of water samples inflight, and negligible depletion, which was evaluated using iodine as a test analyte. Bubble mitigation studies utilized a hand operated centrifuge device to effect phase separation inside a Teflon bag prior to sample collection.

METHODS AND MATERIALS

Instrumentation

In-flight and ground-based CSPE measurements were made using a BYK Gardener Color Guide spin d/8° diffuse reflectance spectrophotometer. Color-matching analyses were performed using a BYK Gardner Color Guide Plus diffuse reflectance spectrophotometer.

A motorless centrifuge, which consisted of a rotating clamp and base, was used in the bubble mitigation studies. Stainless steel hemostats and various sizes of plastic clips were also evaluated as a means to maintain isolation of entrapped air following phase separation.

Procedures

Silver(I) solutions. Sample solutions containing silver(I) were prepared in opaque Teflon bottles by diluting a silver atomic absorption standard (Aldrich) with deionized water. Five solutions were prepared by pipetting a predetermined mass of silver standard into a bottle and bringing the solution to a final mass of 100 g. The silver(I) concentrations were verified by inductively-coupled plasma mass spectrometry (ICP-MS.)

Iodine solutions. Iodine sample solutions were prepared by diluting a volumetric iodine standard solution (Fixanal, Riedel-de Haen) with deionized water. Each solution was prepared in a 500-mL glass volumetric flask, and then stored in black Teflon bottles. Iodine concentrations were verified by the Leuco Crystal Violet method prior to the experiments.

pH solutions. Buffered water samples with pH values ranging from 7.0 to 10.0 were prepared by dissolving the appropriate amount of buffer salt (sodium phosphate, TRIS, or sodium carbonate) in 0.1 M sodium nitrate so that the final solution had a buffer concentration of 0.1 M. The final solution pH was adjusted using either 0.01 M sodium hydroxide or 0.1 M sulfuric acid, as appropriate. All solution pH values were verified using a pH meter.

Silver(I) membranes. A solution of 5-(4-(dimethylamino)benzylidene)rhodanine (DMABR) was prepared by dissolving 0.1526 g of DMABR in 50 mL of dimethyl formamide in a 250 mL-volumetric flask. In order to dissolve the DMABR, the solution was sonicated for approximately 5 minutes. Once the DMABR was dissolved, the solution was brought to volume with methanol. A 3% (by mass) solution of Brij-30 was prepared by pipetting 3.073 g of the surfactant into a Nalgene bottle and bringing the solution to a final mass of 100.4 g with deionized water.

Silver(I) membranes were prepared by passing 10.0 mL of the DMABR solution through 3M Empore SDB-XC extraction membranes using a glass filtration assembly and a mechanical vacuum pump. A pressure difference of ca. 2 in of Hg was required to cause the solution to flow through the membrane. After the DMABR solution had passed through the membrane, the pressure difference was maintained for ca. 10 s to remove residual solvent. At this point, the funnel portion of the filter assembly was removed and wiped clean with methanol and a Kimwipe to remove residual droplets of DMABR solution. The cleaned funnel was then replaced and 5.0 mL of the Brij-30 solution was passed through the membrane using a pressure difference of ca. 3.5 in of Hg. Once the solution had passed, the pressure difference was increased to ca. 20 in Hg for approximately 30 s to dry the membrane. Membranes were allowed to dry overnight in a dark drawer and then cut into 13-mm disks.

Iodine negligible depletion membranes. A solution of molecular weight 10,000 poly(vinylpyrrolidone) (PVP) was prepared by dissolving 1.0 g of PVP in 50 mL of 1:9 methanol:water (by volume). This solution was then brought to a final volume of 100 mL with 1:9 methanol:water.

Iodine negligible depletion membranes were prepared by wetting a Whatman 0.45 μm nylon membrane with several drops of a 1:9 methanol/water solution prior to passing 10 mL of the PVP solution through the membrane using a glass filtration assembly and a mechanical vacuum pump. A pressure difference of ca. 2 in Hg was required to cause the solution to flow through the membrane. Once the solution had passed, the pressure difference was increased to remove residual solvent and dry the membrane. Membranes were stored approximately 5 hours in a sealed plastic bag before being cut into 13-mm disks.

pH membranes. A solution containing 5.0 $\mu\text{g/mL}$ of the sodium salt of thymol blue was prepared by dissolving the appropriate mass of the thymol blue salt in deionized water. A 3% (by mass) solution of Brij-30 was prepared by pipetting 3.073 g of the surfactant into a Nalgene bottle and bringing the solution to a final mass of 100.4 g with deionized water.

The pH membranes were prepared by treating 3M Empore Anion-SR anion exchange membranes with 10 mL methanol. The methanol was pulled through the membrane using a glass

filtration apparatus and a mechanical vacuum pump. A pressure difference of ca. 1 in Hg was required to effect passage of the methanol. The membranes were then exposed to 5 mL of the 3% Brij-30 solution using a pressure difference of ca. 3.5 in Hg. After the Brij-30 solution passed through the membrane, the pressure difference across the membrane was increased to ca. 20 in Hg, and maintained for 45 s. At this point, the vacuum was removed and 10.0 mL of the thymol blue solution was pipetted onto the membrane surface. A pressure difference of ca. 3.5 in Hg was then applied until the solution passed completely through the membrane. The pressure differential was then increased to ca. 20 in Hg and held for 1 minute to remove residual solvent. The membranes were then dried overnight on a paper towel in a dark drawer and stored in individual plastic bags a foil-wrapped box until they were cut into 13-mm disks for use.

CSPE cartridges. After being cut into 13-mm disks, all CSPE cartridges were loaded into Swinnex polypropylene filter holders. The filter holders are constructed with Luer fittings that allowed simple interfacing with a syringe (inlet) and a waste bag (outlet). Additionally, the holders contained an O-ring that defined the exposure area on the membrane disk and formed an internal seal.

RESULTS AND DISCUSSION

Silver(I) flight. Silver(I) CSPE membranes were prepared and loaded into cartridges the day prior to the microgravity flight. The morning of the flight, 1 mL disposable syringes were pre-filled with 1.0-mL volumes of the silver(I) solutions. Sufficient syringes and CSPE cartridges were prepared to perform six replicate analyses with each silver(I) concentration both on the ground and in flight. The syringes and cartridges were color-coded to simplify data recording during the flight. Ground and flight experiments were performed simultaneously, with efforts taken to mimic the thermal environment on the aircraft in the ground laboratory.

Data collected during the ground and flight experiments are plotted in Figure 1. Although the flight data show somewhat higher standard deviations than the ground data, the agreement between the two data sets was excellent. The most likely cause of the increased uncertainty in the flight data is effectiveness of the drying step in microgravity. When CSPE analyses are performed, a portion of the sample volume remains above the membrane until it is displaced by air in the drying step. It is believed that disruption of this liquid plug during the high-gravity portion of the parabola led to incomplete membrane drying. If the plug is disturbed, it is possible that the drying air would follow the path of least resistance and go through the disk without displacing the residual sample plug. Since this phenomenon is caused by the high g portion of the flight, it is not expected to be a serious issue during experiments performed on the ISS. The only other notable problem during the flight experiments was the distortion of one of the 0.6 ppm silver(I) membranes. The membrane was scraped as it was loaded into the sample locator, but the spectrum was still acquired. Due to the limited number of microgravity periods during the flight, it was not possible to repeat the measurement.

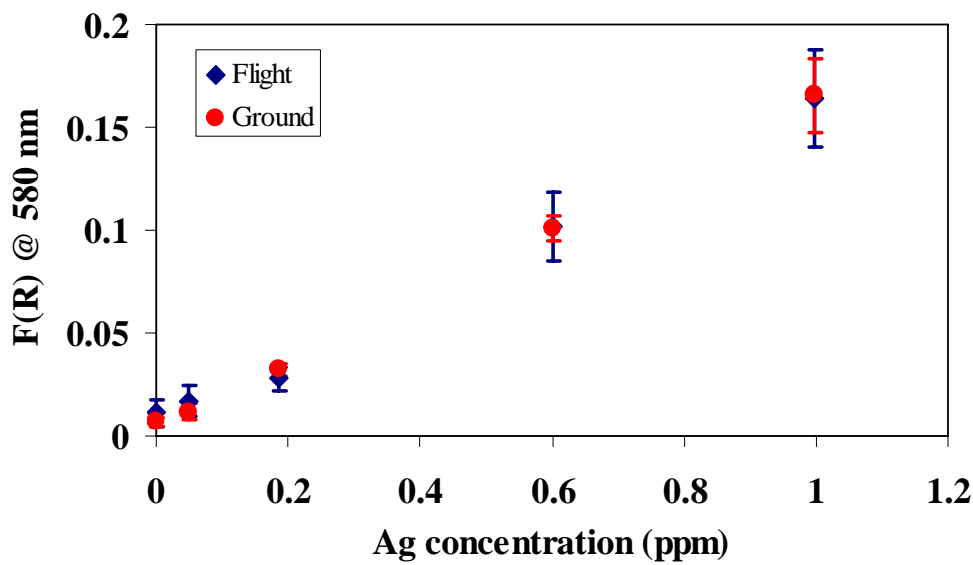


Figure 1. Ground and flight results from silver(I) experiments.

Iodine negligible depletion flights. Iodine negligible depletion membranes were prepared and loaded into cartridges prior to the microgravity flight. Iodinated water samples were stored in Teflon sample bags, and glass syringes were used to collect and meter water samples. During the microgravity flights, iodine syringes were filled during the 1 g turnaround portions of the flight in an effort to minimize entrapped air in the samples. Two separate flights were dedicated to iodine determinations with negligible depletion. During each set of experiments, six replicate analyses were performed on each iodine solution. Ground and flight experiments were performed simultaneously, with efforts made in the ground laboratory to mimic the thermal environment on the aircraft.

This series of flights were the first evaluations of negligible depletion in a microgravity environment. Negligible depletion is an equilibrium methodology that eliminates the need to de-bubble water samples prior to CSPE analysis⁵. As an air-water mixture is passed through a negligible depletion membrane, the target analyte partitions between the stationary phase (membrane disk) and the mobile phase (sample solution). Eventually, equilibrium is established and a steady-state concentration is reached in both phases. Applying this concept to CSPE, as long as the minimum sample volume required to reach equilibrium is passed through the membrane disk, the amount of air in the sample should become irrelevant.

Previous experience with iodine analysis using negligible depletion has indicated that ca. 6-mL of sample is required to establish a steady-state response from the membrane surface (equilibrium). During the negligible depletion flights and the ground experiments, 10-mL samples of iodinated water were analyzed to establish a response curve for negligible depletion. Then, 20-mL samples and 5-mL samples were analyzed in an effort to demonstrate negligible depletion. Since the 20-mL sample exceeds the minimum volume required to establish equilibrium, the response was expected to be the same as the response from the 10-mL samples. The response from the 5-mL samples was expected to be slightly less than the 10-mL samples because the required equilibrium volume would not pass through the membrane disk. The results from these trials were in reasonable agreement with expectations. Unfortunately the data

collected for the response curve did not show the same precision as earlier ground-based experiments. The data from both negligible depletion flights and the ground studies is being reanalyzed in an effort to better understand the results that were obtained.

pH flight. CSPE membranes for the pH experiments were prepared and loaded into cartridges prior to the microgravity flight. Samples of the pH solutions were pre-loaded into 1-mL disposable syringes for both the flight and ground experiments. Sufficient syringes and CSPE cartridges were prepared to perform five replicate analyses with each pH solution both on the ground and in flight. All syringes and cartridges were color-coded to simplify data recording during the flight. Ground and flight experiments were performed simultaneously, with efforts taken to mimic the thermal environment on the aircraft in the ground laboratory.

These pH CPSE experiments were the first demonstration of a color-matching analysis. Unlike other CSPE methods that utilize $F(R)$ values at a single wavelength for analyte quantification, color matching uses integrated spectral data to match the sample spectrum with a standard spectrum stored on the instrument. The standard spectra were collected from solutions with pH values in the same range as the flight solutions and labeled with the corresponding pH. In flight, the Color Guide Plus returned the label of the standard spectrum that most closely matched the sample solution. Importantly, this is the first demonstration of a CSPE analysis that provided real-time data during microgravity flights.

Table 1 shows the results for the C-9 flights and the results for an identical analysis performed on the ground. Five repetitions were performed of each pH sample on both ground and flight, with the exception of the pH 7.43 sample. In this case, an extra analysis was performed on the ground, as the membrane disk was damaged during the experiment process. The first column of each table displays the actual pH of the solution as measured using a standard pH meter. The second and third columns show the results of color matching for the ground and C-9 experiments, respectively. The average value of the flight samples was within 0.2 pH units of the actual pH for all four samples tested, while the average for the ground study was within 0.3 pH units of the actual solution value. All data points were included in the table, which illustrates that the damage caused to the membrane disk had little, if any, effect on the overall measurement.

Table 1. Summary of ground and flight pH experiments.

Solution pH	Ground Match	Flight Match
7.43	7.2	7.3
	7.2	7.0
	7.2	7.2
	7.0	7.4
	7.0	-
Average	7.1	7.2
8.19	8.0	7.9
	8.0	7.9
	8.0	8.1
	8.0	8.1
Average	8.0	8.0
8.86	8.6	8.5
	8.6	8.8
	8.6	8.7
	8.5	8.6
Average	8.6	8.7
9.31	9.2	9.2
	9.2	9.2
	9.2	9.0
	9.2	9.2
Average	9.2	9.2

Bubble mitigation flight. Flight evaluations of the motorless centrifuge were performed with deionized water loaded in Teflon bags. Several drops of red food coloring were added to each of the experimental bags to accentuate the appearance of the air bubbles in the water samples. The sample bags were prepared to contain predetermined air-water mixtures (10% air, 33% air, and 50% air).

The motorless centrifuge is a rotating clamp that was attached to the top of an experimental table using Velcro. During the microgravity portions of the flight, a sample bag was clamped in the centrifuge and rotated to separate the air and liquid phases (Figure 2). The bag was then clamped midway along its length with either a hemostat or a plastic clamp to isolate the phases (Figure 3). This spinning and clamping was accomplished during a single weightless period.



Figure 2. Sample bag being rotated in the motorless centrifuge.

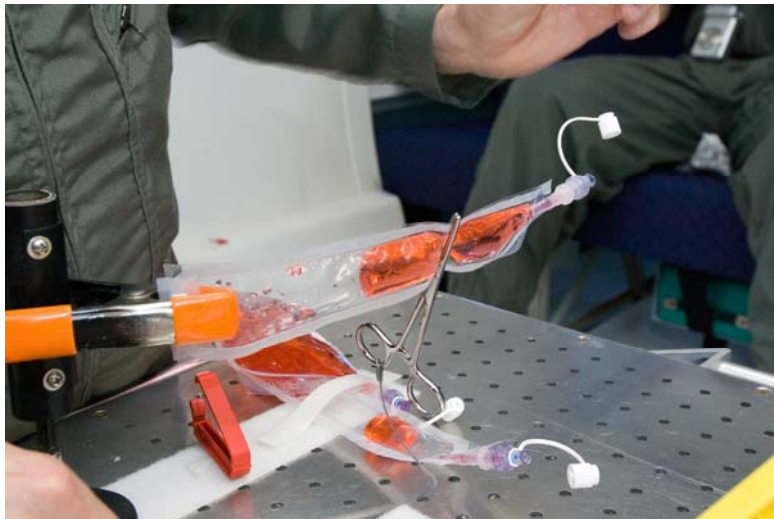


Figure 3. Air pocket isolated in sample bag using hemostat.

During the next parabola, a valve assembly was attached to the sample bag and a 1-mL sample volume was collected in a plastic syringe. The valve assembly consisted of a small check valve and a 4-mL waste bag. Once the sample syringe was connected to the valve assembly, the syringe plunger was pumped several times to remove residual air from the sampling port and then fill the sample syringe. Once the sample was collected, photographs were taken to verify that no air was trapped in the water sample. This process was repeated with each air-water mixture.

After 10 parabolas were flown using the valve assembly during sample collection, 10 parabolas were used to assess sample collection without the valves. After the sample bag was spun and clamped, no valve assembly was attached. Instead, several 1-mL volumes were collected into the syringe and dispensed into a waste bag before the final sample collection.

The motorless centrifuge and associated valve assembly proved to be very effective, repeatedly yielding syringes with bubble-free water. On one occasion, a small air bubble was observed in a syringe. The volume of this air bubble was estimated to be approximately 0.05 mL. It was noted

that the bubble appeared during the trials with the valve assembly that utilized the plastic clamp for phase isolation.

CONCLUSIONS

Despite the presence of a few minor problems, the silver(I) CSPE data clearly showed excellent agreement between ground and flight results. These results verify that the chemistry utilized in the silver(I) method is not affected by the absence of gravity. The iodine negligible depletion analysis did provide some promising results, but, the lack of precision in the collected data indicates that the method requires further refinement and ground testing. The motorless centrifuge system was successful in isolating air bubbles from water samples in Teflon bags. The hemostat appeared to be more reliable than the plastic clamp when used to keep the phases separated. Both the valving system and the syringe refilling provided bubble-free samples, and both could be useful on orbit depending on the application.

Based on these results, future microgravity flights will focus on cradle-to-grave analyses for silver(I) and iodine using the standard CSPE methods. These flights will combine the lessons learned about sample handling in microgravity with the refinements made to the CSPE methods so that the entire analysis, including sample collection and volume determination, will be performed in microgravity.

REFERENCES

1. Arena, M. P.; Porter, M. D.; Fritz, J. S., *Analytica Chimica Acta* 2003, 482, 197
2. Arena, M. P.; Porter, M. D.; Fritz, J. S., *Analytical Chemistry* 2002, 74, 185-190.
3. Porter, M.; Arena, M.; Weisshaar, D.; Mudgett, P.; Rutz, J.; Benoit, M., In *KC-135 and Other Microgravity Simulations*; Space and Life Sciences Directorate, Human Adaptation and Countermeasures Office, Lyndon B. Johnson Space Center: Houston, TX, August, 2001, pp 168-177.
4. Porter, M. D.; James, J.; Packham, N.; Dias, N.; Gazda, D. B.; Hazen-Bosveld, A.; Lipert, R. J.; Ponton, L. M.; Kuo, M.; Rutz, J. A.; Straub, J. E.; Schultz, J., *Colorimetric Solid Phase Extraction Measurements of Spacecraft Drinking Water Contaminants. KC-135 and Other Microgravity Simulations Summary Report*; Space and Life Sciences Directorate, Human Adaptation and Countermeasures Office, Lyndon B. Johnson Space Center. August 1, 2004, 2004, 85-97.
5. Nardi, L., *Journal of Chromatography, A* 2003, 985, 85-91.

PHOTOGRAPHS:

JSC2006E24709 to JSC2006E24775
JSC2006E24848 to JSC2006E24883
JSC2006E24964 to JSC2006E24993

VIDEO:

- Zero G June 19 – 23, 2006 flights, Master: 721253

Videos available from Imagery and Publications Office (GS4), NASA/JSC.

CONTACT INFORMATION

Marc Porter, Ph.D
42 Spedding Hall
Department of Chemistry
Institute for Combinatorial Discovery
Iowa State University
Ames, IA 50011
515-294-6433
mporter@porter1.ameslab.gov

Appendix

Background Information about the C-9 and the Reduced Gravity Program

The Reduced-Gravity Program, operated by the NASA/Johnson Space Center (JSC), provides engineers, scientists, and astronauts alike, a unique opportunity to perform testing and training in a weightless environment but without ever having to leave the confines of the Earth's orbit. Given the frequency of space shuttle missions and the construction and habitation of the International Space Station, the Reduced-Gravity Program provides a truly ideal environment to test and evaluate space hardware and experimental procedures prior to launch.

The Reduced-Gravity Program was established in 1959 to investigate the reactions of humans and hardware during operations in a weightless environment. A specially modified C-9 turbojet, flying parabolic arcs, produces periodic episodes of weightlessness lasting 20-25 seconds. The C-9 is sometimes also flown to provide short periods of lunar (1/6) and Martian (1/3) gravity. Over the last 35 years, approximately 100,000 parabolas have been flown in support of the Mercury, Gemini, Apollo, Skylab, Space Shuttle, and Space Station programs.

Excluding the C-9 Flight Crew and the Reduced Gravity Program Test Directors, the C-9 accommodates seating for a maximum of 20 other passengers. The C-9's cargo bay provides a test area that is approximately 45 feet long, 104 inches wide, and 80 inches high. The aircraft is equipped with electrical power, overboard venting system, and photographic lights. When requested and available, professional photography and video support can be scheduled to document in-flight activities.

A typical flight lasts 2 to 3 hours and consists of 30 to 40 parabolas. The parabolas are flown in succession or with short breaks between maneuvers to allow time for reconfiguring test equipment.

For additional information concerning flight weeks sponsored by the Johnson Space Center's Human Adaptation and Countermeasures Department or other Reduced-Gravity Program opportunities, please contact:

Todd Schlegel, MD
Technical Monitor
Human Adaptation and Countermeasures
NASA Lyndon B. Johnson Space Center
Mail Code: SK
Houston, TX 77058
Telephone: (281) 483-9643

NASA Lyndon B. Johnson Space Center
Reduced-Gravity Office, Ellington Field
Mail Code: CC43
Houston, TX 77034
Telephone: (281) 244-9211

Explore the Zero Gravity Experiments and Aircraft Operations Web pages at:

<http://zerog.jsc.nasa.gov/>

<http://jsc-aircraft-ops.jsc.nasa.gov>

REPORT DOCUMENTATION PAGE			Form Approved OMB No. 0704-0188	
Public reporting burden for this collection of information is estimated to average 1 hour per response, including the time for reviewing instructions, searching existing data sources, gathering and maintaining the data needed, and completing and reviewing the collection of information. Send comments regarding this burden estimate or any other aspect of this collection of information, including suggestions for reducing this burden, to Washington Headquarters Services, Directorate for Information Operations and Reports, 1215 Jefferson Davis Highway, Suite 1204, Arlington, VA 22202-4302, and to the Office of Management and Budget, Paperwork Reduction Project (0704-0188), Washington, DC 20503.				
1. AGENCY USE ONLY (Leave Blank)	2. REPORT DATE September 2006	3. REPORT TYPE AND DATES COVERED NASA Technical Memorandum		
4. TITLE AND SUBTITLE C-9 and Other Microgravity Simulations			5. FUNDING NUMBERS	
6. AUTHOR(S) Prepared by: Space and Life Sciences Directorate Human Adaptation and Countermeasures Office				
7. PERFORMING ORGANIZATION NAME(S) AND ADDRESS(ES) Lyndon B. Johnson Space Center Houston, Texas 77058			8. PERFORMING ORGANIZATION REPORT NUMBERS S-984	
9. SPONSORING/MONITORING AGENCY NAME(S) AND ADDRESS(ES) National Aeronautics and Space Administration Washington, DC 20546-0001			10. SPONSORING/MONITORING AGENCY REPORT NUMBER TM-2006-213727	
11. SUPPLEMENTARY NOTES				
12a. DISTRIBUTION/AVAILABILITY STATEMENT Available from the NASA Center for AeroSpace Information (CASI) 7121 Standard Hanover, MD 21076-1320 Category: 99			12b. DISTRIBUTION CODE	
13. ABSTRACT (Maximum 200 words) This document represents a summary of medical and scientific evaluations conducted aboard the C-9 or other NASA-sponsored aircraft from June 30, 2005, to June 30, 2006. Included is a general overview of investigations manifested and coordinated by the Human Adaptation and Countermeasures Office. A collection of brief reports that describe tests conducted aboard the NASA-sponsored aircraft follows the overview. Principal investigators and test engineers contributed significantly to the content of the report, describing their particular experiment or hardware evaluation. Although this document follows general guidelines, the format of individual reports varies to accommodate differences in experiment design and procedures. This document concludes with an appendix that provides background information concerning the Reduced Gravity Program.				
14. SUBJECT TERMS Weightlessness, weightlessness simulation, parabolic flight, zero gravity, aerospace medicine, astronaut performance, bioprocessing, space manufacturing.			15. NUMBER OF PAGES 202	16. PRICE CODE
17. SECURITY CLASSIFICATION OF REPORT Unclassified	18. SECURITY CLASSIFICATION OF THIS PAGE Unclassified	19. SECURITY CLASSIFICATION OF ABSTRACT Unclassified	20. LIMITATION OF ABSTRACT Unlimited	
